Studies of Calcium Channels in Cultured Neuroblastoma and Muscle Cells Using Monoclonal Antibodies

A thesis presented by

HELEN JANE PHILLIPS

For the degree of Doctor of Philosophy in the University of London.

Department of Pharmacology, Royal Free Hospital School of Medicine.

March 1992

ABSTRACT

The calcium channel from skeletal muscle is composed of five subunits: α_1, α_2, ß, γ and δ. The α_1 subunit contains the ion channel pore and a dihydropyridine binding site but a role for the α_2 subunit is unclear. In this study the role of the α_2 subunit in the functioning of the dihydropyridine-sensitive calcium channel has been investigated. More specifically, monoclonal antibodies raised against this subunit from rabbit skeletal muscle t-tubule membranes were used as probes to study the functioning of the channels using primarily electrophysiological methods.

In order to study the action of the monoclonal antibodies on voltage-dependent calcium channels, whole-cell patch clamp recordings were made from neuroblastoma and muscle cell lines. In the mouse neuroblastoma x rat glioma hybrid (NG 108 15) cells at a holding potential of -40mV, two components of current were present: a dihydropyridine-sensitive current (L-type) and a dihydropyridine-insensitive current. At a holding potential of -80mV an additional transient (T-type) component was also present. After incubating the cells for 24 hours with the antibody, of the seven monoclonal antibodies tested, only one (mAb 11.14) had an effect on the whole cell currents. This monoclonal antibody selectively reduced the dihydropyridine-sensitive (L-type) component of current and decreased the time to peak of the current. However when it was applied acutely to the bath during whole-cell recording, it had no effects on the inward calcium channel currents. Potassium-stimulated ^{45}calcium flux experiments confirmed the effect of mAb 11.14 after 24 hour incubation with the cells, by reducing the stimulated calcium flux whilst none of the other antibodies

produced a significant effect.

Monoclonal antibody 11.14 was also tested on a mouse muscle cell line (BC_3H1). These cells had two components of calcium channel current. The major component was dihydropyridine-sensitive and had both slow activation and inactivation rates. The second dihydropyridine-insensitive component was much smaller and could be isolated by using a holding potential of -40mV. Of two antibodies (against the α_2 subunit) tested after 24 hour incubation with the cells, again only mAb 11.14 had an effect. However, on these cells the antibody appeared to increase the rate of activation of the dihydropyridine-sensitive component without the corresponding reduction in amplitude. This effect was also observed when the antibody was applied acutely and suggests that the α_2 subunit possibly has a role in directly modulating dihydropyridine-sensitive calcium channel function.

The results presented from both cell types indicate that there must be antigenic differences between dihydropyridine-sensitive channels and the other channel types seen in these cells since the antibody only affected dihydropyridine-sensitive channels. In addition they indicate that the α_2 subunit is present in NG 108 15 cells and must be in close association with the α_1 subunit (where the pore is located) enabling it to affect the functioning of the channel.

CONTENTS

LIST OF TABLES

LIST OF ILLUSTRATIONS

ACKNOWLEDGEMENTS

I would like to thank my supervisor, Professor D.Wray, for the help, guidance and encouragement that he has provided throughout the project. I am also indebted to Dr R.I.Norman for his advice concerning the biochemical aspects of the project. I would also like to acknowledge my gratitude to Drs. R.I.Norman and T.M.Harrison for the production of the monoclonal antibodies used in this work.

Thanks are also due to the staff in the Pharmacology Department at the Royal Free Hospital Medical School for their much appreciated help and support. Finally, thanks to Dave for his patience and the use of his computer.

CHAPTER 1

INTRODUCTION

Voltage-sensitive calcium channels exist in skeletal, cardiac and smooth muscle cells as well as other excitable and secretory cells. They translate changes in membrane potential into an intracellular calcium signal. This increase in free cytosolic calcium initiates a number of cellular responses, including muscle contraction and release of hormones and neurotransmitters. The 1,4-dihydropyridines are potent blockers of one type of voltage-dependent calcium channel. The experiments reported in this thesis were carried out to investigate a possible functional role of the α_2 subunit of the dihydropyridine-sensitive calcium channel using monoclonal antibodies against this subunit as probes. The studies were carried out in both mouse neuroblastoma x rat glioma hybrid cells (NG 108 15) and a mouse muscle cell line (BC_3H1). In this introduction the properties of the voltage-dependent calcium channels found in a wide range of tissues will be discussed, with particular attention paid to those present in neuronal and skeletal muscle preparations. In addition the current knowledge on the subunit structure of the dihydropyridine-sensitive calcium channel will be reviewed.

The concentration of free calcium in the cytoplasm is normally at a very low level, less than 0.1μM. When this concentration rises it initiates many important processes. The extracellular concentration is in the millimolar range so there is a large concentration gradient across the cell membrane. An increase in the free cytoplasmic calcium concentration can come from two sources: i. from intracellular stores and ii. from the extracellular space by an increase in permeability of the plasma membrane

due to the opening of voltage operated calcium channels, with calcium flowing down its electrochemical gradient (Reuter, 1983).

Currents through calcium channels can be carried by calcium, strontium and barium. These currents still occur when the extracellular solution is sodium free or in the presence of tetrodotoxin which blocks inward sodium current. However cobalt, magnesium, lanthanum and cadmium block the currents at concentrations less than 10mM. Also certain organic drugs and toxins block some types of calcium currents (Hagiwara & Byerly, 1981). Sodium ions can go through calcium channels in the absence of calcium but are strongly inhibited in the presence of even low calcium concentrations.

Multiple types of calcium channels have been found which have been classified according to the differences in their pharmacology, gating and ionic conductance (for review see e.g. Tsien *et al.*, 1988). At least three distinct types of voltage-gated calcium channel have so far been identified: T, N and L (for alternative terminology see below), although other voltage-gated calcium channels have been described which do not fit precisely into this classification.

In sensory neurons the co-existence of three types of calcium channels have been identified by use of cell-attached patch and whole cell recordings (Nowycky, Fox & Tsien, 1985). There is a low-threshold, rapidly inactivating calcium current which has been named T-type. This channel is activated by steps to depolarisations positive to -70mV and inactivates with a time constant of about 20-50ms at 0mV. It shows steady-state inactivation at relatively depolarised holding potentials e.g.-40mV. It conducts calcium as well as barium (Fox, Nowycky & Tsien, 1987) and has a single channel conductance of about 8pS in 110mM barium. The dihydropyridines have no

marked effect on the channel but it is blocked by inorganic calcium channel blockers, particularly nickel.

Two types of high-threshold calcium currents have been distinguished, L and N. The L-type current is a very slowly inactivating (>500ms) current which can be activated by large depolarizing steps to potentials more positive than around -20mV. It is not inactivated at a steady-state potential of e.g. -40mV. The channels are sensitive to the dihydropyridines e.g. nitrendipine, phenylalkylamines e.g. verapamil and benzothiazepines e.g. diltiazem and are more sensitive to block by the inorganic ion, cadmium, than nickel. It conducts barium better than calcium (Fox, Nowycky & Tsien, 1987) and has a single channel conductance of around 25pS in 110mM barium.

The other high-threshold activating channel is the N-type. It needs fairly large depolarizing steps to potentials more positive than -20mV to be activated, from a strongly negative holding potential. It has an inactivation rate of about 50-80ms in sensory neurons, which is intermediate between the other types of channel described. The inactivation rate,however, varies greatly between neurons with a time constant of about 500ms in sympathetic neurons (Hirning, 1988). The single channel conductance is about 13pS in 110mM barium (the channel conducts barium better than calcium). The channel is not affected by the dihydropyridines but is blocked by ω-conotoxin (McCleskey *et al.*, 1987) and by cadmium.

In skeletal muscle two types of calcium current have been found. One is a slowly activating current which also inactivates very slowly, with a time constant for inactivation of around 1s (Sanchez & Stefani, 1978; Donaldson & Beam, 1983; Cota, Nicola Sira & Stefani, 1984). These channels are often called "slow" calcium channels although their voltage-dependence is similar to that of the L-type channel, requiring

large depolarisations for activation. They are blocked by D-600 and dihydropyridines (McCleskey, 1985), like other L-type channels, and are consequently sometimes also referred to as dihydropyridine-sensitive calcium channels. The other type of calcium channel found in skeletal muscle requires a low threshold for activation like the T-type described in neurons and is activated at a fast rate (Cota & Stefani, 1986; Garcia & Stefani, 1987). It is not sensitive to the dihydropyridines (Arreola, Calvo, Garcia & Sanchez, 1987). However, in contrast to T-type channels it does not inactivate rapidly (Cota & Stefani, 1986). A T-type channel is seen in developing skeletal muscle during the first three weeks after birth (Cognard, Lazdunski & Romey, 1986; Beam, Tanabe & Numa, 1989).

BC_3H1 cells are a mouse muscle cell line. When differentiated these cells have been found to express two functional types of calcium channels (Caffrey, Brown & Schneider, 1987) which correspond to those found in the t-tubules of skeletal muscle (Almers & McCleskey, 1984; Cota & Stefani, 1986). The "slow" calcium current is activated with a time constant of around 100ms which is comparable with "slow" calcium channels found in t-tubules of skeletal muscle (time constant of activation 100-300ms) and is dihydropyridine-sensitive (Caffrey, Brown & Schneider, 1987; Morton, Caffrey, Brown & Froehner, 1988). The "fast" calcium current is activated at quite negative potentials and is slowly inactivating, with a time constant for inactivation in both BC_3H1 cells and skeletal muscle of 500-5000ms and is dihydropyridine-insensitive (Caffrey, Brown & Schneider, 1987).

It is clear from the channels seen in skeletal muscle that not all calcium channels will fit precisely into the T, N, and L classification. In particular calcium channels in invertebrates have been found to be very difficult to group with those of

vertebrates (e.g. Lees, Pearson & W.-Wray, 1989; Pelzer, S. *et al.*, 1989). More evidence for a larger variety of channel types in both vertebrates and invertebrates comes from the identification of a fourth type of calcium channel, the P channel (Llinas, Sugimori, Lin & Cherksey, 1989; Llinas, Sugimori & Cherksey, 1989). The P channel was first described in Purkinje cells hence the notation, but has since been shown to be present in the squid giant synapse and optic lobe (Llinas, Sugimori, Lin & Cherksey, 1989). It is a high threshold channel which is not blocked by ω-conotoxin or the dihydropyridines but is sensitive to a toxin from funnel-web spiders (Llinas, Sugimori, Lin & Cherksey, 1989). This channel may be contributing to the high threshold, dihydropyridine and ω-conotoxin insensitive current which has been recorded in a variety of neurons (Scroggs & Fox, 1992) and which was particularly apparent in cerebellar Purkinje cells (Regan, Sah & Bean, 1991).

Most investigations have centred on L-type channels since they are highly sensitive to the dihydropyridines and are present in a large number of tissues. They are found in cardiac (e.g. Nilius, Hess, Lansman & Tsien, 1985) and smooth muscle (e.g. Benham, Hess & Tsien, 1987), most neurons (e.g. Nowycky, Fox & Tsien, 1985; Hirning *et al.*, 1988) and neuronal cell lines (e.g. Narahashi, Tsunoo & Yoshii, 1987; Peers *et al.*, 1990), as well as some secretory cells e.g. pancreatic ß cells (Ashcroft, Rorsman & Trube, 1989) and "non-excitable" cells e.g. fibroblasts (Chen *et al.*, 1988). L-type channels as mentioned above are characterized by their block by organic calcium channel antagonists. The three groups of drugs appear to bind at different but allosterically interacting sites on the calcium channel (Glossmann *et al.*, 1984). The sites are referred to as the 1,4-dihydropyridine, the verapamil and the diltiazem binding sites, after the drugs used to characterise them. Each of the receptor sites can

exist in low and high affinity binding states with the distribution in each state regulated by drugs, ions and temperature. When the diltiazem site is occupied, the binding of 1,4-dihydropyridine channel blockers is increased. Similarly binding of the 1,4-dihydropyridine antagonists stimulates diltiazem binding. In contrast binding of the 1,4-dihydropyridine agonists is inhibitory for diltiazem binding. When the verapamil site is occupied there is also a negative allosteric action on the binding of diltiazem as well as on the binding of the 1,4-dihydropyridines. The divalent cations also affect binding. For high affinity 1,4-dihydropyridine binding, divalent cations are required but they inhibit diltiazem or verapamil binding. High affinity binding is also dependent on temperature, with maximum binding of all three drug types usually occurring at temperatures lower than 10°C. Therefore, at temperatures above this a large proportion of the receptors are in the low affinity state. Binding of the 1,4-dihydropyridines antagonists is also strongly modulated by membrane potential (Sanguinetti & Kass, 1984). These compounds show a greater degree of block when the current is measured from a depolarised holding potential.

These antagonists reduce outward as well as inward flux through calcium channels without slowing the rate of current activation. The block by any of these organic drugs is antagonised by raising the external calcium concentration, but this is not by competition for the same binding site as calcium (Lee & Tsien, 1983).

The mechanism of action of the dihydropyridine antagonists and agonists is thought to be by favouring a particular mode of gating and not by plugging the pore (Hess, Lansman & Tsien, 1984). Untreated single calcium channels show multiple modes of gating. "Mode 1" is the most common form of gating in the absence of drug. It is characterised by rapid bursts of short channel openings, approximately 1ms

duration. The probability of the channel being open is low at small depolarisations but high at stronger depolarisations. Open time histograms can be fitted by a single exponential, indicating one open state and closed times by the sum of two exponentials indicating two closed states. "Mode 0" is when the channel is unavailable for opening and this mode of gating is favoured by the dihydropyridine antagonists. "Mode 2" is characterised by long openings, about 20ms, and brief closures. The probability of the channel being open is high even at smaller depolarisations. The distributions of the open and closed times can still be explained by one open state and two closed but the values of the rate constants are different. Dihydropyridine agonists e.g. Bay K 8644 favour mode 2 (Hess, Lansman & Tsien, 1984; Fox, Nowycky & Tsien, 1987a). This mode of gating only occurs at a frequency of 1% in the absence of drug.

Not all the dihydropyridines though are in fact pure antagonists or agonists but can show mixed effects. For instance, nitrendipine at lower doses favours mode 0 gating (i.e. an antagonist like action) with a reduction in the proportion of sweeps with openings. However it also displays an increase in mode 2 gating, with a larger number of sweeps with long open times and shorter closed times (i.e. agonist like action). At higher concentrations of nitrendipine there is an increase in the percentage of sweeps with no openings, which at 10μM nitrendipine approaches 100%. Therefore the inhibitory effect generally observed for nitrendipine is a net effect of the antagonist as well as agonist component (Hess, Lansman & Tsien, 1984).

The effects of the dihydropyridines on the L-type currents vary between tissues. For example, in chick dorsal root ganglion (DRG) cells, which express all three types of calcium channel, nifedipine (a dihydropyridine) had no effect on

calcium currents in 28 out of the 56 cells (Kasai, Aosaki & Fukuda, 1987) at a concentration of 5μM, which would cause total block of L-type channels in cardiac or smooth muscle (Bean *et al.*, 1986; Sanguinetti & Kass, 1984). In the remaining cells which gave an effect with nifedipine, the reduction in current was only 5-50%. Also in other studies at depolarized holding potentials where the inhibition should be maximal (Sanguinetti & Kass, 1984) the block seen by dihydropyridines was still only around 60% (Rane, Holz & Dunlap, 1987; Fox, Nowycky & Tsien, 1987). Furthermore, in bullfrog and rat DRG neurons, dihydropyridine blocking drugs also have little effect on a current that by its slow inactivation and voltage dependence would be classified as L-type (Bean, 1989). This limited effect also occurs if the cell is held at a relatively depolarized potential. This suggests that neuronal calcium channels have a lower sensitivity to the dihydropyridines than muscle L-type channels or alternatively that the sustained current is not entirely due to L-type channels.

Verapamil may not be specific for L-type channels. Although it blocks the L-type and not T-type in rat and chick DRG cells (Fedulova, Kostyuk & Veselovsky, 1985), in hippocampal neurons it reduces both L- and T-type currents (Yaari, Hamon & Lux, 1987). In addition in DRG cells the concentrations that are required to block the high threshold currents are ten times higher than those needed to block purely L-type channels in cardiac cells, which may indicate that N-type as well as L-type channels are blocked (Bean, 1989).

Most L-type channels are modulated by cAMP-dependent protein kinase, which phosphorylates L-type channels. This increases the channel opentime and decreases the interval between channel openings so increasing the probability that the channel is open by several fold. This has been found for the calcium channels in both isolated

cardiac cells (Trautwein *et al.*, 1987) as well as the purified dihydropyridine-sensitive channel complex from skeletal muscle reconstituted into artificial lipid bilayers (Flockerzi *et al.*, 1986). A fairly small proportion however of L-type channels in cardiac cells (around 20%) will still open in the absence of cAMP stimulated phosphorylation (Brum, Osterrieder & Trautwein, 1984), indicating that cAMP-dependent phosphorylation is not necessarily essential for L-type channel opening.

During repetitive stimulation L-type currents progressively decrease in amplitude (rundown). This effect is seen in whole cell recordings in cells that are not dialysed internally with MgATP (Fedulova, Kostyuk & Veselovsky, 1985; Forscher & Oxford, 1985; Robertson & Taylor, 1986) and in isolated patches where the cytoplasmic side of the patch is exposed to a standard intracellular saline solution (Armstrong & Eckert, 1987). This effect has been studied in Helix neurones and two processes appear to contribute to rundown. One process could be due to a calcium-dependent proteolysis while the other appears to be due to dephosphorylation (Chad & Eckert, 1986). A variety of methods have been used to decrease the inactivation due to dephosphorylation. The most successful appears to be the addition of either the catalytic subunit of cAMP-dependent protein kinase with MgATP (Armstrong & Eckert, 1987) or the presence of an ATP regeneration system of creatine phosphate and creatine phosphokinase together with MgATP (Forscher & Oxford, 1985).

ω-conotoxin is a 27 amino acid polypeptide from the venom of the marine snail, *Conus geographus*. In many vertebrate neurons it produces persistent block of N- and L-type channels but only a weak reversible block of T-type (McCleskey *et al.*, 1987), although it has been suggested that it is specific for N-type channels (Kasai, Aosaki & Fukuda, 1987). Block is however tissue specific, since it blocks the high

threshold currents in neurons of vertebrates but not in skeletal, cardiac or smooth muscle (McCleskey *et al.*, 1987). Another possible blocker of N-type current is gadolinium. In NG 108 15 neuroblastoma cells gadolinium selectively blocks a component of the calcium current (Docherty, 1988). If an analogy is drawn between the three components of current observed in these cells and those in sensory neurons, the gadolinium-sensitive current probably corresponds to N-type.

A few potential blocking drugs selective for T-type channels have been proposed. These include amiloride in neuroblastoma cells and dorsal root ganglion neurons (Tang, Presser & Morad, 1988), phenylhydantoin in hippocampal neurons (Yaari, Hamon & Lux, 1987) and flunarizine in N1E-115 neuroblastoma cells (Wang, Karpinski, Wu & Pang, 1990). However, so far none of the potential blocking drugs have allowed the purification, isolation and biochemical characterization of the T-type channel.

Many neurotransmitters have been found to affect calcium channel function. The most investigated example is the increase in L-type current seen with ß-adrenoceptor stimulation in cardiac cells (e.g Reuter, 1983; Trautwein *et al.*, 1987). Agonist binding to the ß-adrenoceptor activates adenylate cyclase which results in an increase in cAMP. This binds to the regulatory subunit of cAMP-dependent protein kinase which liberates the catalytic subunit resulting in phosphorylation of the channel or a closely related protein. Phosphorylation of the channel, as discussed earlier, increases the probability that it is open. An increase in L-type current is also seen with ß-adrenoceptor stimulation in frog sympathetic neurones again by a process involving cAMP (Lipscombe & Tsien, 1987). But in hippocampal neurones ß-adrenoceptor activation results in an increase in N-type channel activity (Gray & Johnston, 1987).

However, α_2-adrenoceptor stimulation by noradrenaline, causes a decrease in N-type current in frog sympathetic neurones (Kongsamut, Lipscombe & Tsien, 1989) and in rabbit vesical parasympathetic neurones (Akasu, Tsurusaki & Tokimasa, 1990). This decrease in N-type current possibly has a role in the inhibitory effect of noradrenaline on its own release. It is postulated that noradrenaline acts on an α_2-like adrenoreceptor to decrease N-type current via a process mediated by a G-protein (i.e. GTP-binding protein). In dorsal root ganglion neurones however, noradrenaline appears to reduce the L-type calcium current also with a G-protein as the signal transducer (Holz, Rane & Dunlap, 1986).

Other neurotransmitters which have been found to inhibit calcium channels include: GABA (B) in chick, rat and cat dorsal root ganglion neurones (Dunlap & Fischbach, 1981; Dolphin & Scott, 1986; Robertson & Taylor, 1986); adenosine in chick and rat dorsal root ganglion neurones, an action mediated by a GTP-binding protein (Kasai & Aosaki, 1989; Dolphin & Scott, 1987); and opioids in NG 108 15 cells (Hescheler, Rosenthal, Trautwein & Schultz, 1987); for reviews see Tsien *et al.*, 1988 and Hofmann *et al.*, 1987. In many cases it appears that GTP-binding proteins are intermediate between the neurotransmitter receptor and the calcium channel, coupling either directly or indirectly to the channel.

In skeletal muscle, unlike cardiac and smooth muscle, only 5% or fewer of the total number of dihydropyridine receptors are in fact functional calcium channels (Schwartz, McCleskey & Almers, 1985). Extracellular calcium entry is not required to trigger contraction (Almers, McCleskey & Palade, 1985). Depolarisation of skeletal muscle releases calcium from the sarcoplasmic reticulum without the need for calcium entry through dihydropyridine-sensitive channels. This is in contrast to the situation

in cardiac muscle where calcium enters through an L-type like channel and the entry triggers a large release of calcium from the sarcoplasmic reticulum (Tanabe *et al.*, 1990). It is possible that in skeletal muscle the dihydropyridine receptors mainly act not as calcium channels but as voltage-sensors in excitation-contraction coupling (Rios & Brum, 1987).

Since the dihydropyridines, such as nitrendipine and PN200-110, bind with high affinity and specificity to L-type channels they have been used extensively in its purification and characterization (e.g. Curtis & Catterall, 1984; Borsotto *et al.*, 1984; Flockerzi, Oeken & Hofmann, 1986). The transverse-tubules of skeletal muscle are particularly rich in binding sites for the dihydropyridines (Fosset *et al.*, 1983). For this reason most of the biochemical investigations have concentrated on this system. This has assumed that these receptors are equivalent to or associated with a calcium channel (e.g. Curtis & Catterall, 1984; Borsotto *et al.*, 1984; Flockerzi, Oeken & Hofmann, 1986).

From such studies of purified receptors, the dihydropyridine receptor from skeletal muscle is thought to be composed of five subunits: α_1, α_2 disulphide linked to δ, ß and γ (Takahashi *et al.*,1987; Catterall *et al.*, 1989). Under non-reducing conditions the α_1 subunit has a molecular weight of approximately 175kDa, $\alpha_2\delta$ 167kDa, ß 54kDa and γ 30kDa. However, under reducing conditions the disulphide bond is broken and the molecular weight of the α_2 subunit is reduced to approximately 143kDa (Leung, Imagawa & Campbell, 1987) while 24-27kDa components appear which have collectively been called, δ (Morton & Froehner, 1987; Takahashi *et al.*, 1987). The α_1 and ß subunits contain cAMP-dependent protein kinase phosphorylation sites whereas α_2, γ and δ do not (Curtis & Catterall, 1985; Hosey, Borsotto &

Lazdunski, 1986; Nastainczyk *et al.*, 1987). α_1 and γ are the most hydrophobic and therefore probably the principal transmembrane polypeptides (Takahashi *et al.*, 1987). α_2 and δ have some hydrophobic regions whilst ß appears to have none. The hydrophobicity of the α_2 subunit is weak, indicating that it has only limited transmembrane domains and it, therefore, appears unlikely that the ion channel is formed jointly by α_1 and α_2 (Takahashi *et al*, 1987). The α_2, γ and δ subunits are glycosylated and have estimated core polypeptides of 105kDa, 20kDa and 17kDa respectively (Catterall *et al.*, 1989; Jay *et al.*, 1991). The α_1 subunit contains the DHP and phenylalkylamine binding sites since [^{3}H]azidopine and [^{3}H]LU 49888 both label a band of approximately 165kDa even after reduction of disulphide bonds (Vaghy *et al.*, 1987; Sieber *et al.*, 1987; Striessnig *et al.*, 1987). Using specific anti-α_1 polyclonal antibodies or α_2-specific lentil lectin-agarose it has been shown that α_1, α_2, ß, γ and δ behave as a complex in the presence of digitonin or CHAPS but in the presence of Triton X-100 the $\alpha_2\delta$ complex dissociates from α_1ßγ (Takahashi *et al.*, 1987). As the $\alpha_2\delta$ complex is fairly weakly associated with the α_1 complex it has been argued that it is just a persistent impurity (Froehner, 1988). However, the $\alpha_2\delta$ complex remains associated with the α_1ßγ complex in detergents where the functional properties of the calcium channel are preserved upon purification (Flockerzi *et al.*, 1986).

From these studies, Takahashi *et al.* (1987) proposed a model (figure 1.1). The α_1 subunit is suggested to form the ion channel-forming pore since it has the largest hydrophobic domains, the DHP binding site and cAMP-dependent phosphorylation sites. The ß subunit is proposed to be intracellular since it had no hydrophobic regions but has cAMP-dependent phosphorylation sites and γ appears to have at least one transmembrane region since it is hydrophobic. The γ is composed of approximately

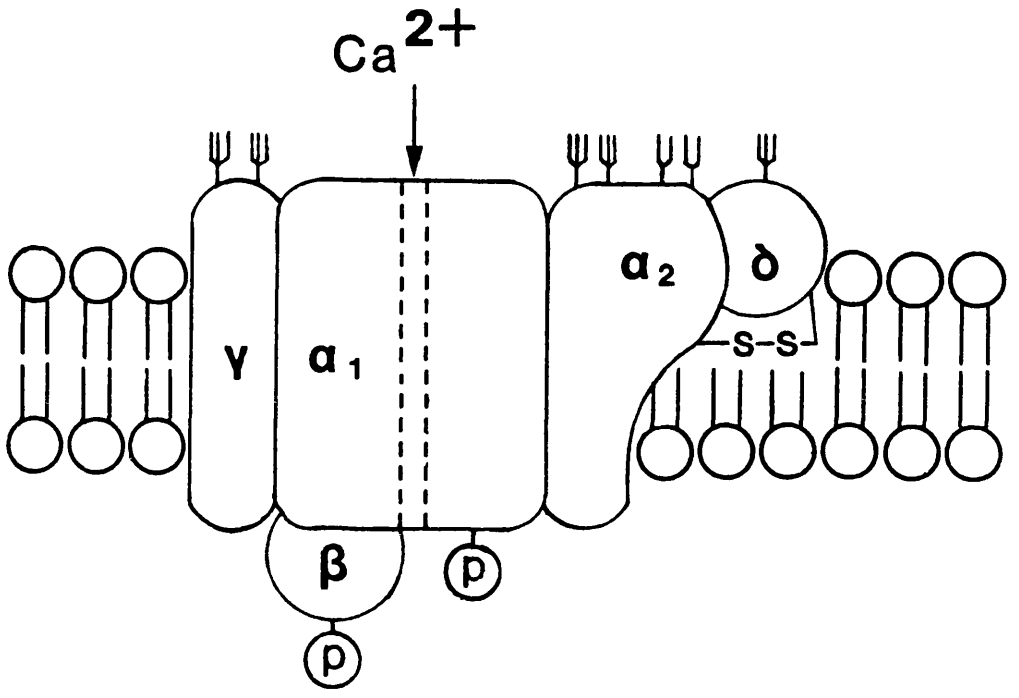

Legend for Figure 1.1 Proposed model of the subunit structure of the dihydropyridine-sensitive calcium channel.

Structure of dihydropyridine-sensitive calcium channel showing the proposed sites of cAMP-dependent phosphorylation (P) and glycosylation (Ψ).

30% carbohydrate and appears to be similar to the β_1 subunit of rat brain and skeletal muscle sodium channels. The α_2 subunit is disulphide linked to δ subunit. These subunits are glycosylated and do not have large hydrophobic domains indicating that they are unlikely to be important in the formation of the ion channel.

The purified dihydropyridine receptor complex (α_1, α_2, β, γ and δ subunits), has been reconstituted into artificial lipid bilayers to show that it can still function as a calcium channel (Flockerzi *et al.*, 1986; Talvenheimo, Worley & Nelson, 1987). When reconstituted the purified receptor gave a single channel conductance of 16-20pS, similar to the value found in bilayer recordings of single Ca^{2+} channels from solubilized skeletal muscle t-tubule membranes (Rosenberg *et al.*, 1986) and cell-attached recordings from L-type Ca^{2+} channels (Cavalie, Ochi, Pelzer & Trautwein, 1983). The currents through the reconstituted channels were blocked by gallopamil, a phenylalkylamine, and Bay K 8644 increased the probability of the channels being open by inducing long term channel openings. Phosphorylation of the receptor complex by cAMP-dependent kinase also increased the probability of the channel being open. This data shows that the purified complex can be reconstituted to form a functional calcium channel.

By cloning studies and sequencing of cDNA, the complete amino-acid sequence of the rabbit skeletal muscle dihydropyridine receptor (α_1 subunit) has been determined (Tanabe *et al.*, 1987). It is very similar to the sequence found for the voltage-dependent sodium channel (Noda, 1984; Noda, 1986). Indeed, of the proposed amino acid sequence, 29% is identical with the sequence of the α subunit of the rat brain sodium channel with an additional 36% being substitutions of chemically similar amino acids. The sequence is composed of 1873 amino-acids with a calculated

molecular weight of 212,018. There are four ~~internal~~ domains (I-IV), which exhibit sequence homology between themselves. Each internal domain has five hydrophobic segments (S1, S2, S3, S5 and S6) and one positively charged one, S4. This also corresponds to the situation found in the sodium channel where there is evidence that the positive charges in segment S4 are involved in voltage-sensing (Stuhmer *et al.*, 1989). The model proposed for the channel orientates the carboxyl and amino-termini on the cytoplasmic side of the membrane, the seven potential cAMP-dependent sites on the cytoplasmic side and two of the five potential N-glycosylation sites on the extracellular side.

Antibodies raised against a peptide which represents the C-terminal amino-acid residues from the predicted sequence, recognised a 212kDa protein on immunoblots that was previously undetected (De Jongh, Merrick & Catterall, 1989). The size is as predicted for the full length of the α_1 subunit from cDNA cloning. The 175kDa protein previously identified may arise from proteolytic cleavage of the C terminus from the 212kDa form. Both forms are phosphorylated by cAMP-dependent protein kinase and are present in transverse-tubular membranes. The C-terminal segment however, present in the 212kDa form, contains several of the potential phosphorylation sites and the fraction of this form identified was small. It has been proposed that the two forms may have separate functions, the 212kDa protein having a function in ion conductance, since the proportion of dihydropyridine receptors that function as calcium channels in situ is also small (Schwartz, McCleskey & Almers, 1985) and these are known to be modulated by phosphorylation, while the 175kDa form may perform the other proposed function of dihydropyridine receptors as the voltage-sensor in excitation-contraction coupling.

The primary sequence of the rabbit skeletal muscle α_2 subunit has also been obtained by cloning studies. In contrast to the α_1 subunit, it does not have sequence homology with other known proteins. The protein consists of 1106 amino acids with a calculated molecular weight of 125,018. This differs from the observed molecular weight of 140kD under reducing conditions as determined by SDS gel electrophoresis, which could be due to glycosylation (18 potential sites). There are 3 hydrophobic regions which may represent transmembrane domains although the majority is hydrophilic. If the signal sequence of the α_2 is cleaved where expected and all 3 hydrophobic regions are transmembrane, the amino terminus would be extracellular and the carboxyl terminus intracellular. With this proposed transmembrane topography 8 of the potential N-glycosylation sites would be extracellular. The δ subunit is thought to be encoded by the same gene as the α_2 subunit. The sequences predicted for the various δ subunit components were found to be contained in the C terminal tail of the α_2 sequence (De Jongh, Warner & Catterall, 1990; Jay *et al.*, 1991). Therefore it is proposed that the δ and α_2 subunits come from a single precursor polypeptide which undergoes post-translational proteolytic cleavage (De Jongh, Warner & Catterall, 1990).

The primary sequence of the rabbit skeletal muscle ß subunit (again obtained by cloning studies) is consistent with it being a protein associated with the intracellular side with several potential phosphorylation sites. It is a mainly hydrophilic protein and has no homology with any other known protein (Ruth *et al.*, 1989).

In contrast the primary sequence of the rabbit skeletal muscle γ subunit shows the presence of four transmembrane regions and two potential glycosylation sites. Glycosylation probably accounts for the difference between the observed molecular

weight by SDS gel electrophoresis of 32kDa and the calculated molecular weight of 25,058Da. This protein is not homologous with any other known protein (Bosse *et al.*, 1990).

L-type channels are the predominant type found in the heart. However the proteins that form the cardiac L-type channel have been difficult to purify because they are present in very low amounts in cardiac membranes. At present it appears that cardiac L-type channels are composed of at least two peptides which occur in approximately equal amounts after purification and have molecular weights of 185kDa and 140kDa under reducing conditions (Hosey *et al.*, 1989). Under non-reducing conditions the 140kDa peptide has a molecular weight of 180kDa and appears to be comparable with the α_2 subunit of skeletal muscle (Takahashi & Catterall, 1987; Cooper *et al.*, 1987). Photoaffinity labelling studies have demonstrated that the 185kDa peptide contains the receptors for both the dihydropyridine and phenylalkylamine antagonists (Hosey *et al.*, 1989). This peptide therefore, appears to be comparable with the α_1 subunit seen in skeletal muscle. However the 185kDa peptide was not phosphorylated by cAMP-dependent protein kinase (unlike the α_1 subunit of skeletal muscle). This is surprising since it is well known that L-type channels in cardiac muscle are regulated by cAMP-dependent phosphorylation (see earlier). One possible reason for its apparent lack of ability to serve as a substrate for cAMP-dependent protein kinase is that it may not be in the proper conformation in the detergent solution. Therefore, it cannot be assumed that regulation of L-type channels in cardiac tissue by cAMP-dependent phosphorylation does not occur via the phosphorylation of this peptide. At present only the above two peptides have been identified. However in earlier attempts to purify this channel small peptides were

found (32-60kDa) but these were thought to be due to problems with proteolysis.

The cardiac dihydropyridine receptor from rabbit is composed of 2171 amino acids with a calculated molecular weight of 242,771 (Mikami *et al.*, 1989). The amino acid sequences of the cardiac and skeletal muscle dihydropyridine receptors (α_1 subunit) are 66% homologous. The sequence similarities suggest that this receptor has the same proposed transmembrane topography as that in skeletal muscle. The sequence corresponds to the skeletal muscle α_1 subunit and the α subunit of the voltage-dependent sodium channel in that it contains four homologous domains. Each domain again has 5 hydrophobic transmembrane segments and one positively charged transmembrane segment.

The primary sequences of the dihydropyridine receptors from both smooth muscle and brain have also been deduced (Koch *et al.*,1989; Koch, Ellinor & Schwartz, 1990; Biel *et al.*, 1990). These sequences show around 70% homology with the rabbit skeletal muscle dihydropyridine receptor and share the same proposed transmembrane topography.

In addition, the primary sequence of a voltage-dependent calcium channel from rabbit brain, which is not sensitive to dihydropyridines or to ω-conotoxin, has also been deduced by cloning studies. This channel exists in two isoforms which differ by a 423 nucleotide insert and have calculated molecular weights of 257,337 and 273,217 (Mori *et al.*, 1991). The primary sequences of the skeletal muscle and cardiac dihydropyridine receptors share around 40% homology with this voltage-dependent calcium channel. The sequence similarities again suggest that this calcium channel has the same transmembrane topography as that proposed for the dihydropyridine-sensitive calcium channels from skeletal, cardiac, smooth muscle and brain, with four

homologous domains, each domain again having 5 hydrophobic transmembrane segments and one positively charged transmembrane segment.

The primary sequence similarities between the dihydropyridine-sensitive calcium channels from a number of tissues and the dihydropyridine-insensitive calcium channel from brain has led to the suggestion that the multiple classes of voltage-dependent calcium channels have evolved from a common ancestor. From this ancestral calcium channel two main groups have appeared which show different sensitivities to the dihydropyridines. Further diversity in calcium channels between tissues and within tissues appears to be due to both the expression of distinct genes and alternative splicing of these genes (e.g. Perez-Reyes *et al.*, 1990; Hui *et al.*, 1991; Snutch *et al.*,1991; for review see Tsien, Ellinor & Horne, 1991).

The α_1 subunit of skeletal muscle appears to form the channel. A monoclonal antibody specific for this subunit has been shown to directly inhibit calcium currents in cultured muscle cells (Morton *et al.*, 1988). Furthermore, the homology with the sodium channel suggests that the α_1 subunit is the ion channel pore and possibly the voltage-sensor (Stuhmer *et al.*, 1989). More direct evidence has come from experiments in which the expression of the α_1 subunit has resulted in functional calcium channels. This type of evidence has been produced by a variety of methods. Firstly, in experiments in which the isolated α_1 subunit was reconstituted into artificial lipid bilayers, the channel activity observed was sensitive to voltage, D600, BayK 8644 and cAMP-dependent protein kinase and had a single channel conductance of 20pS (Pelzer, D. *et al.*, 1989). This single channel activity is comparable with that seen for the 20pS channel in purified (Flockerzi *et al.*, 1986) or solubilized (Rosenberg *et al.*, 1986) dihydropyridine-receptor complex preparations (i.e. containing

multiple subunits) and also the L-type channel recorded from cell-attached preparations (Cavalie *et al.*, 1983). Secondly, injection of an expression plasmid that carries cDNA encoding the α_1 subunit of skeletal muscle into cultured muscle cells from dysgenic mice (which lack calcium currents and excitation-contraction coupling) restores both the slow calcium current and excitation-contraction coupling (Tanabe *et al.*, 1988). Similarly, when murine L cells which contained no calcium channels were transfected with a plasmid as above, calcium channels were expressed (Perez-Reyes *et al.*, 1989). Finally, the cardiac α_1 subunit has also been shown to be sufficient to form a functional dihydropyridine-sensitive calcium channel (Mikami *et al.*, 1989). Messenger RNA derived from cardiac α_1 subunit cDNA, injected into Xenopus oocytes gave inward currents which were suppressed by cadmium or nifedipine but which increased in the presence of Bay K 8644.

Less direct evidence for the role of the α_1 subunit within the complex has come from developmental studies. In rat skeletal muscle, the levels of the α_1 subunit are quite low at birth and during the first 10 days, they then rise dramatically until day 20 when they almost reach the levels found in adult muscle (Morton & Froehner, 1989). This rise is consistent with the association of the α_1 subunit with the t-tubule system and a role in excitation-contraction. The t-tubules although present at birth are only rearranged into the transverse orientation 10-15 days after birth (Edge, 1970) at which time there is a decrease in excitation-contraction latency from 6ms to 2.8ms, close to that seen in adult muscle (Chaplin *et al.*, 1970). The increase in level of the subunit also corresponds to the increase in the slow calcium current seen in rat skeletal muscle (Beam, Tanabe & Numa, 1989).

The function of the α_2 subunit has not yet been determined although it has

been found in every dihydropyridine receptor preparation purified. In contrast to the α_1 subunit the α_2 subunit has been found to be present in large amounts in rat skeletal muscle at birth and only increases slightly in adults. This has lead to the suggestion that the α_1 and α_2 subunits may not be part of the same complex in vivo and that their co-purification is a result of association after solubilization (Morton & Froehner, 1989). However another possibility is that the α_2 subunit may associate with other types of functional calcium channels or other proteins, in addition to the dihydropyridine receptor, in possibly a regulatory or structural manner (Morton & Froehner, 1989). One such channel appears to be the N-type channel from mammalian brain (Ahlijanian, Striessnig & Catterall, 1991).

Evidence that the α_2 subunit does have a role in the channel complex has come from studies in which the mRNA specific for the α_2 subunit is co-injected into Xenopus oocytes with mRNA from the cardiac (Mikami *et al.*, 1989; Singer *et al.*, 1991) or smooth muscle (Biel *et al.*, 1990) α_1 subunit. With both subunits present higher calcium channel activity was observed than with only the α_1 subunit present. In addition when the cardiac α_1 subunit was co-expressed with the skeletal muscle α_2 the activation and inactivation rates of the channels increased (Singer *et al.*, 1991). A similar result has been found in a study in which oocytes were co-injected with mRNA specific for a brain calcium channel and with skeletal muscle α_2, ß, or γ subunit specific mRNA (Mori *et al.*, 1991). The calcium channel activity expressed, increased somewhat with either α_2 or ß alone and dramatically with these two in combination. However, the brain calcium channel expressed was a high threshold channel which was dihydropyridine and ω-conotoxin insensitive and these properties did not change with co-expression with any of the other subunits. Neither did the

addition of subunits affect the characteristics of the macroscopic current.

Additional evidence for a role for the α_2 subunit has come from purified preparations where the α_1 subunit was apparently absent. In these preparations the ability to bind dihydropyridines was retained (Borsotto *et al.*, 1984; Curtis & Catterall, 1984; Norman *et al.*, 1987). Also one such preparation, composed of only one major polypeptide with a molecular weight of 150kDa under reducing conditions comparable with α_2, was still found to reconstitute functional voltage-sensitive calcium channels when incorporated into artificial lipid bilayers (McKenna *et al.*, 1987). Furthermore in experiments which investigated the effect of deglycosylation on dihydropyridine binding, it was found that only a small proportion (about 25%) of the dihydropyridine binding sites remained available after enzymatic deglycosylation (Norman, Burgess & Harrison, 1989). The α_2 subunit was reduced in molecular weight by this deglycosylation from 140kDa to 130kDa while the unglycosylated α_1 subunit would not be expected to be affected by deglycosylation. However γ and δ are also glycosylated and so possibly contribute to this effect. Taking into account all of the above evidence it appears that the α_2 subunit may have a more important role in calcium channel structure and function than is recognized at present.

The ß subunit is a substrate not only for cAMP-dependent protein kinase but also for protein kinase C and a protein intrinsic to skeletal muscle triads (Imagawa, Leung & Campbell, 1987; Nastainczyk *et al.*, 1987). It is tightly associated with the α_1 subunit and indeed a monoclonal antibody against the ß subunit activated >10 fold above control levels calcium channels reconstituted into planar lipid bilayers (Vilven *et al.*, 1988). In addition, as mentioned earlier, co-injection into oocytes of mRNA for the ß subunit from skeletal muscle with mRNA specific for a brain calcium channel

increased the level of calcium channel activity observed (Mori *et al.*, 1991). Therefore, it seems that the ß subunit may be involved in regulation of channel activity.

The γ subunit has both extracellular and transmembrane domains. Its properties are similar to those of the $ß_1$ subunit of the sodium channel, which has been suggested to have a role in stabilizing the structure of the main subunit of the sodium channel (Catterall, 1988).

Results on the tissue distribution of the α_1 and α_2 subunits differ. When monoclonal antibodies specific for each of the subunits were used as probes the monoclonal antibody specific for the α_1 subunit could only detect protein in skeletal muscle (Morton & Froehner, 1989), whereas monoclonal antibodies against the α_2 subunit could detect protein in skeletal muscle, brain, heart and lung, and to a lesser extent in kidney, liver and spleen (Morton & Froehner, 1989; Norman *et al.*, 1987). This difference in tissue distribution seen between the α_1 and α_2 subunits could possibly be due to the monoclonal antibody for the α_1 subunit being against a variable region of the protein, since the primary sequence of this subunit is known to vary between tissues (Tanabe *et al.*, 1987; Mikami *et al.*, 1989; Mori *et al.*, 1991; Biel *et al.*, 1990). Using RNA blot analysis of total rabbit RNA from a number of tissues, with skeletal muscle α_1 and α_2 subunit cDNA probes, the α_1 cDNA probe could detect mRNA in skeletal muscle and more weakly in heart and aorta, whereas the α_2 cDNA probe could detect mRNA of a number of tissues including again skeletal muscle, heart, aorta and brain (Ellis *et al.*, 1988). Similarly a cardiac α_1 subunit cDNA probe could detect mRNA of skeletal muscle, heart, brain and stomach, in blot analysis of various rabbit tissues (Mikami *et al.*, 1989). It, therefore, appears that similar subunits

to the α_1 and α_2 are present in a variety of tissues as has been confirmed directly for the α_1 subunit in skeletal muscle, cardiac muscle, smooth muscle and brain (Tanabe *et al.*, 1987; Mikami *et al.*, 1989; Biel *et al.*, 1990; Mori *et al.*, 1991).

The monoclonal antibodies used in these studies were raised against the highly purified α_2 component of the dihydropyridine receptor of skeletal muscle by Dr Norman's group (Norman *et al.*, 1987). Of the 31 antibodies produced, four specifically bound to the denatured 140kDa subunit under reducing conditions (i.e. denatured α_2 subunit). One of the 4 antibodies was used to test for immunocrossreactivity between species. It was found to bind to an α_2 component of skeletal muscle membranes from rabbit, rat, mouse and frog (identified by molecular weight), indicating that the α_2 subunit is similar between species.

There is not only a similarity in size between the α_2 component in different species (Norman *et al.*, 1987) but also in primary sequence (Norman *et al.*, 1987a) and the extent of glycosylation (Burgess & Norman, 1988). The similarity in the primary sequence was suggested because of comparable immunoreactive bands observed between species in immunoblots following limited tryptic digestion. This shows that not only is the primary sequence preserved with respect to the antibody binding sites but also the sites where trypsin cleavage will occur.

Complete deglycosylation of the reduced α_2 subunit of rabbit, rat, and mouse skeletal muscle membranes results in a "core polypeptide" of approximately 105kDa in all cases. This indicates that in each of these species approximately 25% of the total mass of the α_2 subunit is composed of carbohydrate residues (Burgess & Norman, 1988).

In this thesis, the experiments reported in Chapter 3 show the effects of

monoclonal antibodies raised against the α_2 subunit on calcium channel function in cultured mouse neuroblastoma x rat glioma hybrid (NG 108 15) cells. The effects of long term incubation of the cells with the antibody were studied using the whole cell patch clamp technique as well as potassium-stimulated ^{45}calcium flux. Only one antibody showed an effect on the calcium channel currents. This antibody was further tested by applying it directly to the bath during whole cell recording. Some of these results have been previously published (Wray, Phillips, Harrison & Norman, 1989; Harrison, Norman, Phillips & Wray, 1990; Wray, Norman & Phillips, 1990; Phillips, Wilson, Baldwin, Norman & Wray, 1991). One possibility for the lack of effect of most of the antibodies on the NG 108 15 cells may be that there are antigenic differences between the calcium channels in neuroblastoma cells and skeletal muscle t-tubules against which the antibodies were raised. For this reason the effect of the antibodies was further tested on mouse muscle cells (BC_3H1) in which we predicted that the calcium channels would be more similar to those against which the antibodies were raised. The results obtained in these investigations are given in Chapter 4.

Three batches of mAb 11.14 ascitic fluid were used during these experiments. The experiments investigating the effects of mAb 11.14 on the differentiated NG 108 15 cells after both 24 hours incubation and acute application, used one batch. The investigations on the effect of mAb 11.14 in the presence of nitrendipine and the ^{45}calcium flux experiments also on the differentiated NG 108 15 cells used another batch and the final batch was used in the studies on the effect of mAb 11.14 after 24 hours incubation and acute application to the BC_3H1 cells. However, due to the limited supplies of the mAbs, the remainder from each batch was mixed in with the new batch prior to using.

CHAPTER 2

METHODS

I. Preparation of antibody

Monoclonal antibodies were raised against highly purified α_2 subunit of the 1,4-dihydropyridine receptor of skeletal muscle by Dr Norman's group (Norman, Burgess, Allen & Harrison, 1987). A monoclonal antibody against Gyrase B was used as a control. The concentration of each of the antibodies in the ascitic fluid was estimated at approximately 1mg/ml. These antibody preparations were dialysed twice against Hartmann's solution (approx. 3hrs each time) and then overnight against the solution to which they were to be added. They were spun to remove large impurities and then filtered through a sterile 0.22μm filter. For experiments investigating the long term effects of the antibodies on channels, the antibodies were applied to the culture media approximately 24 hours before recording, while for acute application the antibodies were added to the bath during recording. In each case the concentration in the bath was approximately 50μg/ml (approximately 0.3μM).

II. Culture of NG 108 15 cells

Stocks of undifferentiated NG 108 15 cells were kept frozen in liquid nitrogen and retrieved approximately every 2 months. When required the cells were thawed rapidly and transferred to 800ml flasks (Nunclon) with 40ml of growth media. They were grown under humid conditions in a incubator kept at 37°C and ~~10%~~ gassed with 10% CO_2 in air. ~~CO_2~~. The basic media was 88.5% Dulbecco's Modified Eagles Medium (4500mg/l glucose,

Gibco) with 8.8% foetal calf serum (Sera-lab). To this was added 1.8% HAT supplement (0.1mM hypoxanthine, 0.4μM aminopterin and 160μM thymidine, Gibco), 0.9% L-glutamine (Gibco), and penicillin (final conc. 88units/ml) and streptomycin (final conc. 88μg/ml) to prevent microbial infection. The cells were frozen in the above media but with the foetal calf serum content doubled and with 10% dimethylsulphoxide (DMSO, Sigma) also added. New stocks of cells were frozen each time some were retrieved.

The flasks were divided every 3-4 days, as necessary, under sterile conditions, at which time a proportion were plated out. The plates were coated in poly-L-lysine hydrobromide (Sigma) to aid adhesion for 2 hours before plating out the cells. To split the flasks of cells they were ~~spun~~ centrifuged at 1000rpm for 5 minutes and then resuspended in 10ml of fresh media, of which 0.5ml were applied to each 60mm culture dish to give a density of approximately 0.5 million cells per plate. They were either used for recordings 3 or 4 days after plating for undifferentiated cells or in later experiments were differentiated as follows. Cells were plated out in the same way to give a density of 0.5 million cells / 35mm culture dish (Nunclon). Three days after plating, the medium on the dishes was exchanged for a medium containing 10μM prostaglandin E_1 (Sigma), 50μM 3-isobutyl-1-methyl-xanthine (IBMX, Sigma) (Docherty, 1988) and only 1% foetal calf serum. PGE_1 has been shown to cause the intracellular level of cAMP to rise (Hamprecht, 1977), while IBMX is an inhibitor of cAMP phosphodiesterase activity. After differentiation the cells were fed with a 1% foetal calf serum media every 2-3 days. Cells were used for experiments 4-6 days after induction of differentiation.

III. Culture of BC_3H1 cells

The BC_3H1 cells required very similar culture conditions to those described above for NG 108 15 cells. The cells were unfrozen every 2 months and grown in flasks containing 40ml of media. The growth media was Dulbecco's Modified Eagles medium as above, however the glucose concentration was doubled to 9000mg/l. Again 8.8% foetal calf serum, L-glutamine and penicillin and streptomycin were added as above, but omitting HAT. The flasks of cells needed to be divided approximately once a week. The cells adhered strongly to the flasks so 5ml trypsin-EDTA (0.05% trypsin and 0.02% EDTA in special salt solution, Flow) was added to the cells to detach them from the flask. The effect of the trypsin was curtailed by adding a large quantity of the growth media. The cells were removed by gently tapping the flask and spun at 1000rpm for 5 minutes. The media was removed and the cells resuspended in 10ml of fresh media, 0.025ml of which was added to each plate and to this 1ml of growth media. After 4 days the medium was exchanged for fresh medium containing only 0.05% foetal calf serum; this induces differentiation of the cells (Spizz *et al.*, 1986). Every 3-4 days after induction of differentiation the cell medium was changed for fresh 0.05% foetal calf serum medium. The cells were used for electrophysiological recordings 17-20 days after induction of differentiation.

IV. Solutions used for whole cell patch clamp recordings

For the whole cell patch clamp recordings the culture media was removed from the plate of cells and replaced by the extracellular recording solution. This contained in mM: NaCl 130, KCl 3, $MgCl_2$ 0.6, $NaHCO_3$ 1.0, HEPES 10, glucose 4, $BaCl_2$ 10, tetraethylammonium (TEA-Br) 25 and tetrodotoxin (TTX) 2.5μM. The pH was

adjusted to 7.3-7.4 with NaOH and the osmolarity was left unchanged at approximately 335 mosmols (measured value). The solution was filtered with a 0.22μm pore filter to remove any small impurities before being washed over the cells. Approximately 5ml of the recording solution were washed over the cells to allow for complete exchange and finally 1ml was left for recording purposes.

The recording solution used barium as the charge carrier instead of calcium for a number of reasons. Firstly, Ba^{2+} gives larger whole cell L-type (but not T-type) currents than Ca^{2+}, the increase in L-type current being largely due to increased single channel conductance (see Introduction). Also external Ba^{2+} suppresses the K^+ current through delayed rectifier channels which could otherwise obscure Ca^{2+} channel currents (e.g. Hille, 1984). Lastly the use of Ba^{2+} as the charge carrier instead of Ca^{2+} reduces Ca^{2+}-mediated inactivation of the channels (Eckert & Tillotson, 1981). The extracellular solution also contained tetrodotoxin to block inward sodium currents (Quandt & Narahashi,1984) and tetraethylammonium to minimize potassium currents (e.g. Hagiwara & Byerly, 1981).

In experiments where nitrendipine was present in the extracellular solution, it was dissolved in ethanol at a concentration of 2mg/ml. This was diluted to the required concentration (5μM) in the extracellular solution to give only a small final ethanol content of 0.09% v/v. Verapamil hydrochloride (Cordilox, Abbott) was obtained already in solution at a concentration of 2.5mg/ml. This was also diluted in the recording solution to the required concentration. Both the above drugs are light sensitive and so were handled in low intensity light conditions with a sodium lamp. When using these drugs the microscope light was left on for the minimum amount of time possible.

Patch electrodes were filled with a solution containing, in mM: CsCl 140, EGTA 1.1, $MgCl_2$ 2, $CaCl_2$ 0.1 and HEPES 10, pH adjusted to 7.3 with CsOH and osmolarity to 310 mosmols with sucrose. In this solution, which forms the intracellular solution, Cs^+ replaces K^+ as the major cation in order to further minimise currents through K^+ channels (Hagiwara & Byerly, 1981). EGTA was present to buffer Ca^{2+} to a low concentration, pCa approximately 8 (Dolphin & Scott, 1987). Electrodes were used which had a resistance of 3-8 MΩ when filled with this solution. The electrodes were filled with the solution after it had been filtered with a 0.22μm pore filter to remove any small particles.

In some of the experiments which involved long term recording from the NG 108 15 cells, other substituents were added to the pipette solution to prevent rundown (see Introduction). These were: disodium creatine phosphate 20mM, creatine phosphokinase 50U/ml and adenosine 5'-triphosphate (ATP, magnesium salt) 5mM. The measured osmolarity with the addition of these substances was 323mosm.

V. Patch electrode preparation

Patch electrodes were pulled using a Kopf 720 electrode puller by a 2 stage process using thin-walled fibre-fill electrode glass (Clark's GC 150TF-15,external diameter 1.5mm). They were coated with Sylgard resin which thickens the walls and so reduces the electrode capacitance, as follows. The electrode was mounted on a micromanipulator under a microscope with a heated coil of nichrome wire also in view. Sylgard was applied to the electrode over the pulled part near to the tip. The electrode was then moved into the coil to cure the Sylgard. Electrodes were not fire-polished as this was found to be of no advantage. The electrodes were back-filled with

filtered solution just prior to being used (Hamill *et al.*, 1981).

VI. Whole cell recordings

Two sets of experimental equipment were used for these experiments; containing either an Axoclamp-2 or Axopatch-1C amplifier. All tests and corresponding controls were done on the same set-up. The filled patch electrode was connected to the headstage of the amplifier via a AgCl coated Ag wire contained in the electrode holder. The holder had a sidearm to which was attached silicone tubing and a 3-way tap, which allowed negative pressure to be applied by mouth to the inside of the electrode. The current and voltage outputs were connected to D.C.-coupled oscilloscope amplifiers (Tektronix 5A22N, 5A21N) to display signals recorded by the patch electrode. The signals were fed into two channels of an FM tape recorder (Racal 4DS, 7.5 inches/sec tape speed). The current signal was also followed on a chart recorder (Gould BS-272) at a chart speed of 20mm/min in order to monitor changes in holding current. The current signal was low-pass filtered at 1kHz by the Axoclamp and 2.5kHz by the tape recorder for the Axopatch. All experiments were performed at room temperature, 22-24°C.

For experiments with the Axoclamp the plate of cells containing 1ml of the extracellular solution were mounted on the microscope (Zeiss, X400 magnification). In the "Bridge" mode of the amplifier the resistance of the electrode was checked by applying a hyperpolarising current pulse of 0.1nA (20msec duration, 2Hz frequency) and backing off the resulting voltage step using the calibrated bridge balance control. This allowed the electrode resistance to be read off directly. Electrodes were used which had resistances between 3-8MΩ. Cells were selected which were isolated from

all others and with as small processes as possible. The electrode was advanced towards the cell with first a coarse manipulator (Prior) and then using a 3-plane hydraulic micromanipulator (Narishige MO-103M) until it just touched the surface of the cell. During this procedure 0.1nA pulses (20msec duration, 2Hz frequency) were passed so that when the electrode touched the cell membrane this was seen on the oscilloscope as an increase in the voltage step response to the pulse, i.e an increase in resistance. Very gentle suction was applied which caused the formation of a high resistance seal between the electrode and cell membrane. The mode of the amplifier was then changed into 'direct current clamp'. This uses a sample and hold circuit which enables the voltage at the tip to be sampled and stored in between each current step. The voltage response was followed on a monitor while passing repetitive 0.1nA current pulses (50msec duration, 2Hz frequency). The capacitance neutralization was changed until the voltage response decayed most rapidly to a horizontal baseline. This compensates for the electrode capacitance.

If the seal between the cell and the electrode reached larger than 1GΩ a greater suction was applied which ruptured the sealed area of the membrane. The process of going into whole cell mode was followed on the oscilloscope. A change was seen in the voltage response from a near square pulse, in response to the current pulse, to a slow time course response due to the charging up of the cell membrane.

To measure cell capacitance, a series of hyperpolarising current pulses (0.1nA, 300msec duration, 0.5Hz frequency) were applied and the corresponding voltage changes were recorded, allowing the capacitance of the cell to be calculated (see below) which is proportional to the cell membrane area. It was important that the voltage response had reached a plateau, and therefore the duration of the current pulse

needed to be varied from cell to cell.

The amplifier was then switched into discontinuous single voltage clamp mode. The voltage clamp gain was increased so that the observed membrane potential followed the command potential as well as possible (within 97%).

The membrane potential was firstly clamped at -80mV and 200ms duration voltage steps were applied. Firstly, 20 small hyperpolarising (10mV) steps were applied at a frequency of 0.5Hz. These steps were for capacitance and leak subtraction. The stimulation frequency was then switched to 0.1Hz and hyperpolarising steps of 30mV, 20mV, and 10mV were applied, followed by depolarising steps in 10mV increments from 10-140mV. The cell membrane was then held at -40mV and 20 hyperpolarising steps (10mV) again applied. This was then followed by hyperpolarising steps of 50mV, 40mV, 30mV, 20mV, and 10mV, and depolarizing steps from 10-100mV. In the experiments in which the effect of holding potential was investigated, similar hyperpolarising steps and depolarising steps up to a test membrane potential of +60mV were applied in each case.

In the experiments where the Axopatch-1C amplifier was used, the plate of cells containing 1ml of the extracellular solution were placed on the stage of an inverted phase-contrast microscope (Nikon TMS, x200 magnification). In voltage clamp mode, the resistance of the electrode was checked by applying a voltage pulse of -1mV (20msec duration, 2Hz frequency) and calculating the resistance from the resulting current. Electrodes were used which had resistances between 3-8MΩ, as above. Cells were also selected with the same criteria as above. The electrode was advanced towards the cell with first the coarse manipulator (Narishige MN-3) and then using a 3-plane hydraulic micromanipulator (Narishige MO-203) until it just touched

the surface of the cell. During this procedure 1mV hyperpolarising pulses (20msec duration, 2Hz frequency) were passed so that when the electrode touched the cell membrane this was seen on the oscilloscope as a decrease in the current step response to the pulse, i.e an increase in resistance. The hyperpolarising voltage pulse was increased to 10mV (20msec, 2Hz) and very gentle suction was applied which caused the formation of a high resistance seal between the electrode and cell membrane. If this seal between the cell and the electrode reached larger than 1GΩ (usually approx. 5GΩ) a greater suction was applied or alternatively the "zap" on the Axopatch was used, which ruptured the sealed area of the membrane. "Zap" works by applying a large voltage (1.5V D.C) to the patch for a duration that can be varied but usually 0.1 msec was sufficient. The process of going into whole cell mode could be followed on the oscilloscope. A change was seen in the current response from a square pulse, in response to the voltage pulse, to a form which shows capacitance spikes at the start and finish due to the charging up of the cell membrane.

The mode of the amplifier was then changed into current clamp. For cell membrane capacitance calculation 0.1nA (approx.300msec duration, 0.5Hz frequency) hyperpolarising pulses were applied. This gave a voltage response which corresponds to the charging up of the whole cell membrane. Around 15 such voltage steps were again recorded as for the Axoclamp.

The amplifier was then returned to voltage clamp mode. The cell membrane potential was clamped at -80mV and 200ms voltage steps were applied. The pulse protocol was as for the Axoclamp, detailed above. The holding potential was then changed to -40mV and the protocol followed again as for the Axoclamp.

In the case of the acute studies, after having recorded the above, 70mV

Experiments investigating the effects of test mAbs 11.3 and 11.6 on the undifferentiated NG 108 15 cells, and 10 recordings from mAb 11.14 and control treated differentiated NG 108 15 cells, were made using the Axoclamp-2 amplifier. Also experiments investigating the effect of holding potential on the whole cell calcium channel currents recorded from the differentiated NG 108 15 cells were obtained using the Axoclamp-2 amplifier. All other recordings were made with the Axopatch-1C as the amplifier.

depolarizing pulses were applied repetitively at 0.1Hz for a duration of 200ms. When the current responses to these pulses had reached a roughly constant level the antibody was applied. Antibody was added using a Gilson pipette which was refilled and dispersed several times to aid diffusion. The voltage pulses of 70 mV continued to be applied until the cell was no longer attached. If the current required to hold the cell at -80 ~~or -40mV~~ altered by more than 0.03nA during the experiment, the recording was rejected. In the acute studies, the holding current showed a small jump (approximately 0.03nA) when the antibody was applied, however as this occurred in both control and test cells this was ignored.

In the case of the BC_3H1 cells only a holding potential of -80mV was used. The pulse protocol was the same as for the NG 108 15 cells. However as the current in the BC_3H1 cells is slowly activating the step duration was increased to 300ms. In the acute studies the protocol was altered slightly, depolarizing pulses of 90mV were applied. The antibody was added in the same way although after 10 minutes the continuous pulses were stopped and the original protocol repeated. When complete the cell was again stimulated repetitively at +10mV until an indication that the cell was no longer attached was seen.

VII. Analysis of whole cell recordings

All data was stored on magnetic tape and analyzed later by computer, either an Opus PC V turbo with CED 1401 and Pascal programs, or with equivalent Fortran programs on a Minicomputer (Computer Automation). Both the current and voltage were replayed from the tape recorder, digitized at 5kHz and stored on the hard disc. A cursor was set on either side of the voltage trace to a position corresponding to half

the amplitude of a 10mV step. The computer searched the stored data to find each voltage pulse (i.e. where the cursors were crossed) and corresponding current response, and displayed these on an oscilloscope. For the voltage pulse, the baseline was found by averaging 500 data points, i.e. 100 ms, before the pulse for the NG 108 15 cells and 250 data points (50ms) for the BC_3H1 cells. The total pulse length was measured and the average of the middle third of the voltage pulse taken to obtain the plateau value. The pulse amplitude was calculated from the difference between the baseline and plateau value during each pulse. The voltage pulses for the small 10mV hyperpolarising steps, were measured as above and averaged. All the points in the digitized current traces corresponding to these voltage pulses were also averaged. This averaged pulse was inverted and scaled up appropriately for the larger depolarising pulses, which activated Ca^{2+} channel currents and was subtracted from the original current trace. This results in subtraction of both "leakage" and capacitance currents. Leakage current is the passive cell membrane current seen during the application of voltage pulses. Capacitance transients appeared at the beginning and end of current responses to pulses due to the charging up of the cell membrane and possibly electrode walls, although this could be compensated for during recording and was reduced by Sylgarding electrodes.

For the depolarising test pulses the voltage steps were again measured as above. Cursors were displayed through the baseline and plateau to allow the measurements to be checked by eye. For the current trace (after leak and capacitance subtraction as above) the baseline value was again found before the pulse, by averaging 100ms for NG 108 15 cells and 50ms for BC_3H1 cells. Horizontal cursors were also displayed on the sustained plateau value, found using an average of 50 data

points, 10ms, near the end of the pulse, and on the maximum current value. The maximum current value was found by averaging 10 points, 2ms, around the maximum point to smooth out the noise. A vertical cursor was positioned at the maximum point enabling a visual check of the time to peak of the current, which was also calculated. If no current was present the time to peak could be set to zero to be ignored in later calculations. All cursors could be changed if necessary after visual checks.

Measurements were taken of the sustained inward current amplitude (I_{sus}), the maximum inward current amplitude (I_{peak}) and time to peak amplitude of inward current (TTP). From these a further current value of the difference (I_{diff}) between maximum current and sustained current at each test potential was obtained. Knowing the holding potential (V_{hold}) and using the calculated value of the amplitude of the voltage pulse (V_{pulse}), the test potential (V_{test}) was obtained. Current-voltage curves were plotted for each of the current variables versus test potential for every cell analyzed. The above results were stored on a file for later analysis.

When analyzing an acute recording the method of finding and measuring the voltage pulses and current responses was the same. The initial I-V curve was first obtained as above. Repetitive pulses of 70mV/90mV were then viewed. When the first 70mV/90mV voltage pulse was found and accepted, timing was started (this pulse was taken as time zero). Once time zero was defined, the timings of the other pulses were calculated (from no. of points and digitization rate). The time after starting repetitive 70mV/90mV pulses to adding the antibody was also recorded. From these values a time course graph was plotted for each of the current variables (I_{peak}, I_{sus} and I_{diff}) and also for the time to peak amplitude.

VIII. Analysis of capacitance recordings

Recordings were made, as detailed above, of voltage changes due to current steps for calculation of cell capacitance. Recordings were digitized and stored on the hard disc as for the whole cell data above. A cursor was set under the current recording baseline and the data searched until a current pulse crossed this cursor. The data found was displayed on the oscilloscope and the current pulse amplitude (I) calculated from the difference between the baseline (average of 50ms) and plateau (average of 20ms). The baseline of the voltage trace was again an average of 50ms before the pulse and the plateau of the voltage trace was an average of 20ms taken just before the end of the pulse at a point where it had always plateaued and hence the voltage pulse amplitude (V) was obtained. Cursors were displayed on both the baseline and plateau to allow verification by eye. From these values the cell resistance was calculated (V/I). The rising phase of the current was fitted to an exponential as follows. Natural logarithms of all the values of the difference between the baseline value and the data points between 25% and 75% of the maximum voltage were calculated. The values were plotted versus time (the data points are 0.2ms apart) and a line was fitted to the data by linear regression. The time constant, τ, was calculated from the gradient (τ = 1/gradient) obtained above and divided by the cell resistance to give a value of the cell capacitance.

IX. Presentation of Data

The results for each set of experiments on the control Ab or test Ab were averaged over the cells recorded from for each test potential, and graphs of current versus test voltage plotted. Also each of the current values for every cell were divided

by the cell capacitance for the particular cell. These "capacitance adjusted" values were also averaged for each test potential and graphs plotted as above. The controls and tests were compared using a two-tailed Student's t-test at each test potential with the significance level set at $p<0.05$.

In addition, current-voltage (I-V) curves were plotted for individual cells and from these the test potential at which the maximum inward current occurred found. These potentials were averaged for both the control and test antibody treated cells and also compared using a two-tailed Student's t-test.

In experiments where the antibody was applied acutely, values for the measured parameters were averaged over 1 minute intervals for each separate cell. The values obtained over the minute intervals were then averaged for a number of cells where either the control or test monoclonal antibody was added. Graphs were plotted versus time for each of the measured parameters. Values for control and test monoclonal antibody treated cells were compared over each minute interval using the two-tailed Student's t-test, as above.

X. ^{45}Calcium-flux Experiments

i. Preparation of cells

Ten plates of NG 108 15 cells were plated out for each test condition. The cells were plated out to the same density as in the above experiments and differentiated by the same method. Antibody was applied to the cells approximately 24 hours prior to the experiment.

ii. Solutions for $^{45}Ca^{2+}$-flux

Stimulated flux was taken as a measure of the difference between unstimulated $^{45}Ca^{2+}$-flux and high-potassium-stimulated flux. Unstimulated flux was measured in HEPES-Locke buffer, a solution containing, in mM: 144 NaCl, 2.7 KCl, 1.8 $CaCl_2$, 1.8 $MgCl_2$, 5 glucose and 10 HEPES (pH 7.2). High potassium solution contained, in mM: 144 KCl, 2.7 NaCl, 1.8 $CaCl_2$, 1.8 $MgCl_2$, 5 glucose and 10 HEPES (pH 7.2). $^{45}CaCl_2$ (Amersham) was added to the buffers at an activity of 0.75μCi/ml (stock solution 74MBq/ml) and mixed thoroughly. In experiments where the effect of verapamil hydrochloride was tested it was kept in the dark until just prior to fluxing and then added to the buffers and mixed in natural light but out of direct sunlight.

iii. Flux experiments

The ten plates required for each test were used at the same time (5 unstimulated and 5 stimulated). The culture media was removed from each plate and the cells washed once with phosphate buffered saline and then exposed to the normal or high potassium solution for 1 minute exactly. The plates were then washed 3 times with phosphate buffered saline before 0.5ml (0.5%) Triton X-100 was added to solubilize the cell membranes. After 20-30 minutes the contents of each plate were transferred to a scintillation vial. To this was added 7ml of a scintillation fluid. The vials were mixed thoroughly and counted in a ß-counter (LKB, 1219 Rackbeta). 100μl of normal solution and 100μl of high potassium solution were also counted; these acted as the standards for total counts.

iv. Analysis of flux results

Means of counts per minute were taken of both the unstimulated and stimulated results. The counts per minute for the standards were multiplied by 10 to allow for the fact that this is a count rate for 100µl rather than 1ml. The mean of counts for the unstimulated or stimulated cells was multiplied by the number of moles of calcium present in 1ml of the buffer and divided by the counts per minute of the appropriate standard (adjusted to counts per minute/ml). The results were expressed in nmols of calcium flux. The value of unstimulated flux was subtracted from stimulated to give the total K^+-stimulated flux in moles Ca^{2+}/plate of cells (i.e. 0.5 million).

v. Presentation of results

The values of K^+-stimulated Ca^{2+} flux for each of the experimental repeats were averaged for each of the antibodies. The means and standard errors were plotted on bar graphs. Values of stimulated flux for control and test monoclonal antibody treated cells were compared using the two-tailed Student's t-test.

CHAPTER 3

EFFECT OF MONOCLONAL ANTIBODIES ON CALCIUM CHANNELS IN MOUSE NEUROBLASTOMA X RAT GLIOMA HYBRID (NG 108 15) CELLS

I. Introduction

The α_1 subunit is thought to contain the ion channel pore and also a dihydropyridine binding site (see Introduction). However a role for the α_2 subunit within the channel complex is unclear. For instance, the α_2 subunit may weakly associate with the α_1 during purification although not forming part of the channel complex (Morton & Froehner, 1989). Experiments described here were carried out to investigate the functional role, if any, of the α_2 subunit. A range of monoclonal antibodies raised against this subunit were used as probes and applied to NG 108 15 (neuroblastoma x glioma) cells.

An effect of these antibodies on the functioning of calcium channels was tested using the whole cell patch clamp recording technique with barium as charge carrier (see Methods). Antibodies were applied either for 24 hours or acutely.

Experiments were also carried out to investigate the effects of the antibodies on calcium channels in the same cells by using measurements of potassium-stimulated ^{45}calcium flux (see Methods).

II. Effects of monoclonal antibodies on whole cell calcium channel currents in undifferentiated NG 108 15 cells

Two monoclonal antibody preparations (and controls) were tested for their

effect on the whole cell currents in undifferentiated NG 108 15 cells. The cells were incubated for 24 hours at 37°C with each antibody preparation and electrophysiological recordings made at 22-24°C (see Methods).

Examples of the calcium channel currents evoked from these undifferentiated cells are shown in figure 3.1A. The measured parameters of the currents (I_{sus}, I_{peak} and TTP, see Methods) are shown in figure 3.1B. In most cells held at -80mV, there was only evidence for a single transient component, although rarely there was also a small sustained component. The transient component was clearly seen with small depolarizing steps, for example to -30mV. This current decayed fully within the 200ms test pulse and at these small depolarizing steps is probably due to activation of T-type channels. For larger depolarizing steps (for example to 0mV) a sustained component (presumably L-type) was only seen in a small number of cells (12 out of 63).

For the first antibody tested (mAb 11.3), the current-voltage (I-V) curve for the peak current (I_{peak}) is shown in figure 3.2. The cells were held at a membrane potential of -80mV. The currents plotted are the means from 15 cells in the case of controls and 17 cells in the case of mAb 11.3. There were no significant differences between the peak inward current in control mAb treated cells compared with the mAb 11.3 treated cells. The potential at which the maximum peak inward current occurred for the control cells was -16.3 ± 0.3mV (n=15) which was not significantly different from the mAb 11.3 treated cells (-15.6 ± 2.9mV; n=17). As mentioned above, the sustained component was either absent or small, and furthermore at more positive test potentials was totally obscured by outward currents. Figure 3.3 shows the I-V curve for this sustained component measured at a holding potential of -80mV from the same cells.

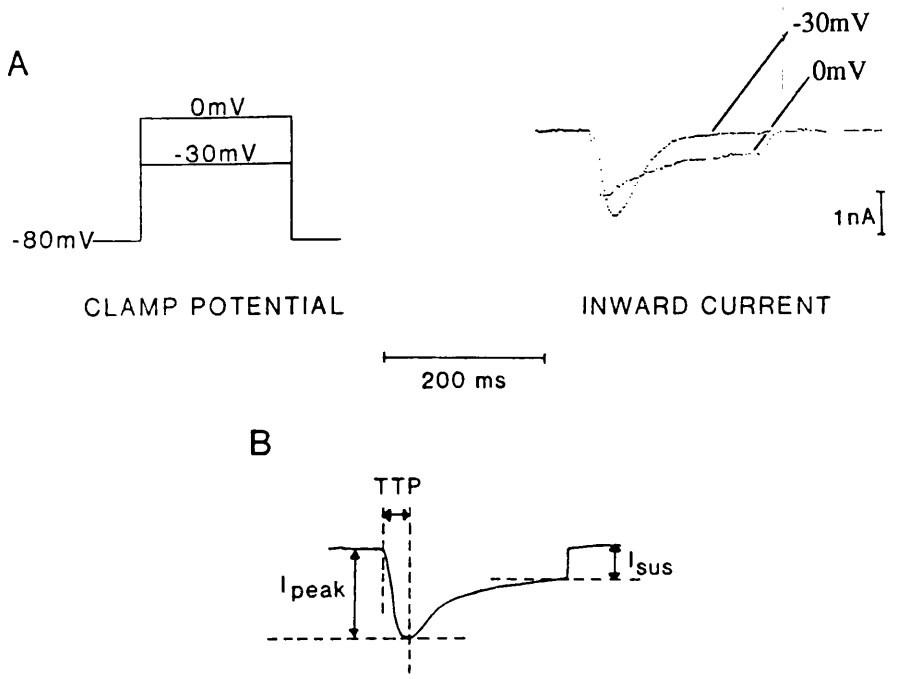

Legend for Figure 3.1

A. Examples of whole cell calcium channel currents in an undifferentiated NG 108 15 cell.

Calcium channel currents evoked in undifferentiated NG 108 15 cells. Currents were evoked in a control mAb treated cell in response to 200ms test depolarisations. Current traces (right) were evoked at different test potentials (left). Leakage and capacitance currents have been subtracted.

B. Parameters measured from whole cell current recordings.

Idealised diagram of calcium channel current illustrating the current parameters measured: I_{sus}, I_{peak} and time to peak (TTP).

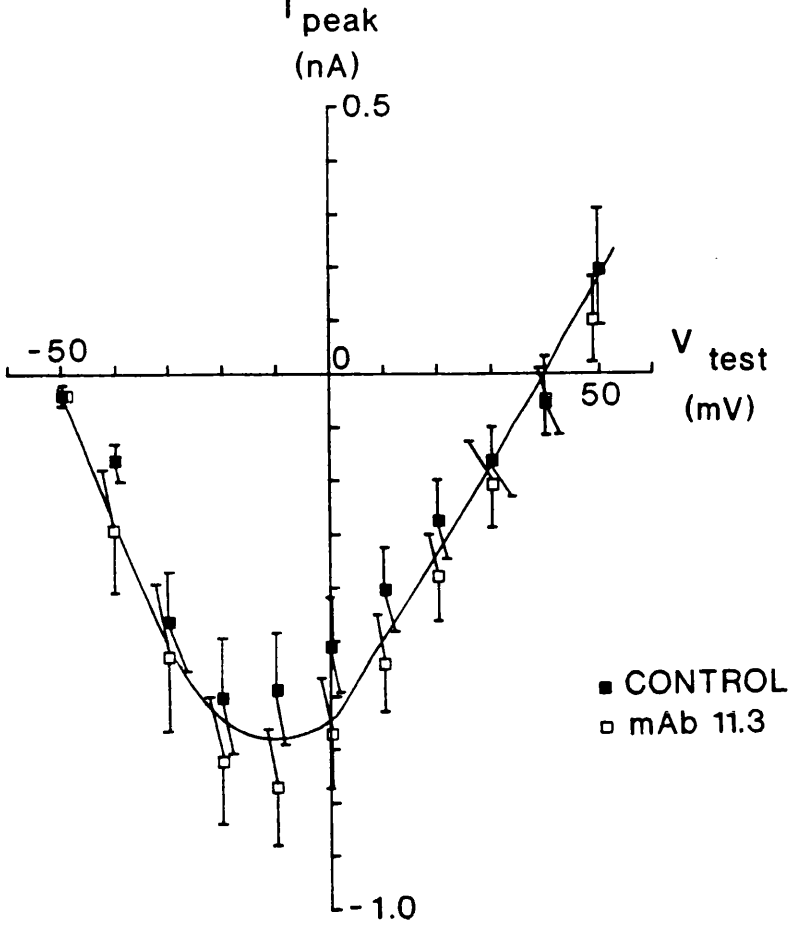

Legend for Figure 3.2 Effect of mAb 11.3 on peak current.

This figure shows the peak inward calcium channel current amplitude (I_{peak}) plotted versus test membrane potential (V_{test}) in control (■) and monoclonal antibody 11.3 (□) treated undifferentiated NG 108 15 cells. All currents were evoked from a membrane holding potential of -80mV. The values plotted are the means ± standard error of the means (one value per cell at each test potential) from 15 control and 17 test treated cells. Potentials at which each current value is plotted are also mean values and the standard errors were always so small that they were covered by the symbol in this and all subsequent figures. Monoclonal antibody 11.3 had no significant effect on peak current amplitude at any test potential studied, therefore one curve has been fitted (by eye) through all data points.

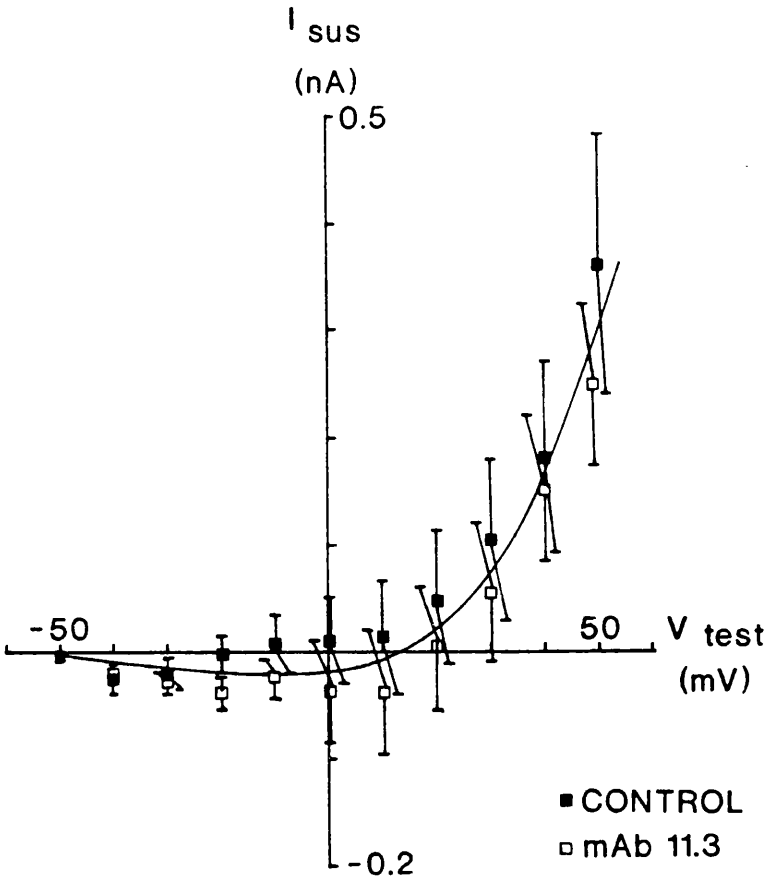

Legend for Figure 3.3 Effect of mAb 11.3 on sustained current.

This figure shows the sustained inward calcium channel current amplitude (I_{sus}) plotted versus test membrane potential (V_{test}) in control (■) and monoclonal antibody 11.3 (□) treated undifferentiated NG 108 15 cells. All currents were evoked from a membrane holding potential of -80mV. The values plotted are the means ± standard error of the means from 15 control and 17 test treated cells. Monoclonal antibody 11.3 had no significant effect on sustained current amplitude at any test potential studied, therefore one curve has been fitted by eye through all data points. Recordings used to construct this figure were the same as those for figure 3.2.

Again the antibody had no significant effect.

Figure 3.4 shows the time to peak of the inward current plotted versus test potential again at -80mV holding potential. The rise time was voltage dependent in both the control and mAb 11.3 treated cells. There were no significant differences between the time to peak inward current between the control antibody treated cells as compared with the test mAb treated cells at any test potential.

Another monoclonal antibody (mAb 11.6) again raised against the α_2 subunit was also tested for its effects on the whole cell calcium channel currents present in undifferentiated NG 108 15 cells. Figure 3.5 shows the I-V curve for the peak current evoked from cells held at a membrane potential of -80mV. The currents plotted are the means from 16 control antibody treated cells and 15 cells incubated with mAb 11.6. There were no significant differences between the peak inward current in mAb 11.6 treated cells compared with the controls. There was also no significant difference between the test potentials at which the peak inward currents were maximal between the control treated cells (-17.5 ± 1.9mV; n=16) and the mAb 11.6 treated cells (-15.6 ± 3.6; n=15).

Sustained components were again small, absent, or even outward at positive potentials (Figure 3.6) and mAb 11.6 again had no significant effect (holding potential of -80mV) in these cells.

Figure 3.7 shows the time to peak of the inward current plotted versus test potential for the same cells at a holding potential of -80mV. There were no significant differences between the mAb 11.6 treated cells as compared with the control antibody treated cells at any test potential.

It therefore appears that neither mAb 11.3 nor mAb 11.6 had any effect on the

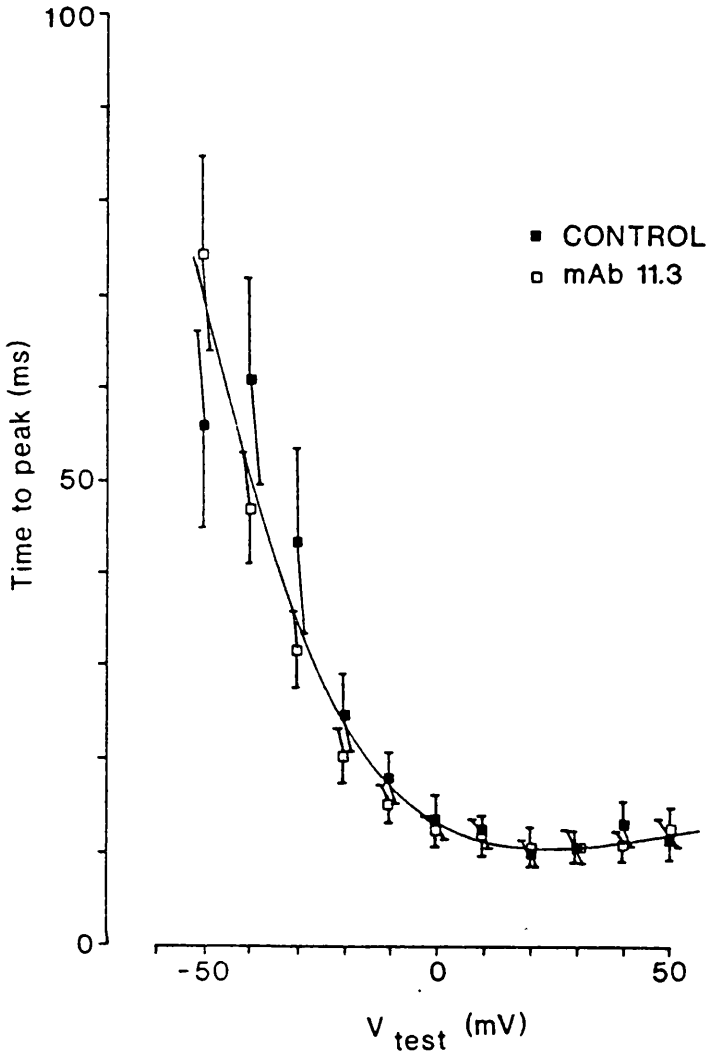

Legend for Figure 3.4 Effect of mAb 11.3 on time to peak inward current.

Plot of time to peak of inward calcium channel currents versus test membrane potential (V_{test}). Currents were evoked from a holding potential of -80mV. Values plotted are means ± S.E.M from 15 control (■) and 17 monoclonal antibody 11.3 (□) treated undifferentiated NG 108 15 cells. Monoclonal antibody 11.3 had no significant effect on times to peak at any test potential studied, therefore one curve has been fitted by eye through all data points. Data were obtained from the same recordings as in figures 3.2 and 3.3.

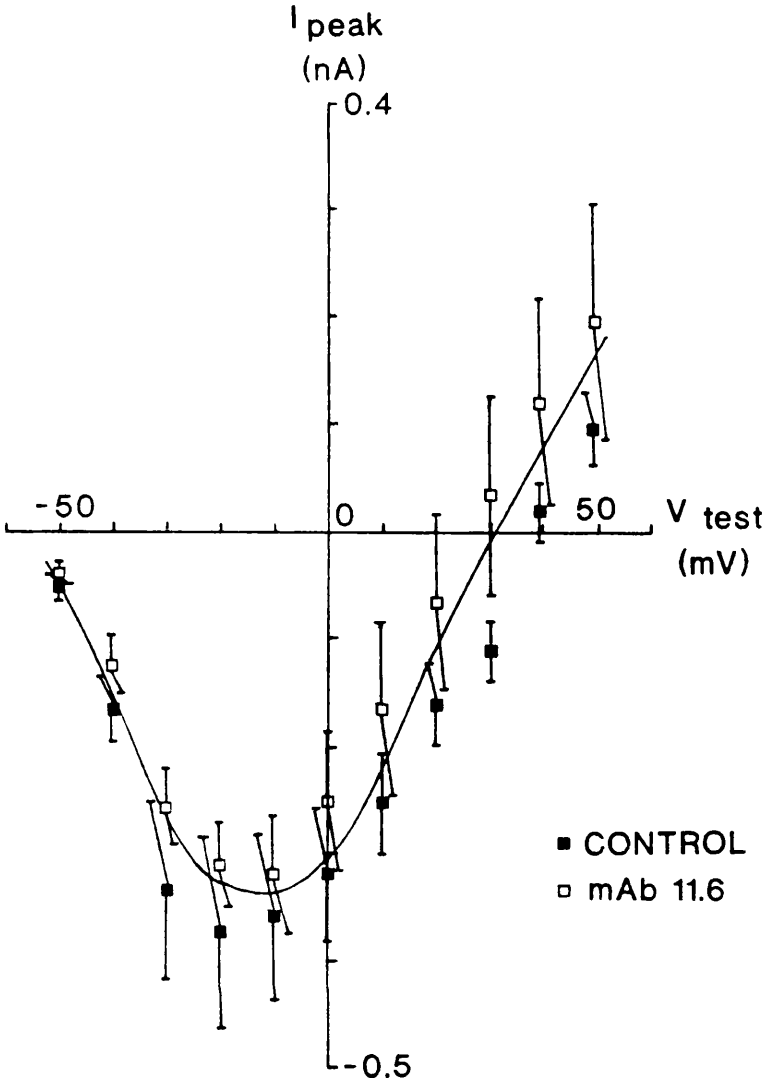

Legend for Figure 3.5 Effect of mAb 11.6 on peak current.

This figure shows the peak inward calcium channel current amplitude (I_{peak}) plotted versus test membrane potential (V_{test}) in control (■) and monoclonal antibody 11.6 (□) treated undifferentiated NG 108 15 cells. All currents were evoked from a membrane holding potential of -80mV. The values plotted are means ± S.E.M from 16 control and 15 monoclonal antibody 11.6 treated cells. Monoclonal antibody 11.6 had no significant effect on peak current amplitude at any test potential studied, therefore one curve has been fitted by eye through all data points.

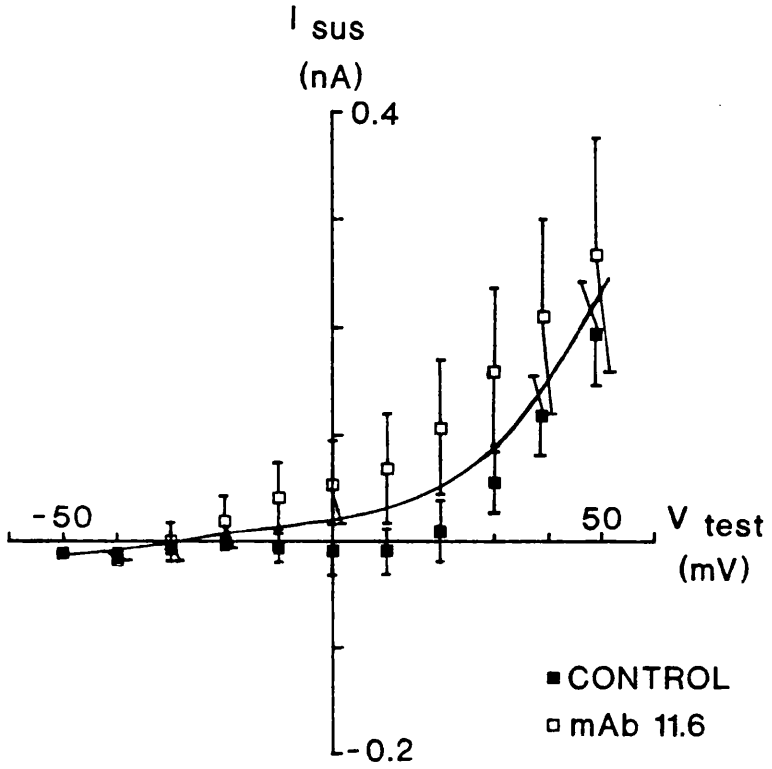

Legend for Figure 3.6 Effect of mAb 11.6 on sustained current.

This figure shows the sustained inward calcium channel current amplitude (I_{sus}) plotted versus test membrane potential (V_{test}) in control (■) and monoclonal antibody 11.6 (□) treated undifferentiated NG 108 15 cells. All currents were evoked from a membrane holding potential of -80mV. The values plotted are means ± S.E.M from 16 control and 15 test treated cells. Monoclonal antibody 11.6 had no significant effect on sustained current amplitude compared with controls at any test potential studied, therefore one curve has been fitted by eye through all data points. Recordings used to construct this figure were the same as those for figure 3.5.

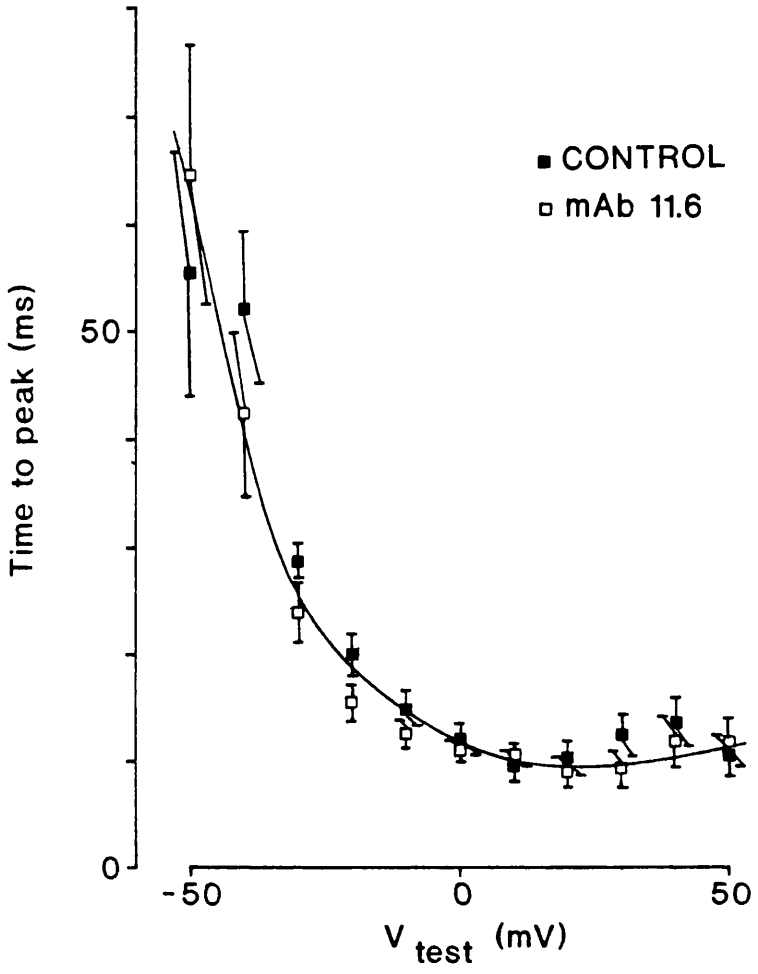

Legend for Figure 3.7 Effect of mAb 11.6 on time to peak current.

Plot of time to peak of inward calcium channel currents versus test membrane potential (V_{test}). Currents were evoked from a holding potential of -80mV. Values plotted are means ± S.E.M from 16 control (■) and 15 monoclonal antibody 11.6 (□) treated undifferentiated NG 108 15 cells. Monoclonal antibody 11.6 had no significant effect on times to peak at any test potential studied, therefore one curve has been fitted by eye through all data points. Data were obtained from the same recordings as in figures 3.5 and 3.6.

T-type calcium channel currents in these cells. On the other hand any effect on L-type currents was unclear since L-type sustained currents were small or absent in these undifferentiated cells. Therefore, all cells in the remaining experiments were differentiated in order to increase the size of the currents.

III. Effect of holding potential on whole cell calcium channel currents in differentiated NG 108 15 cells

Before going on to test effects of antibodies in differentiated NG 108 15 cells the types of calcium channel present were investigated. For this, whole cell currents were recorded at various holding potentials. This also gives an indication of the most appropriate holding potentials to use in subsequent experiments.

Examples of the calcium channel currents evoked from differentiated NG 108 15 cells are shown in figure 3.8. In these cells at least two components of current were seen when the cell membrane potential was held at -80mV. With small depolarizing steps, for example to -30mV, a transient component of current was seen as in the undifferentiated cells. This current again decayed fully within the 200ms test pulse. With larger depolarizing steps, for example to 0mV, a sustained current component was also seen. This sustained component was present in most of the differentiated cells and was larger than that for undifferentiated cells. At a holding potential of -40mV only the sustained component of current was present.

Figure 3.9 shows the I-V curves for the sustained currents (i.e. not including the transient T-type) measured at the various holding potentials studied (-80,-60,-40, -30mV). The sustained current decreased somewhat in magnitude with more depolarized holding potentials (see Figure 3.10A), indicating that it was partially

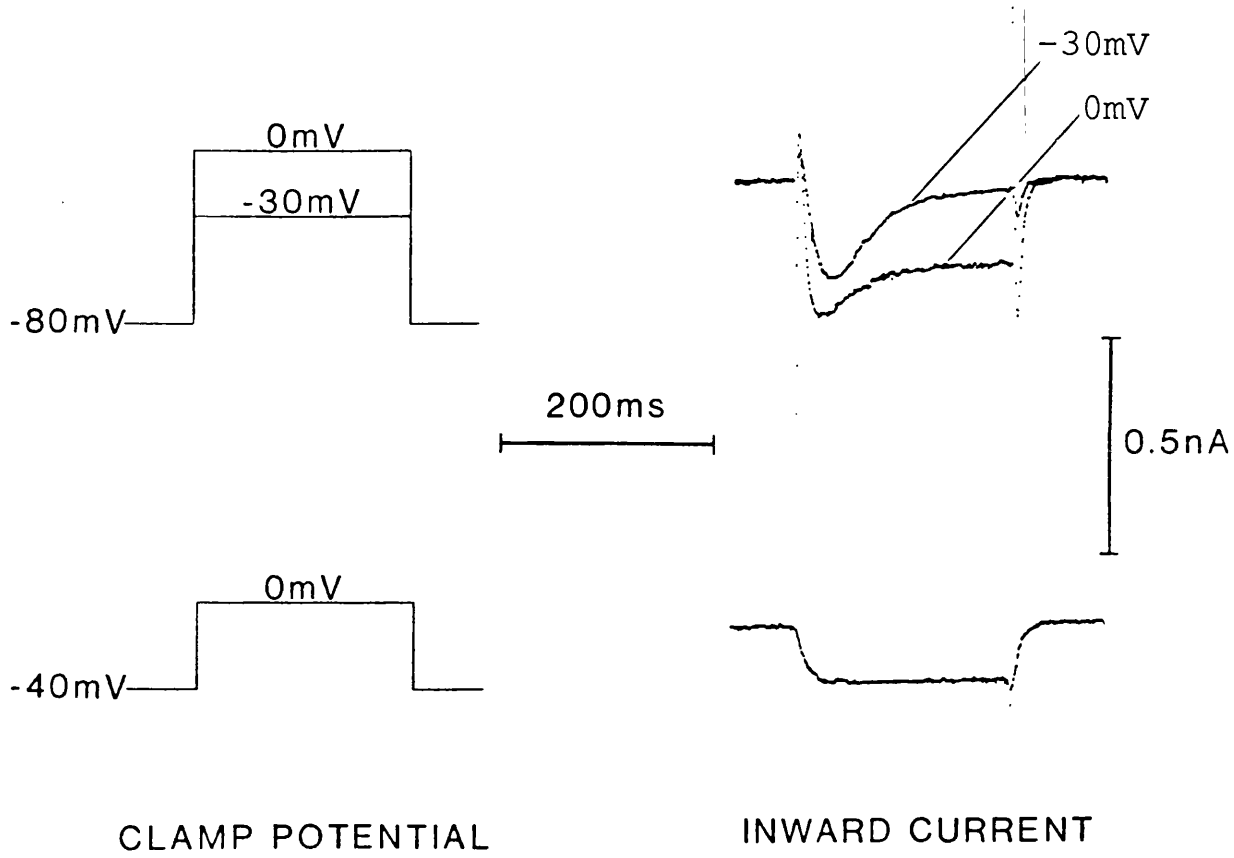

Legend for Figure 3.8 Examples of whole cell calcium channel currents in a differentiated NG 108 15 cell.

Calcium channel currents evoked in an untreated, differentiated NG 108 15 cell in response to 200ms test depolarisation. Current traces (right) were evoked at different clamp potentials (left). Leakage and capacitance currents have been subtracted.

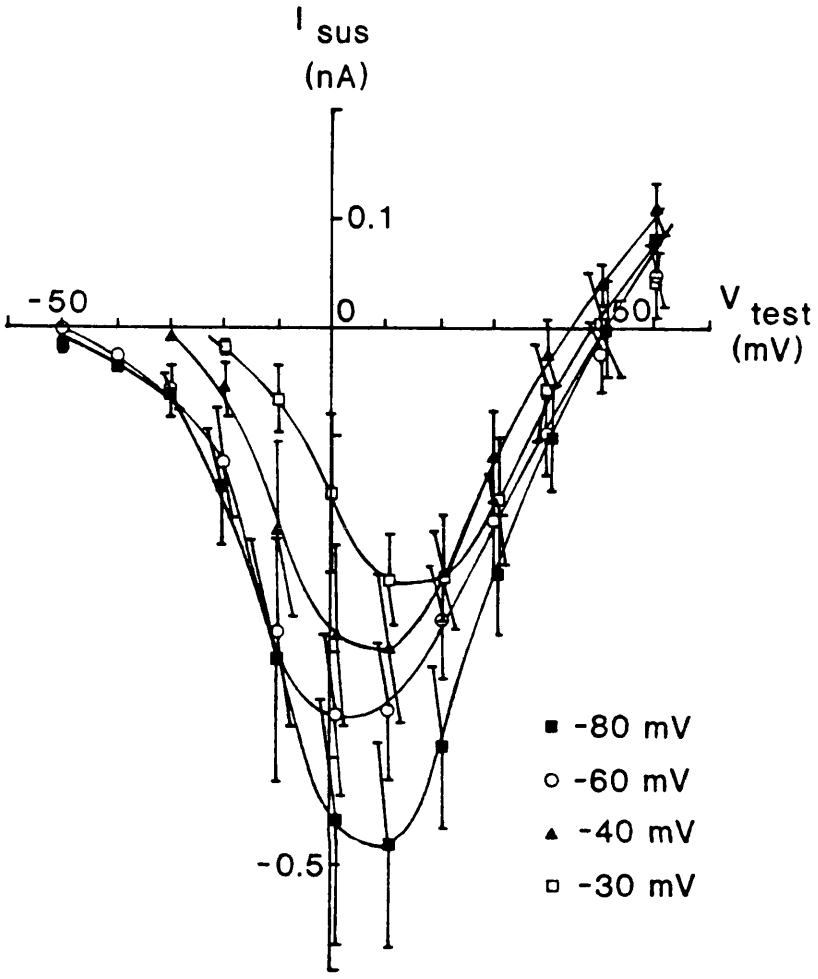

Legend for Figure 3.9 Effect of holding potential on sustained currents.

This figure shows the sustained inward calcium channel current amplitude (I_{sus}) plotted versus test membrane potential (V_{test}), measured in untreated differentiated NG 108 15 cells, held at various membrane holding potentials. Currents were evoked from membrane holding potentials of: ■ -80mV, ○ -60mV, ▲ -40mV and □ -30mV. The values plotted are means ± S.E.M. for 4-9 cells. Curves were fitted by eye.

Figure 3.10

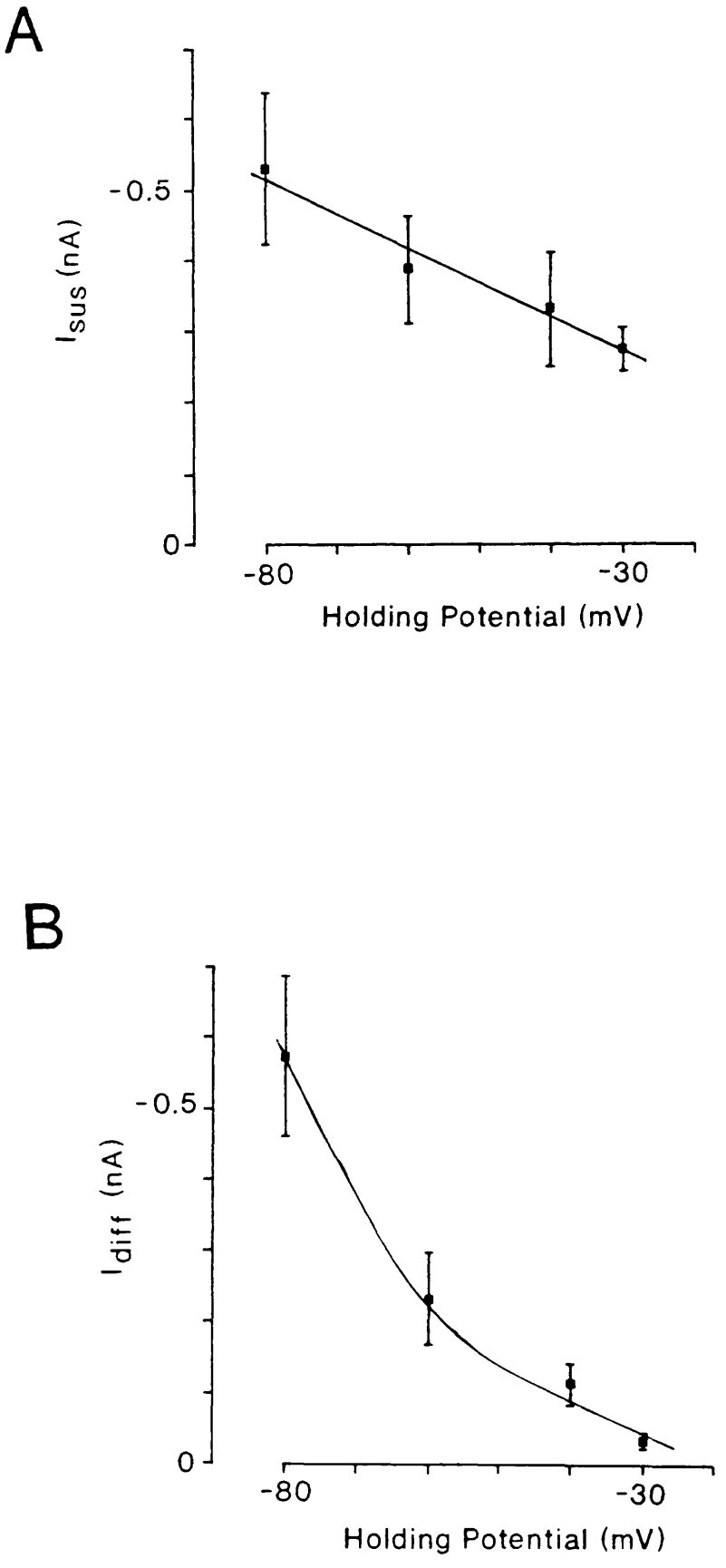
A
-0.5
0
I_{sus} (nA)
-80
-30
Holding Potential (mV)
B
-0.5
0
I_{diff} (nA)
-80
-30
Holding Potential (mV)

Legend for Figure 3.10 Steady-state inactivation of: A. Sustained current,

B. Difference.

The mean ± S.E.M. of the maximum sustained current (A) and I_{diff} (B) (taken from the original curves) are plotted versus the holding potential. The line through the sustained current was fitted by linear regression and through I_{diff} the curve was fitted by eye.

inactivated at the more depolarized holding potentials although still present. The test potential at which the maximum sustained current was evoked (around +8mV) did not change significantly with holding potential (see Table 3.1 and Figure 3.9). This indicates that the sustained current was composed of the same component of current at each of these holding potentials or alternatively more than one component with similar steady-state inactivation properties. If T- and N-type currents were present they would be expected to be inactivated to a greater extent than L-type at the more depolarised holding potentials (Fox, Nowycky & Tsien, 1987) thereby possibly changing the position of the potential for maximum current. Since this did not occur it may be that this sustained current is L-type at all holding potentials. However it is still possible that the sustained current is composed of more than one component (e.g. N and L), if components present were maximally activated over a similar range of test potentials.

The I-V curves for the peak current amplitude measured from the various holding potentials studied are shown in Figure 3.11. It can be seen qualitatively that a low threshold component is progressively lost as the holding potential is depolarized. The potential at which the peak currents were maximal was around 0mV (Table 3.1) at a holding potential of -80mV, whereas for the sustained (L-type) currents this potential occurred at around +8mV (see above). The test potential at which the maximum current was evoked shifted towards +8mV as holding potential was made less negative. This is consistent with the idea that L-type channels can still be activated from more depolarised holding potentials but that other channels (T- and possibly N-type) are inactivated at these less negative holding potentials. This suggests that the peak current in these cells was comprised of at least two components of

Table 3.1

Effect of holding potential on the test membrane potential at which mean inward calcium channel currents were maximal in NG 108 15 cells.

Holding Potential (mV)	Test potential at which currents were maximal (mV)		
	I_{sus}	I_{peak}	I_{diff}
-80	8.0 ± 2.7 (8)	-0.6 ± 3.4 (9)	-16.0 ± 3.8 (9)
-60	4.7 ± 2.4 (7)	2.0 ± 2.3 (7)	-6.0 ± 5.3 (7)
-40	7.0 ± 2.9 (8)	4.6 ± 3.3 (8)	-0.8 ± 2.9 (9)
-30	12.8 ± 5.4 (4)	12.5 ± 5.0 (4)	4.3 ± 3.0 (3)

Legend for Table 3.1 Effect of holding potential on the test membrane potential at which mean inward calcium channel currents were maximal in NG 108 15 cells.

This table shows the test potentials at which the mean inward calcium channel currents were maximal for untreated NG 108 15 cells held at various membrane holding potentials. Values given are means ± S.E.M., averaged in each case from the number of individual current-voltage plots shown in brackets. Significant differences in test potential at which I_{diff} was maximal occurred from a holding potential of -80mV as compared with -40mV and -30mV ($p < 0.05$).

Figure 3.11

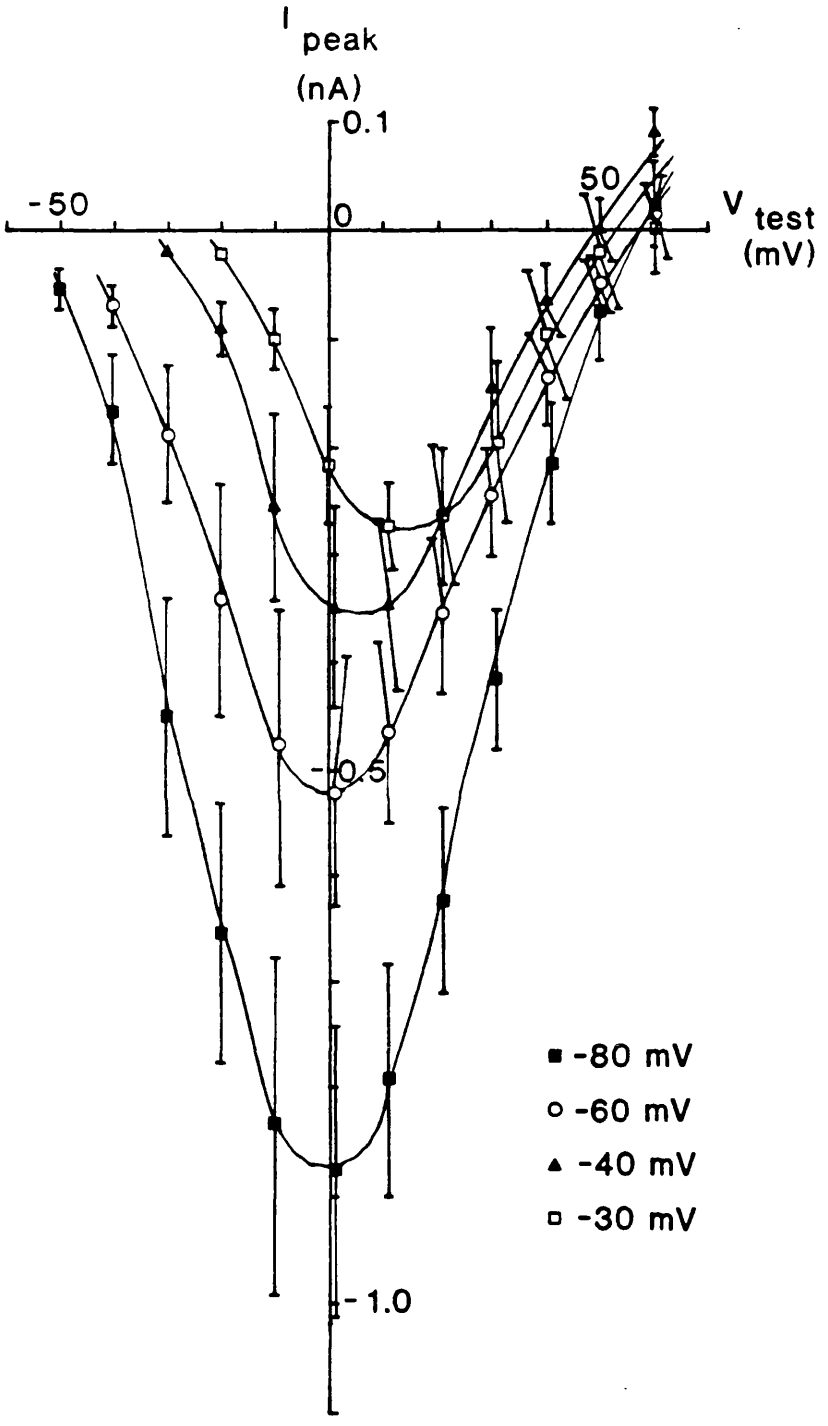

Legend for Figure 3.11 Effect of holding potential on peak currents.

This figure shows the peak inward calcium channel current amplitude (I_{peak}) plotted versus test membrane potential (V_{test}), measured in untreated differentiated NG 108 15 cells, held at various membrane holding potentials. Currents were evoked from membrane holding potentials of: ■ -80mV, ○ -60mV, ▲ -40mV and □ -30mV. The values plotted are means ± S.E.M. for 4-9 cells. Curves were fitted by eye.

current.

In order to investigate this further, I-V curves were also obtained for I_{diff} i.e. I_{peak} - I_{sus} which would give an estimate of the transient component of current (figure 3.12). However it will not be an exact measure of transient current since the sustained current is measured at the end of the pulse and it may show some inactivation during the pulse. This current is mainly T-type since it is not only transient but also is activated at more negative holding potentials like T-type channels but not N- or L-type. The peak I_{diff} is reduced substantially as holding potential is made less negative with only a small proportion of the current seen from a holding potential of -80mV remaining at holding potentials of -40mV and -30mV (see Figure 3.10B). There was a shift to the right in the test potential at which the maximum current occurs as holding potential becomes less negative (see Table 3.1). This shift in test potential was significantly different between currents recorded from cells at a holding potential of -80mV to those held at -40 or -30mV ($p < 0.05$), indicating that a component contributing to I_{diff} at -80mV (i.e. T-type current) is lost at the less negative holding potentials, the remaining current probably being due to inaccurate subtraction of the sustained current (see above).

In summary transient and sustained components appear to be present in these differentiated NG 108 15 cells. The transient component seems to be mainly T-type and the sustained component mainly L-type. There was no clear evidence for a third component (N-type) from these experiments using holding potential although the possibility of such a component could not be ruled out either. Holding potentials of -80 and -40mV were chosen for all the following experiments with monoclonal antibodies. These potentials were chosen because a holding potential of -40mV gave

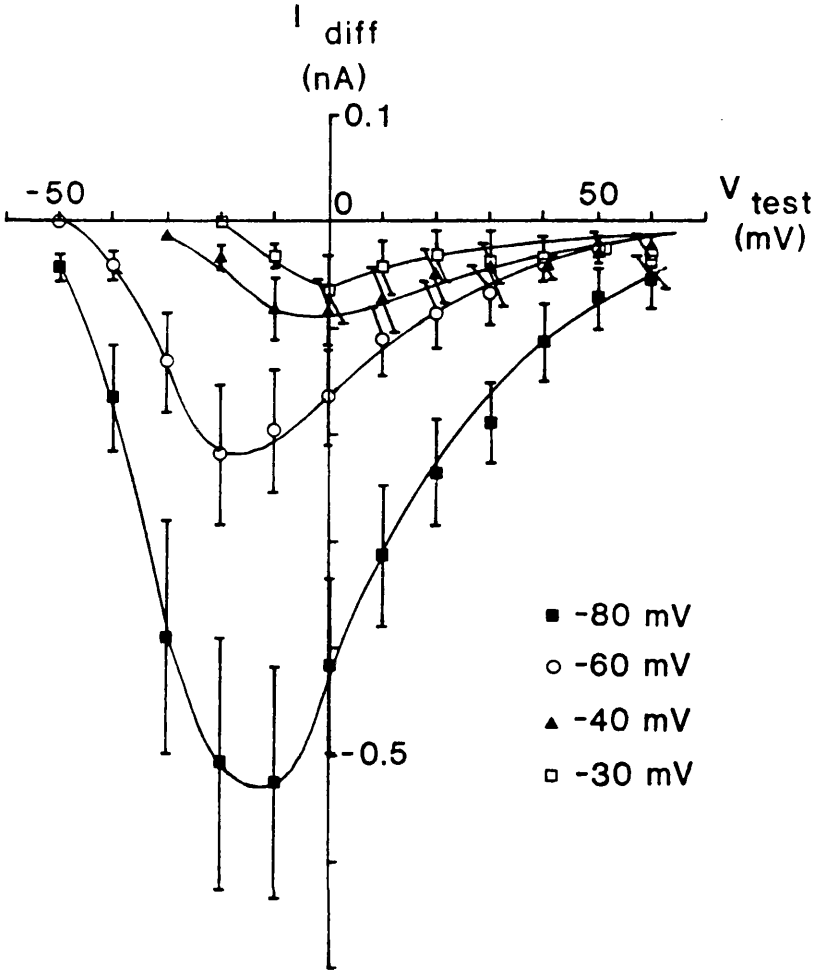

Legend for Figure 3.12 Effect of holding potential on I_{diff}.

This figure shows a plot of the difference between the peak and sustained inward calcium channel current amplitudes (I_{diff}) versus test membrane potential (V_{test}), measured in untreated differentiated NG 108 15 cells, held at various membrane holding potentials. Currents were evoked from membrane holding potentials of: ■ -80mV, ○ -60mV, ▲ -40mV and □ -30mV. The values plotted are means ± S.E.M. for 4-9 cells. Curves were fitted by eye.

good separation of the sustained L-type current without causing too much of its inactivation. On the other hand relatively clear T-type currents can be seen at a holding potential of -80mV with small depolarising steps. The main difference between differentiated and undifferentiated cells is that the sustained L-type current is larger (similar in amplitude to T-type) in the differentiated cells.

IV. Effects of monoclonal antibodies on whole cell calcium channel currents in differentiated NG 108 15 cells

The effects on calcium channels of five monoclonal antibodies raised against the α_2 subunit of the calcium channel from rabbit muscle t-tubules were tested on differentiated NG 108 15 cells. Whole cell currents were recorded after incubation for 24 hours in the presence of either control or test monoclonal antibody.

In these experiments the peak current amplitude (I_{peak}), the sustained current amplitude (I_{sus}) and the time to peak current were measured for cells held at a membrane potential of -80mV. For cells held at a membrane potential of -40mV, the amplitude of the sustained current was recorded. The various values were averaged over cells treated with control or test antibodies at each of the test potentials.

For each of the five monoclonal antibodies studied (11.14, 11.15, 11.23, 11.29 and 11.30) the I-V curve for the sustained component of inward current (I_{sus}) at a holding potential of -40mV was obtained (figures 3.13, 3.14, 3.15, 3.16 and 3.17 respectively). The currents plotted are the means from 14-26 cells for each control and for each of the test monoclonal antibodies. There were no significant effects on the sustained inward current amplitudes by test antibodies 11.15, 11.23, 11.29 and 11.30 as compared with controls at any test potential. There were however, significant

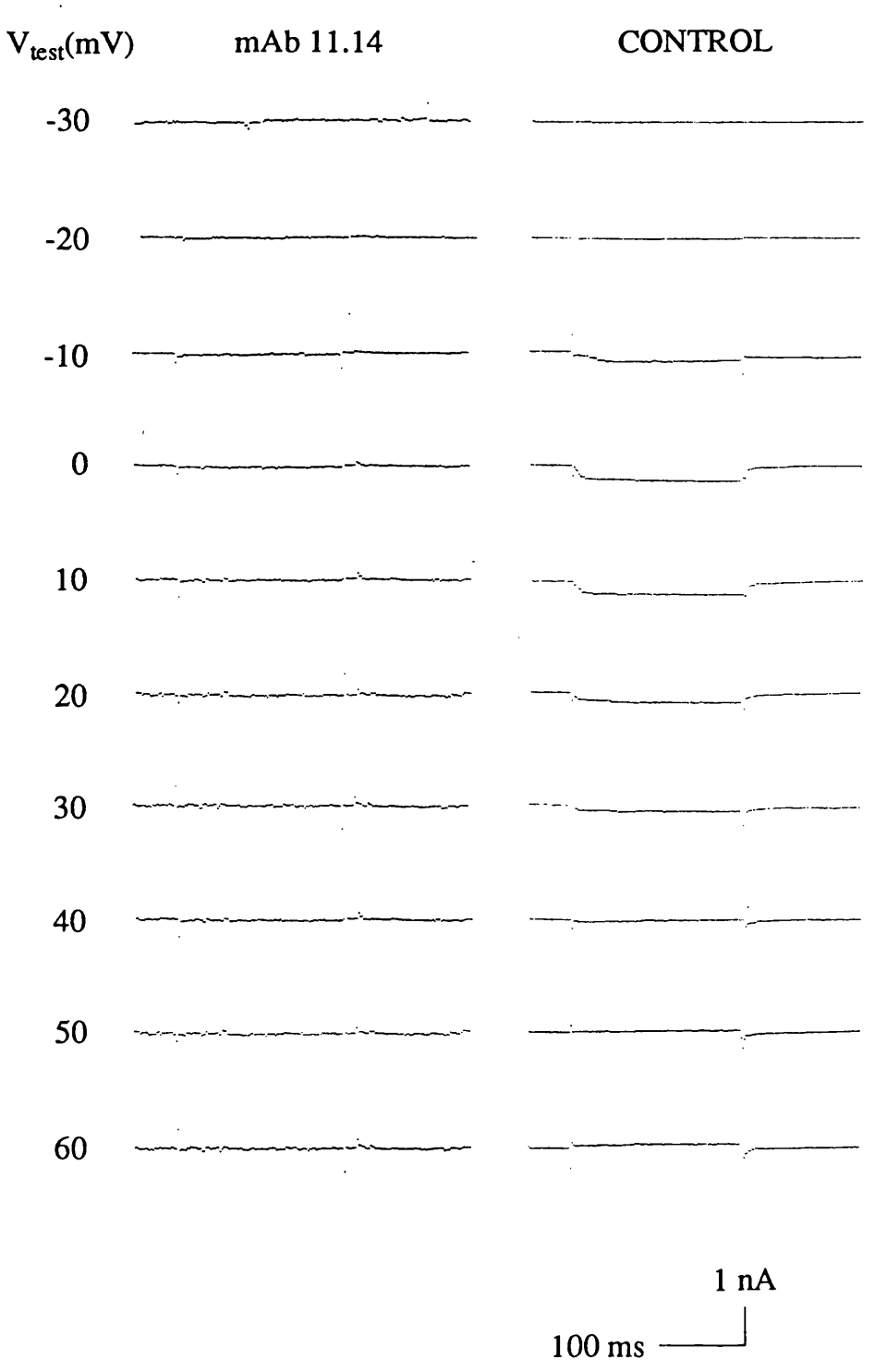

Examples of typical whole cell calcium channel currents in differentiated NG 108 15 cells treated with either control or mAb 11.14. The cells were held at a potential of -40mV. All records are leak and capacitance subtracted.

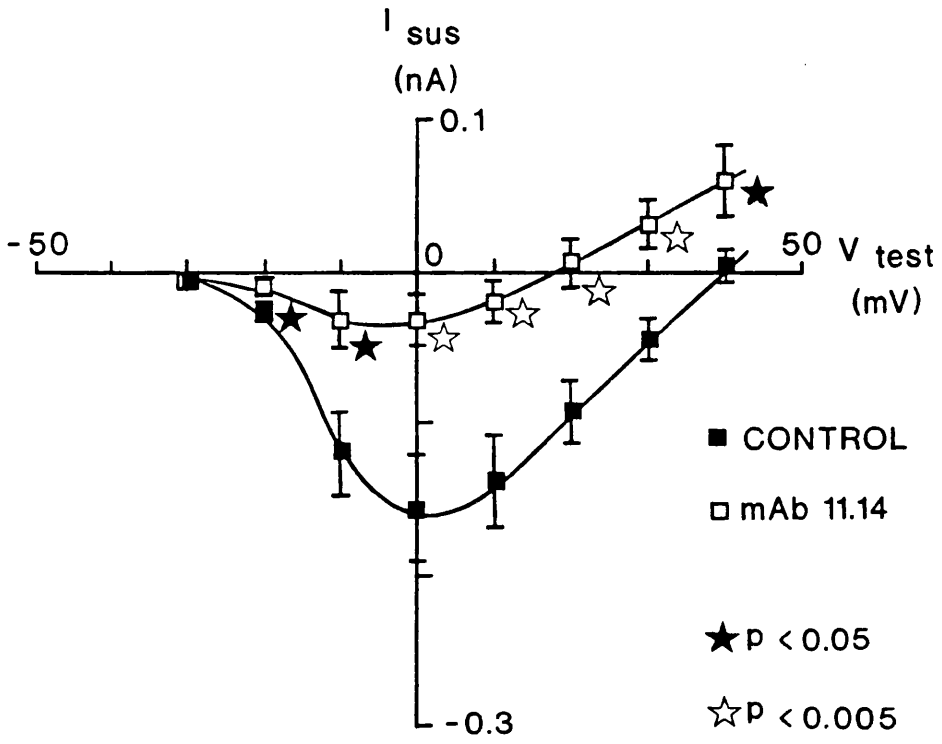

Legend for Figure 3.13 Effect of mAb 11.14 on sustained current (holding potential -40mV).

This figure shows the sustained inward calcium channel current amplitude (I_{sus}) plotted versus test membrane potential (V_{test}), measured in 15 control (■) and 15 monoclonal antibody 11.14 (□) treated differentiated NG 108 15 cells. All currents were evoked from a membrane holding potential of -40mV and the values plotted are means ± S.E.M.. Curves were fitted by eye. Significant reductions in calcium channel current amplitude by monoclonal antibody 11.14 as compared with controls: ★ $p < 0.05$, ☆ $p < 0.005$.

Table 3.5 Effect of mAb 11.14 on capacitance adjusted sustained current (holding potential -40mV).

mAb 11.14		Control	
V_{test}±S.E.M.(mV)	I_{sus}±S.E.M.(AF^{-1})	V_{test}±S.E.M.(mV)	I_{sus}±S.E.M.(AF^{-1})
-29.93 ± 0.04	-0.03 ± 0.05	-29.89 ± 0.07	-0.11 ± 0.04
-19.83 ± 0.10	-0.20 ± 0.16	-19.73 ± 0.11	-0.43 ± 0.13
-9.67 ± 0.18	-0.89 ± 0.50	-9.51 ± 0.14	-1.78 ± 0.44
+0.42 ± 0.20	-0.74 ± 0.44 ★	+0.58 ± 0.21	-2.39 ± 0.65
+10.40 ± 0.23	-0.47 ± 0.37 ★	+10.64 ± 0.27	-2.24 ± 0.67
+20.53 ± 0.28	-0.28 ± 0.56 ★	+20.64 ± 0.32	-1.52 ± 0.48
+30.53 ± 0.34	+0.88 ± 0.79	+30.47 ± 0.36	-0.76 ± 0.27
+40.50 ± 0.39	+1.55 ± 1.08	+40.83 ± 0.43	+0.14 ± 0.16
+50.48 ± 0.42	+2.27 ± 1.42	+50.85 ± 0.49	+0.83 ± 0.30
+60.15 ± 0.50	+3.45 ± 2.16	+60.77 ± 0.55	+1.32 ± 0.38

This table shows the capacitance adjusted sustained calcium channel current amplitudes (I_{sus}) evoked from the given test potentials (V_{test}) with a membrane holding potential of -40mV. Values shown are means ± S.E.M from 15 control and 15 mAb 11.14 treated differentiated NG 108 15 cells. Significant reductions by monoclonal antibody 11.14 as compared with controls: ★ $p < 0.05$, ☆ $p < 0.005$.

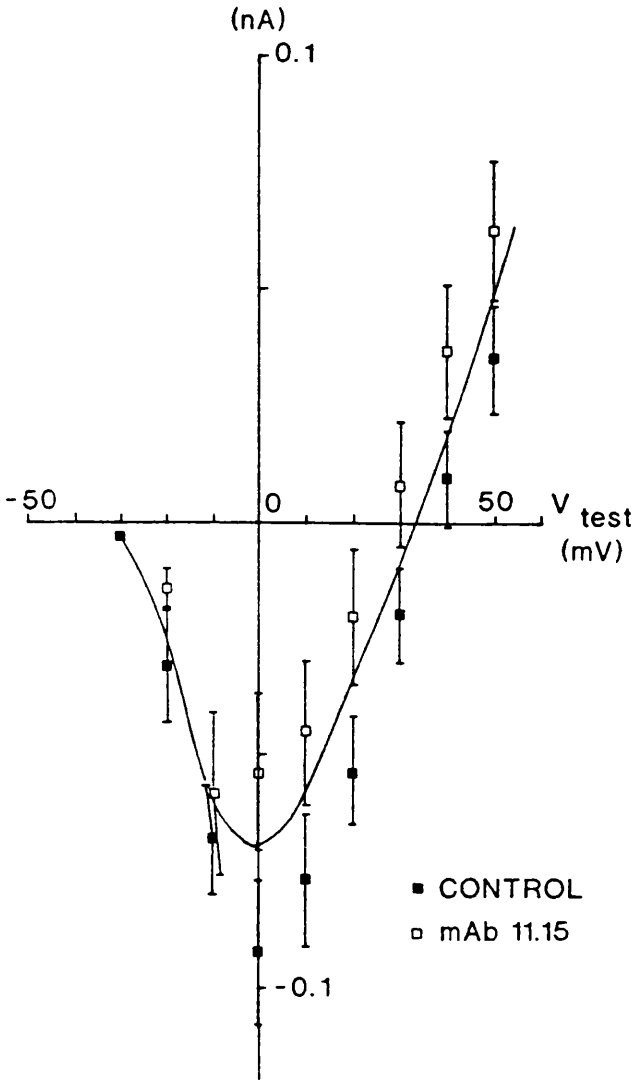

Legend for Figure 3.14 Effect of mAb 11.15 on sustained current (holding potential -40mV).

This figure shows the sustained inward calcium channel current amplitude (I_{sus}) plotted versus test membrane potential (V_{test}), measured in 25 control (■) and 24 monoclonal antibody 11.15 (□) treated differentiated NG 108 15 cells. All currents were evoked from a membrane holding potential of -40mV and the values plotted are means ± S.E.M.. Monoclonal antibody 11.15 had no significant effect on the sustained current amplitude compared with controls at any test potential studied, therefore one curve has been fitted by eye through all data points.

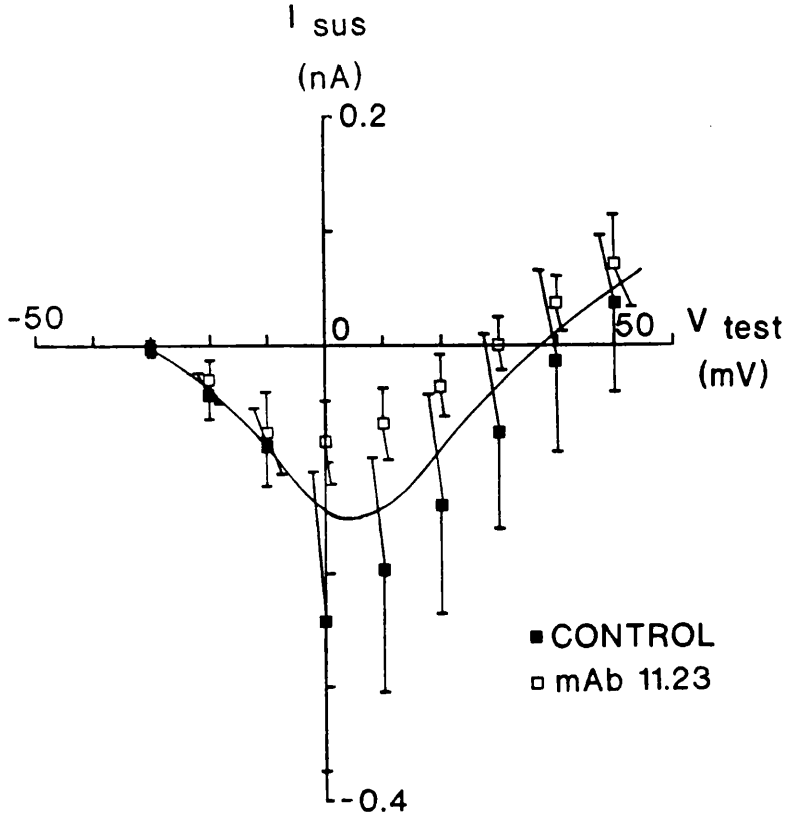

Legend for Figure 3.15 Effect of mAb 11.23 on sustained current (holding potential -40mV).

This figure shows the sustained inward calcium channel current amplitude (I_{sus}) plotted versus test membrane potential (V_{test}), measured in 14 control (■) and 17 monoclonal antibody 11.23 (□) treated differentiated NG 108 15 cells. All currents were evoked from a membrane holding potential of -40mV and the values plotted are means ± S.E.M.. Monoclonal antibody 11.23 had no significant effect on the sustained current amplitude compared with controls at any test potential studied, therefore one curve has been fitted by eye through all data points.

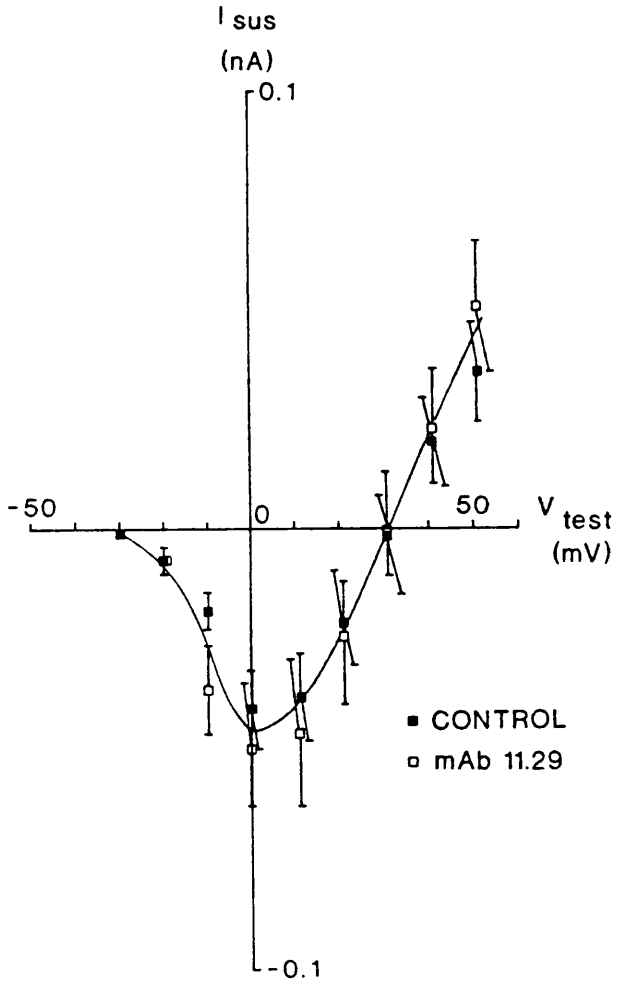

Legend for Figure 3.16 Effect of mAb 11.29 on sustained current (holding potential -40mV).

This figure shows the sustained inward calcium channel current amplitude (I_{sus}) plotted versus test membrane potential (V_{test}), measured in 25 control (■) and 25 monoclonal antibody 11.29 (□) treated differentiated NG 108 15 cells. All currents were evoked from a membrane holding potential of -40mV and the values plotted are means ± S.E.M.. Monoclonal antibody 11.29 had no significant effect on the sustained current amplitude compared with controls at any test potential studied, therefore one curve has been fitted by eye through all data points.

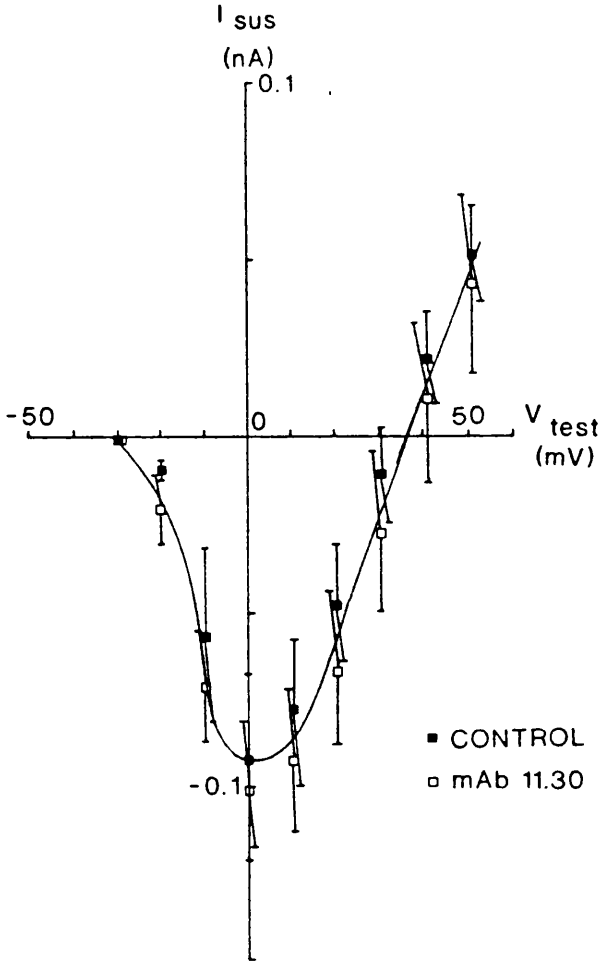

Legend for Figure 3.17 Effect of mAb 11.30 on sustained current (holding potential -40mV).

This figure shows the sustained inward calcium channel current amplitude (I_{sus}) plotted versus test membrane potential (V_{test}), measured in 25 control (■) and 26 monoclonal antibody 11.30 (▫) treated differentiated NG 108 15 cells. All currents were evoked from a membrane holding potential of -40mV and the values plotted are means ± S.E.M.. Monoclonal antibody 11.30 had no significant effect on the sustained current amplitude compared with controls at any test potential studied, therefore one curve has been fitted by eye through all data points.

reductions in the sustained current by mAb 11.14 as compared with controls (figure 3.13), between test potentials of -20 and +40mV. The capacitance adjusted currents (see Methods) showed a similar result.

The test potential at which maximal inward current occurred was calculated for both control and test monoclonal antibody treated cells (see Table 3.2). There were no significant differences between these potentials for any of the test monoclonal antibodies as compared with the corresponding control treated cells. This result was also found for mAb 11.14 which gave a reduction in sustained inward current (see above). This suggests a lack of effect of the antibodies on the voltage dependence of the currents.

The reversal potential for controls (approximately +40mV) and the mAb 11.14 treated cells (approximately +20mV) appears to be different (figure 3.13). A similar apparent change in reversal potential has previously been seen with antibody from Lambert-Eaton myasthenic syndrome patients. The latter antibody also appeared to specifically block L-type currents in NG 108 15 cells. However this apparent change in reversal potential could be fully explained by incomplete block of outward currents which contaminate the calcium channel current, particularly at the larger test potentials (Peers *et al.*, 1990) rather than by any real shift in the reversal potential. For monoclonal antibody 11.14, which does not cause any shift in potential for maximal current, see above, it seems likely that the effect is probably simply a reduction in sustained current without any effect on voltage dependence.

Figures 3.18-3.22 show I-V curves for the sustained component of current for the same monoclonal antibodies as above, 11.14, 11.15, 11.23, 11.29 and 11.30 respectively, but using a holding potential of -80mV. The results are the means of 16-

Table 3.2

Effect of mAbs on the test membrane potential at which mean sustained inward calcium channel currents were maximal (holding potential -40mV) in NG 108 15 cells.

Test monoclonal antibody number	Test potential for maximum I_{sus} (mV)	
	Test mAb	Control
11.14	1.9 ± 2.8 (9)	2.2 ± 1.7 (12)
11.15	-3.5 ± 2.0 (20)	3.5 ± 1.5 (22)
11.23	0.8 ± 2.7 (13)	1.4 ± 2.6 (14)
11.29	4.5 ± 2.7 (16)	6.5 ± 1.7 (17)
11.30	4.0 ± 2.0 (23)	2.3 ± 1.7 (17)

Legend for Table 3.2 Effect of mAbs on the test membrane potential at which mean sustained inward calcium channel currents were maximal (holding potential -40mV) in NG 108 15 cells.

This table shows the test potentials at which the mean sustained inward calcium channel currents were maximal for control and monoclonal antibody treated cells. Values given are means ± S.E.M., averaged in each case from the number of individual current-voltage plots shown in brackets. Some cells had no sustained inward current, particularly those treated with mAb 11.14 since this inhibited the sustained current.

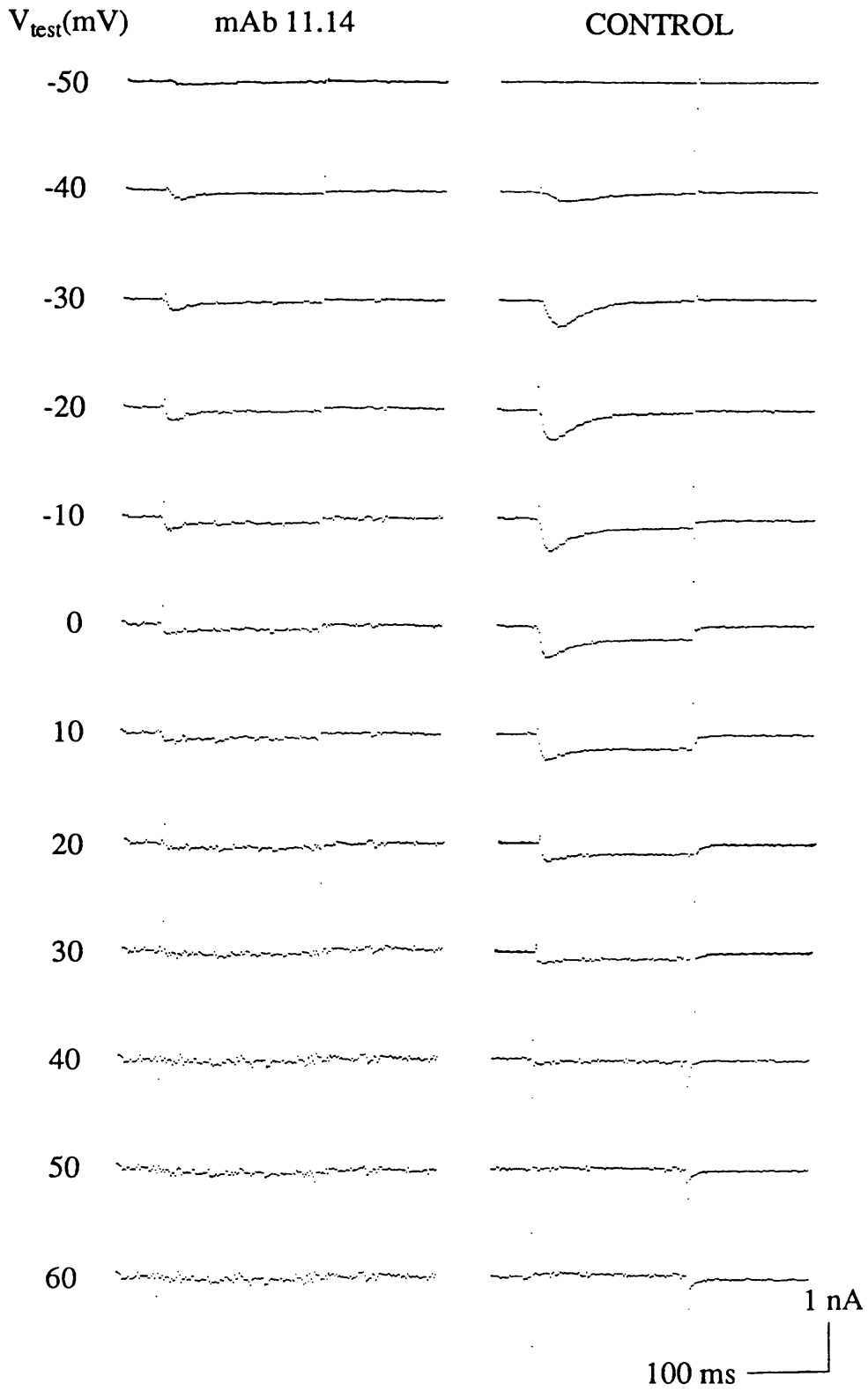

Examples of typical whole cell calcium channel currents in differentiated NG 108 15 cells treated with either control or mAb 11.14. The cells were held at a potential of -80mV. All records are leak and capacitance subtracted.

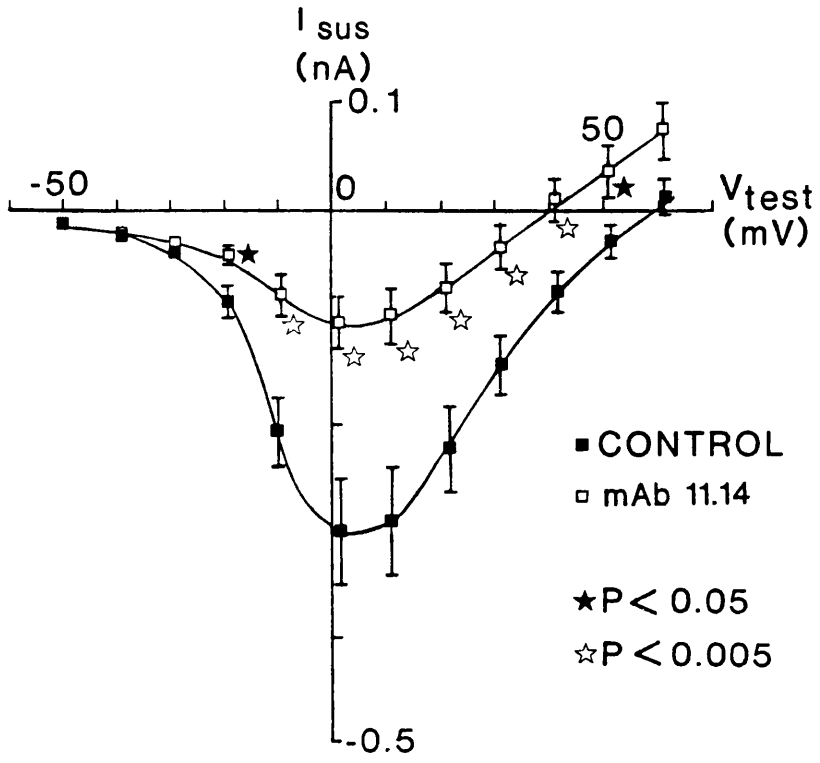

Legend for Figure 3.18 Effect of mAb 11.14 on sustained current (holding potential -80mV).

This figure shows the sustained inward calcium channel current amplitude (I_{sus}) plotted versus test membrane potential (V_{test}), measured in 17 control (■) and 17 monoclonal antibody 11.14 (□) treated differentiated NG 108 15 cells. All currents were evoked from a membrane holding potential of -80mV and the values plotted are means ± S.E.M.. Curves were fitted by eye. Significant reductions by monoclonal antibody 11.14 as compared with controls: ★ $p < 0.05$, ☆ $p < 0.005$.

Table 3.6 Effect of mAb 11.14 on capacitance adjusted sustained current (holding potential -80mV).

mAb 11.14		Control	
V_{test}±S.E.M.(mV)	I_{sus}±S.E.M.(AF^{-1})	V_{test}±S.E.M.(mV)	I_{sus}±S.E.M.(AF^{-1})
-49.73 ± 0.13	-0.25 ± 0.06	-49.55 ± 0.14	-0.19 ± 0.04
-39.53 ± 0.18	-0.31 ± 0.08	-39.32 ± 0.19	-0.51 ± 0.13
-29.51 ± 0.23	-0.42 ± 0.08	-29.26 ± 0.24	-0.61 ± 0.15
-19.33 ± 0.25	-0.70 ± 0.16	-19.16 ± 0.29	-1.29 ± 0.27
-9.31 ± 0.33	-1.64 ± 0.56	-10.07 ± 1.22	-3.15 ± 0.60
+0.79 ± 0.37	-2.14 ± 0.65 ★	+1.37 ± 0.34	-4.57 ± 0.94
+10.92 ± 0.39	-1.83 ± 0.49 ★	+11.23 ± 0.41	-4.53 ± 1.01
+20.90 ± 0.45	-1.13 ± 0.41 ☆	+21.45 ± 0.49	-3.52 ± 0.83
+30.96 ± 0.46	-0.35 ± 0.53 ☆	+31.05 ± 0.51	-2.27 ± 0.55
+40.99 ± 0.67	+0.44 ± 0.77 ★	+41.40 ± 0.60	-1.22 ± 0.33
+50.80 ± 0.57	+1.11 ± 1.07	+51.45 ± 0.65	-0.37 ± 0.24
+60.82 ± 0.60	+1.78 ± 1.28	+61.45 ± 0.70	+0.25 ± 0.26

This table shows the capacitance adjusted sustained calcium channel current amplitudes (I_{sus}) evoked from the given test potentials (V_{test}) with a membrane holding potential of -80mV. Values shown are means ± S.E.M from 17 control and 17 mAb 11.14 treated differentiated NG 108 15 cells. Significant reductions by monoclonal antibody 11.14 as compared with controls: ★ $p < 0.05$, ☆ $p < 0.005$.

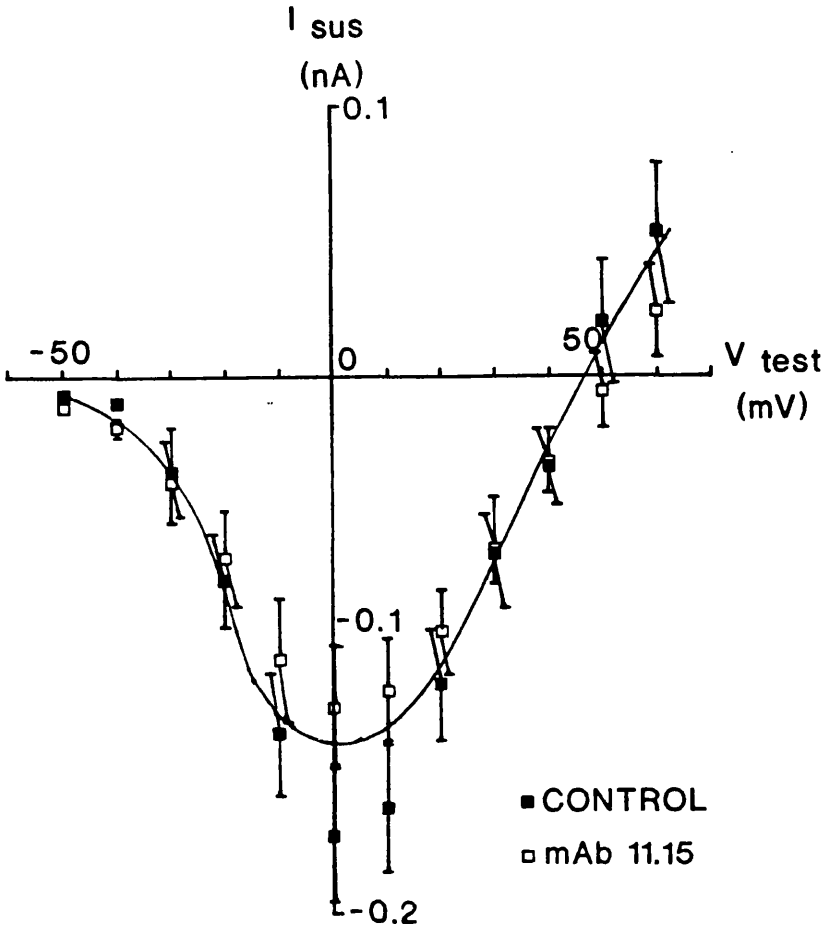

Legend for Figure 3.19 Effect of mAb 11.15 on sustained current (holding potential -80mV).

This figure shows the sustained inward calcium channel current amplitude (I_{sus}) plotted versus test membrane potential (V_{test}), measured in 25 control (■) and 24 monoclonal antibody 11.15 (□) treated differentiated NG 108 15 cells. All currents were evoked from a membrane holding potential of -80mV and the values plotted are means ± S.E.M.. Monoclonal antibody 11.15 had no significant effect on the sustained current amplitude compared with controls at any test potential studied, therefore one curve has been fitted by eye through all data points.

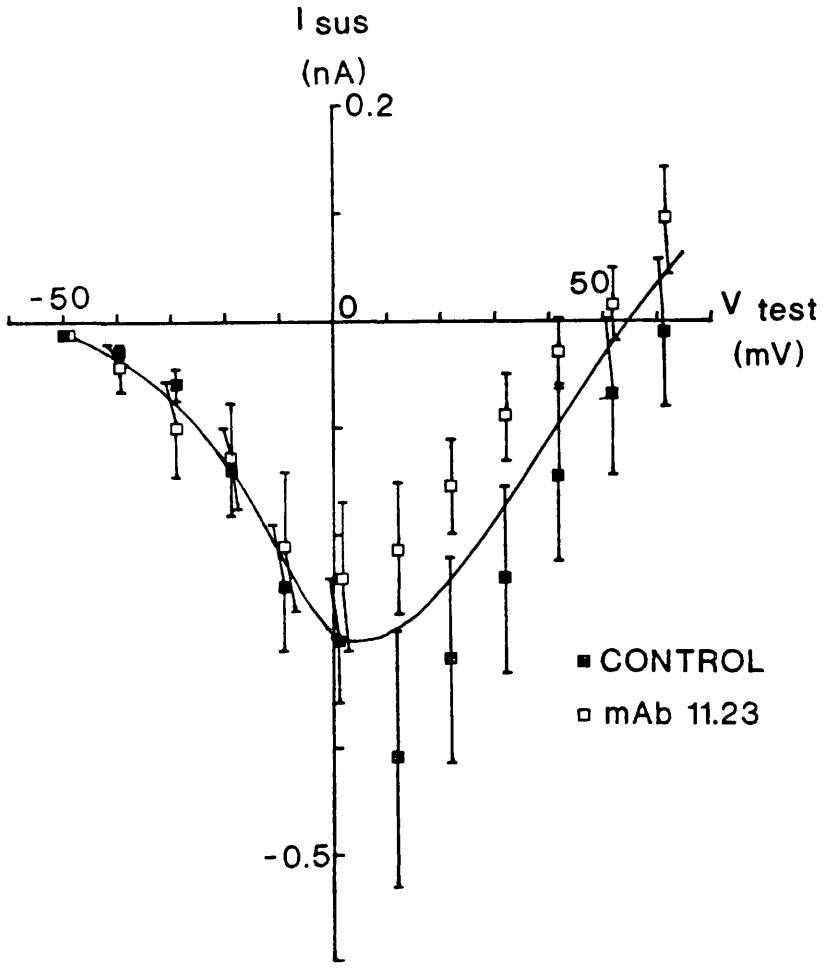

Legend for Figure 3.20 Effect of mAb 11.23 on sustained current (holding potential -80mV).

This figure shows the sustained inward calcium channel current amplitude (I_{sus}) plotted versus test membrane potential (V_{test}), measured in 16 control (■) and 17 monoclonal antibody 11.23 (□) treated differentiated NG 108 15 cells. All currents were evoked from a membrane holding potential of -80mV and the values plotted are means ± S.E.M.. Monoclonal antibody 11.23 had no significant effect on the sustained current amplitude at any test potential studied, therefore one curve has been fitted by eye through all data points.

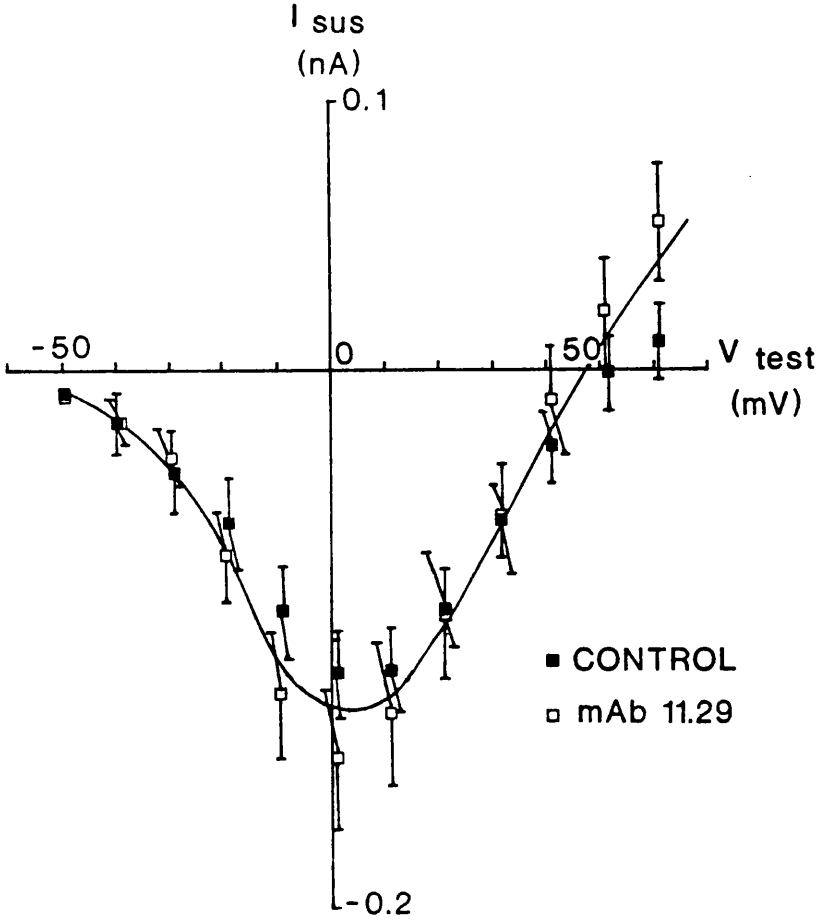

Legend for Figure 3.21 Effect of mAb 11.29 on sustained current (holding potential -80mV).

This figure shows the sustained inward calcium channel current amplitude (I_{sus}) plotted versus test membrane potential (V_{test}), measured in 25 control (■) and 25 monoclonal antibody 11.29 (□) treated differentiated NG 108 15 cells. All currents were evoked from a membrane holding potential of -80mV and the values plotted are means ± S.E.M.. Monoclonal antibody 11.29 had no significant effect on the sustained current amplitude compared with controls at any test potential studied, therefore one curve has been fitted by eye through all data points.

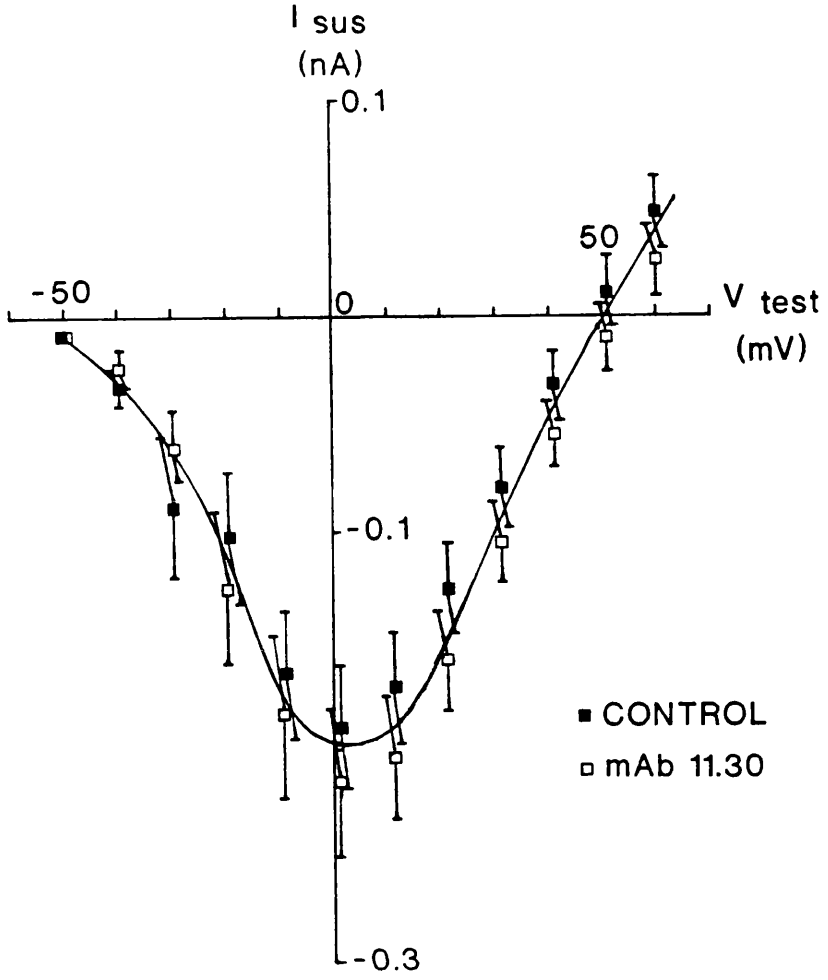

Legend for Figure 3.22 Effect of mAb 11.30 on sustained current (holding potential -80mV).

This figure shows the sustained inward calcium channel current amplitude (I_{sus}) plotted versus test membrane potential (V_{test}), measured in 25 control (■) and 26 monoclonal antibody 11.30 (□) treated differentiated NG 108 15 cells. All currents were evoked from a membrane holding potential of -80mV and the values plotted are means ± S.E.M.. Monoclonal antibody 11.30 had no significant effect on the sustained current amplitude compared with controls at any test potential studied, therefore one curve has been fitted by eye through all data points.

26 cells (same experiments as above) for each control and each test monoclonal antibody. In agreement with the results above at a holding potential of -40mV, there were again no significant reductions in the sustained inward current by mAbs 11.15, 11.23, 11.29 and 11.30 as compared with controls over the range of potentials tested. However there were again significant reductions in the sustained inward current by mAb 11.14 as compared with controls over a range of potentials from -20 to +50mV. Similar results were also found with the capacitance adjusted data. Therefore, as for sustained currents at -40mV, it appears that mAbs 11.15, 11.23, 11.29 and 11.30 had no effects on the sustained currents at -80mV while mAb 11.14 appeared to inhibit them.

As above, the test potentials at which the maximum sustained inward currents occurred were obtained at -80mV holding potential (Table 3.3). There were no significant differences in this potential between control and any of the test antibody treated cells.

Again as for a holding potential of -40mV, the reversal potential for the controls (approximately +60mV) and for mAb 11.14 treated cells (approximately +40mV) appeared to be different (figure 3.18). This effect may again be caused by incomplete block of outward currents rather than by a real shift in reversal potential (see above), so that the net effect of mAb 11.14 appears to be simply a reduction in current with no clear effect on voltage dependence.

I-V curves for the peak current amplitude measured from the same cells are shown in figures 3.23-3.27 for the same mAbs. Currents are averages of 16-26 cells for each control and each test antibody. For small depolarising steps (to potentials < -30mV) where transient (i.e. T-type) currents only were activated, there were no

Table 3.3

Effect of mAbs on the test membrane potential at which mean sustained inward calcium channel currents were maximal (holding potential -80mV) in NG 108 15 cells.

Test monoclonal antibody number	Test potential for maximum I_{sus} (mV)	
	Test mAb	Control
11.14	3.0 ± 0.2 (16)	5.2 ± 1.3 (17)
11.15	4.7 ± 2.8 (23)	2.4 ± 1.6 (25)
11.23	5.0 ± 3.0 (15)	3.8 ± 2.0 (17)
11.29	2.5 ± 2.4 (22)	5.1 ± 2.2 (23)
11.30	3.1 ± 2.6 (17)	0.1 ± 2.7 (23)

Legend for Table 3.3 Effect of mAbs on the test membrane potential at which mean sustained inward calcium channel currents were maximal (holding potential -80mV) in NG 108 15 cells.

This table shows the test potentials at which the mean sustained inward calcium channel currents were maximal for control and monoclonal antibody treated cells (holding potential -80mV). Values given are means S.E.M., averaged in each case from the number of individual current-voltage plots shown in brackets.

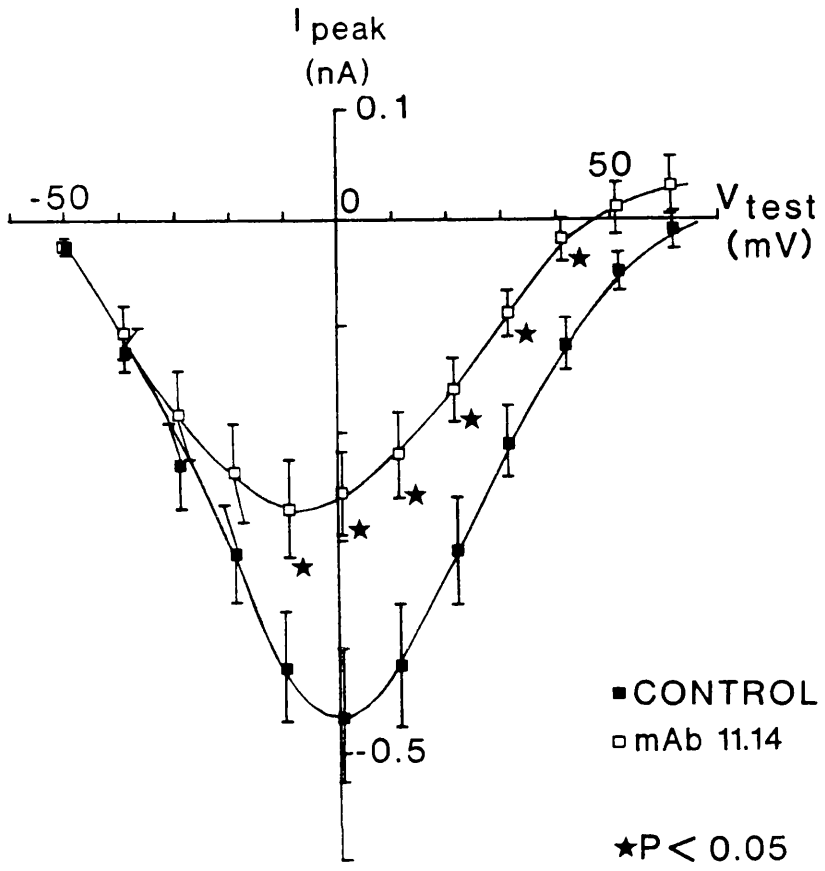

Legend for Figure 3.23 Effect of mAb 11.14 on peak current (holding potential -80mV).

This figure shows the peak inward calcium channel current amplitude (I_{peak}) plotted versus test membrane potential (V_{test}), measured in 17 control (■) and 17 monoclonal antibody 11.14 (□) treated differentiated NG 108 15 cells. All currents were evoked from a membrane holding potential of -80mV and values plotted are means ± S.E.M.. Significant reductions by monoclonal antibody 11.14 as compared with controls:

★ $p < 0.05$.

Table 3.7 Effect of mAb 11.14 on capacitance adjusted peak current (holding potential -80mV).

mAb 11.14		Control	
V_{test}±S.E.M.(mV)	I_{peak}±S.E.M.(AF^{-1})	V_{test}±S.E.M.(mV)	I_{peak}±S.E.M.(AF^{-1})
-49.73 ± 0.13	-0.55 ± 0.20	-49.55 ± 0.14	-0.35 ± 0.07
-39.53 ± 0.18	-1.83 ± 0.68	-39.32 ± 0.19	-1.95 ± 0.52
-29.51 ± 0.23	-2.89 ± 0.85	-29.26 ± 0.24	-4.10 ± 1.52
-19.33 ± 0.25	-3.70 ± 0.97	-19.16 ± 0.29	-5.52 ± 1.89
-9.31 ± 0.33	-4.39 ± 1.11	-10.07 ± 1.22	-6.94 ± 1.90
+0.79 ± 0.37	-4.26 ± 1.03	+1.37 ± 0.34	-7.74 ± 2.09
+10.92 ± 0.39	-3.45 ± 0.74	+11.23 ± 0.41	-6.66 ± 1.62
+20.90 ± 0.45	-2.19 ± 0.46	+21.45 ± 0.49	-4.75 ± 1.20
+30.96 ± 0.46	-1.10 ± 0.52 ★	+31.05 ± 0.51	-3.30 ± 0.79
+40.99 ± 0.67	-0.01 ± 0.71 ★	+41.40 ± 0.60	-1.83 ± 0.45
+50.80 ± 0.57	+0.73 ± 1.02	+51.45 ± 0.65	-0.66 ± 0.30
+60.82 ± 0.60	+1.30 ± 1.19	+61.45 ± 0.70	-0.05 ± 0.33

This table shows the capacitance adjusted peak calcium channel current amplitudes (I_{peak}) evoked from the given test potentials (V_{test}) with a membrane holding potential of -80mV. Values shown are means ± S.E.M from 17 control and 17 mAb 11.14 treated differentiated NG 108 15 cells. Significant reductions by monoclonal antibody 11.14 as compared with controls: ★ $p < 0.05$.

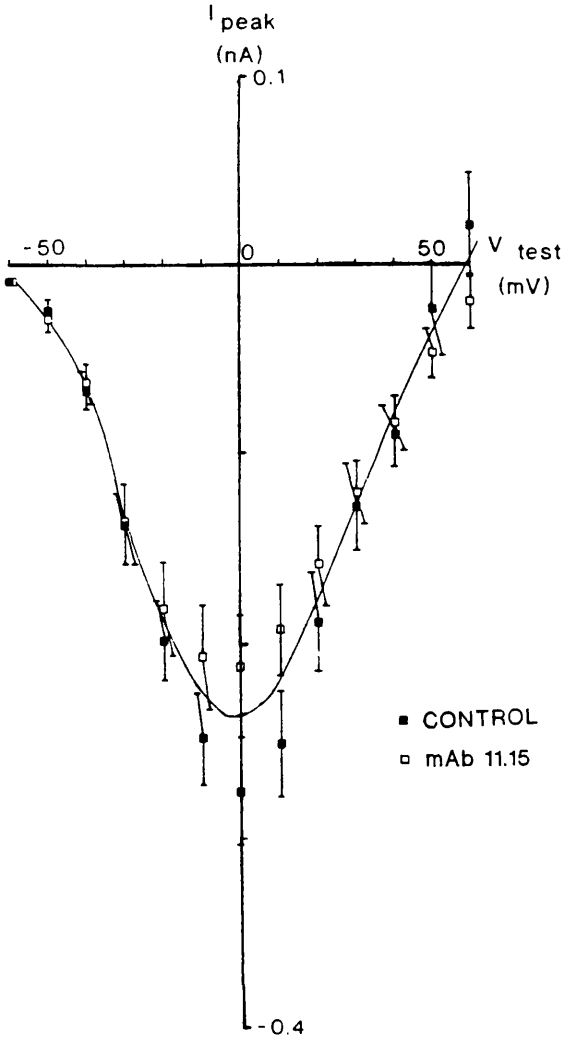

Legend for Figure 3.24 Effect of mAb 11.15 on peak current (holding potential -80mV).

This figure shows the peak inward calcium channel current amplitude (I_{peak}) plotted versus test membrane potential (V_{test}), measured in control (■) and monoclonal antibody 11.15 (□) treated differentiated NG 108 15 cells. All currents were evoked from a membrane holding potential of -80mV. The values plotted are means ± S.E.M from 25 control and 24 monoclonal antibody 11.15 treated cells. Monoclonal antibody 11.15 had no significant effect on peak current amplitude at any test potential studied, therefore one curve has been fitted by eye through all data points.

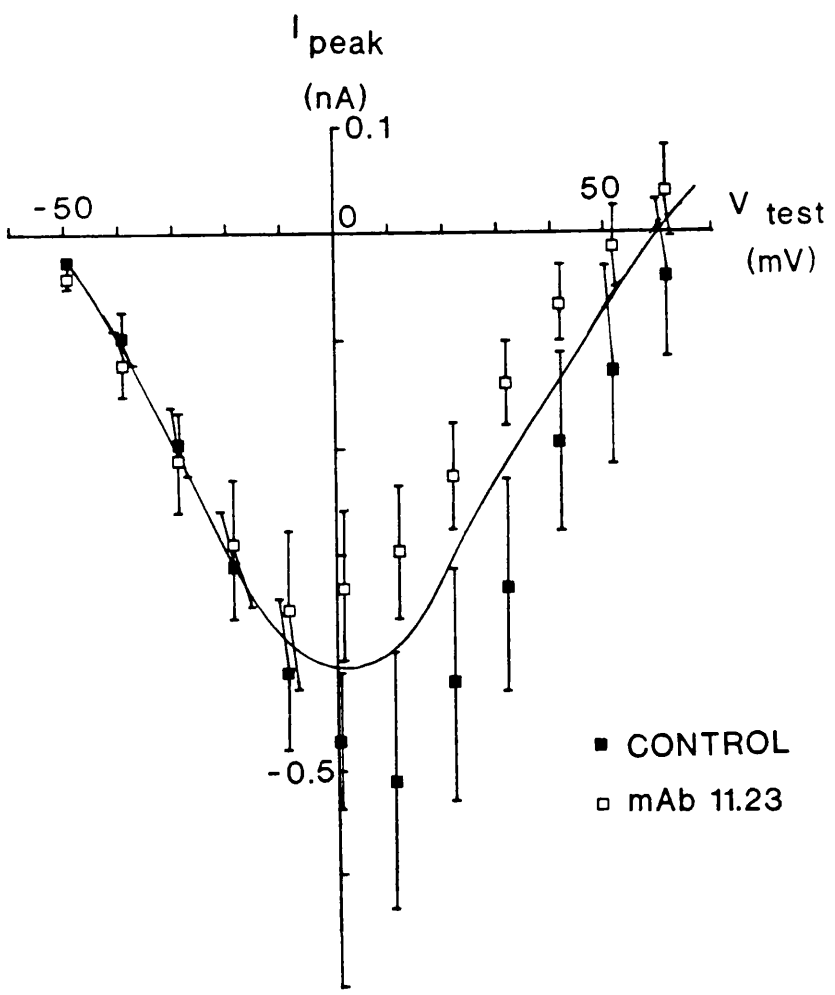

Legend for Figure 3.25 Effect of mAb 11.23 on peak current (holding potential -80mV).

This figure shows the peak inward calcium channel current amplitude (I_{peak}) plotted versus test membrane potential (V_{test}), measured in 16 control (■) and 17 monoclonal antibody 11.23 (□) treated differentiated NG 108 15 cells. All currents were evoked from a membrane holding potential of -80mV and values plotted are means ± S.E.M.. Monoclonal antibody 11.23 had no significant effect on peak current amplitude at any test potential studied, therefore one curve has been fitted by eye through all data points.

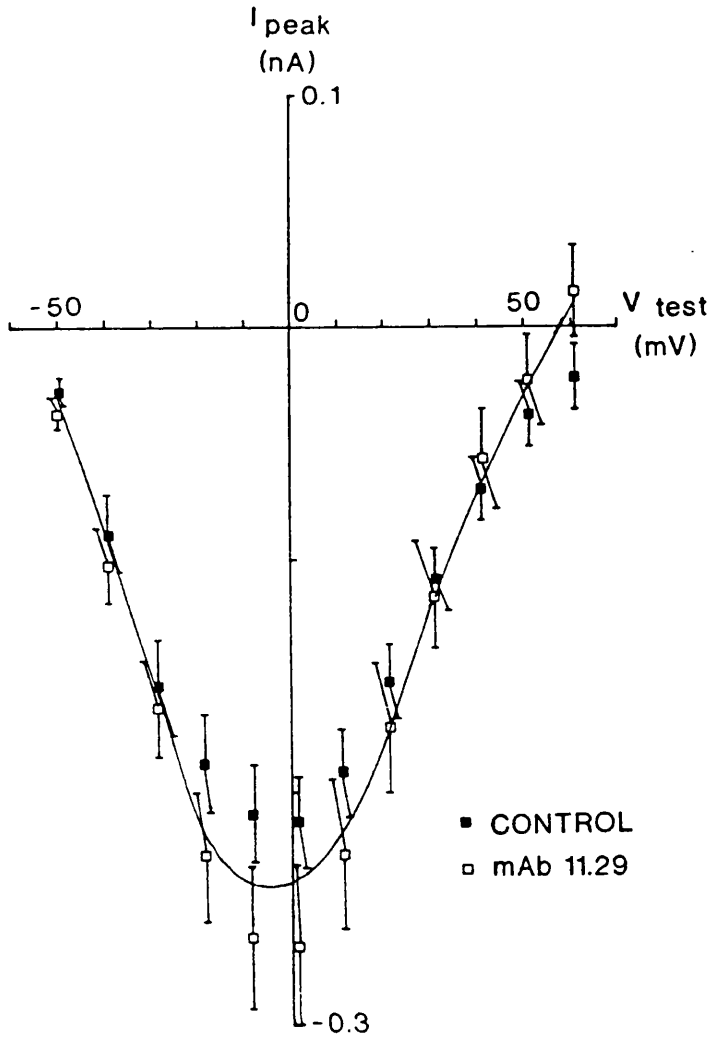

Legend for Figure 3.26 Effect of mAb 11.29 on peak current (holding potential -80mV).

This figure shows the peak inward calcium channel current amplitude (I_{peak}) plotted versus test membrane potential (V_{test}), measured in 25 control (■) and 25 monoclonal antibody 11.29 (□) treated differentiated NG 108 15 cells. All currents were evoked from a membrane holding potential of -80mV and values plotted are means ± S.E.M.. Monoclonal antibody 11.29 had no significant effect on peak current amplitude at any test potential studied, therefore one curve has been fitted by eye through all data points.

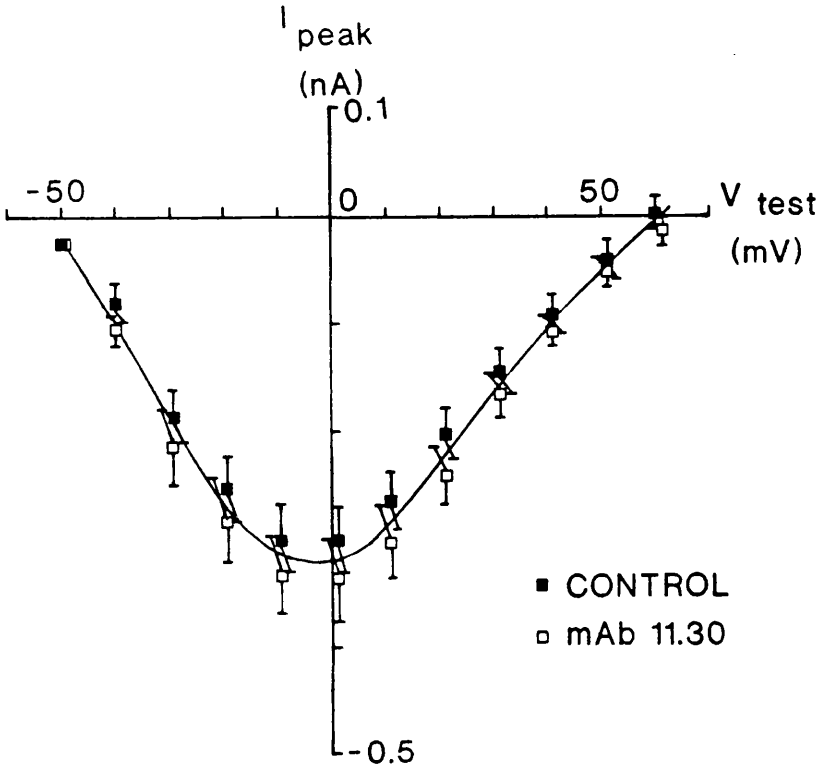

Legend for Figure 3.27 Effect of mAb 11.30 on peak current (holding potential -80mV).

This figure shows the peak inward calcium channel current amplitude (I_{peak}) plotted versus test membrane potential (V_{test}), measured in 25 control (■) and 26 monoclonal antibody 11.30 (□) treated differentiated NG 108 15 cells. All currents were evoked from a membrane holding potential of -80mV and values plotted are means ± S.E.M.. Monoclonal antibody 11.30 had no significant effect on peak current amplitude at any test potential studied, therefore one curve has been fitted by eye through all data points.

significant changes in the measured current amplitude by any of the test monoclonal antibodies compared with controls. For the larger steps, where e.g. L-type channels would also be activated, there were no significant differences between current amplitudes in test antibody treated cells as compared with controls, except for mAb 11.14 where there were significant reductions in peak current. Similar results were again found for the capacitance adjusted data. This indicates firstly, a lack of effect of mAbs 11.15, 11.23, 11.29 and 11.30 on T-type or L-type channels. Secondly, for mAb 11.14, there were significant reductions in the currents evoked at more depolarised potentials, possibly L-type (as seen previously with this mAb for the sustained currents), without any clear action on T-type currents.

For the peak currents, the potentials at which the maximal inward current occurred in the control cells and the test mAb treated cells are shown in Table 3.4. Again, the potentials at which the peak inward currents were maximal were not significantly different between control and test mAb treated cells. A negative-going shift in this potential may have been expected for mAb 11.14 via the block of channels activated at more depolarised potentials (possibly L-type) but not T-type channels (which are activated at the more negative test potentials); however this antibody caused only partial block and only a slight shift in this potential (figure 3.23).

Again there was an apparent shift in the reversal potential between currents in controls and mAb 11.14 treated cells, which can possibly be accounted for as above, rather than by a real shift in reversal potential.

Graphs of the time to peak inward current plotted versus the test potential are shown in figures 3.28-3.32 for the five antibodies tested. These were measured from

Table 3.4

Effect of mAbs on the test membrane potential at which mean peak inward calcium channel currents were maximal (holding potential -80mV) in NG 108 15 cells.

Test monoclonal antibody number	Test potential for maximum I_{peak} (mV)	
	Test mAb	Control
11.14	-7.4 ± 2.6 (17)	-3.2 ± 1.6 (17)
11.15	-7.5 ± 2.6 (24)	-2.6 ± 1.5 (26)
11.23	-7.4 ± 3.5 (17)	-1.4 ± 2.3 (17)
11.29	-9.0 ± 2.1 (25)	-4.1 ± 2.3 (25)
11.30	-6.3 ± 2.1 (25)	-4.0 ± 2.2 (26)

Legend for Table 3.4 Effect of mAbs on the test membrane potential at which mean peak inward calcium channel currents were maximal (holding potential -80mV) in NG 108 15 cells.

This table shows the test potentials at which the mean peak inward calcium channel currents were maximal for control and monoclonal antibody treated cells (holding potential -80mV). Values given are means S.E.M., averaged in each case from the number of individual current-voltage plots shown in brackets.

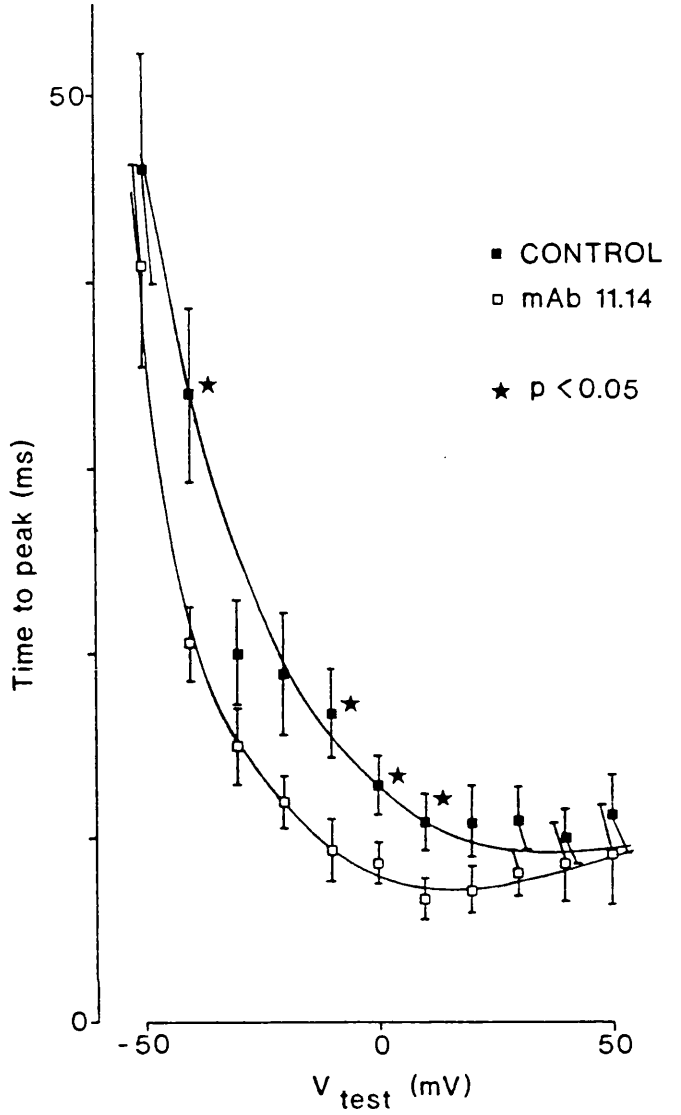

Legend for Figure 3.28 Effect of mAb 11.14 on time to peak current (holding potential -80mV).

This figure shows a plot of time to peak of inward calcium channel currents versus test membrane potential (V_{test}). Currents were evoked from a holding potential of -80mV. Values plotted are means ± S.E.M from 17 control (■) and 17 monoclonal antibody 11.14 (□) treated differentiated NG 108 15 cells. Curves were fitted by eye. Significant reductions by monoclonal antibody 11.14 as compared with controls:

★ $p < 0.05$.

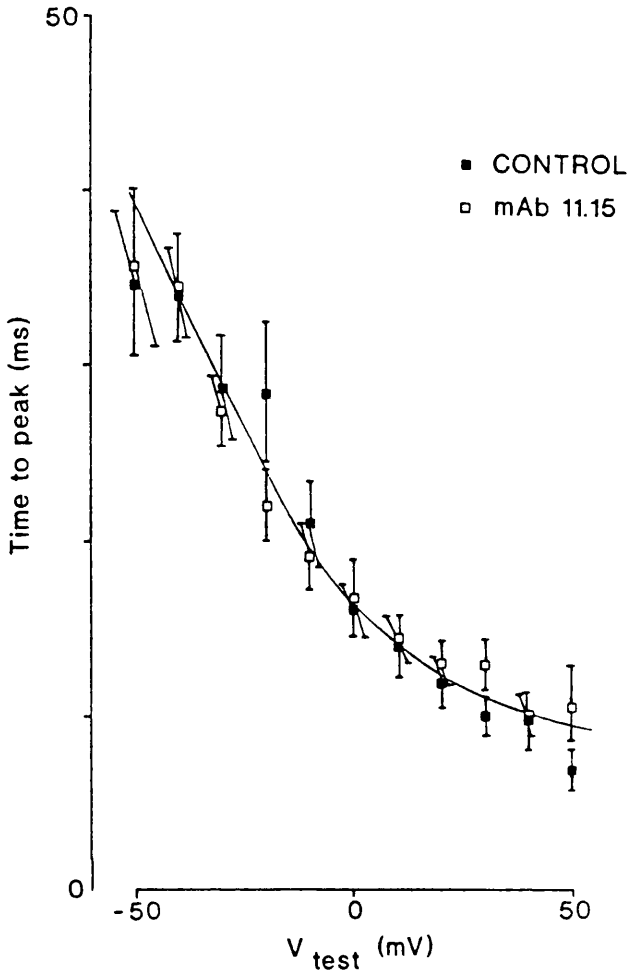

Legend for Figure 3.29 Effect of mAb 11.15 on time to peak current (holding potential -80mV).

This figure shows a plot of time to peak of inward calcium channel currents versus test membrane potential (V_{test}). Currents were evoked from a holding potential of -80mV. Values plotted are means ± S.E.M from 25 control (■) and 24 monoclonal antibody 11.15 (□) treated differentiated NG 108 15 cells. Monoclonal antibody 11.15 had no significant effect on times to peak at any test potential studied, therefore one curve has been fitted by eye through all data points.

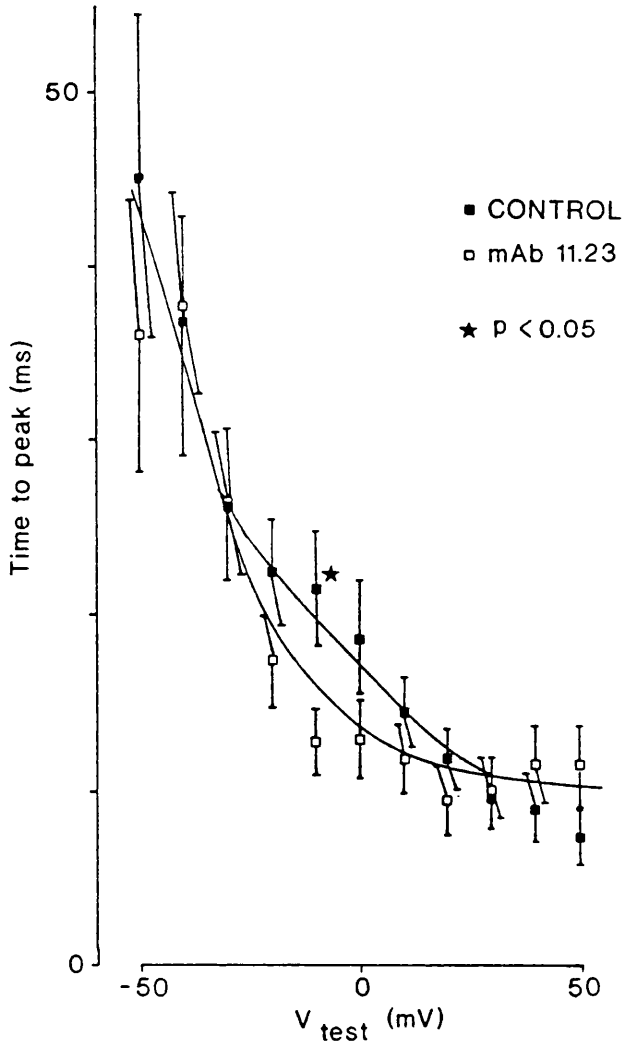

Legend for Figure 3.30 Effect of mAb 11.23 on time to peak current (holding potential -80mV).

This figure shows a plot of time to peak of inward calcium channel currents versus test membrane potential (V_{test}). Currents were evoked from a holding potential of -80mV. Values plotted are means ± S.E.M from 16 control (■) and 17 monoclonal antibody 11.23 (□) treated differentiated NG 108 15 cells. Curves were fitted by eye. Significant reductions by monoclonal antibody 11.23 as compared with controls:

★ $p < 0.05$.

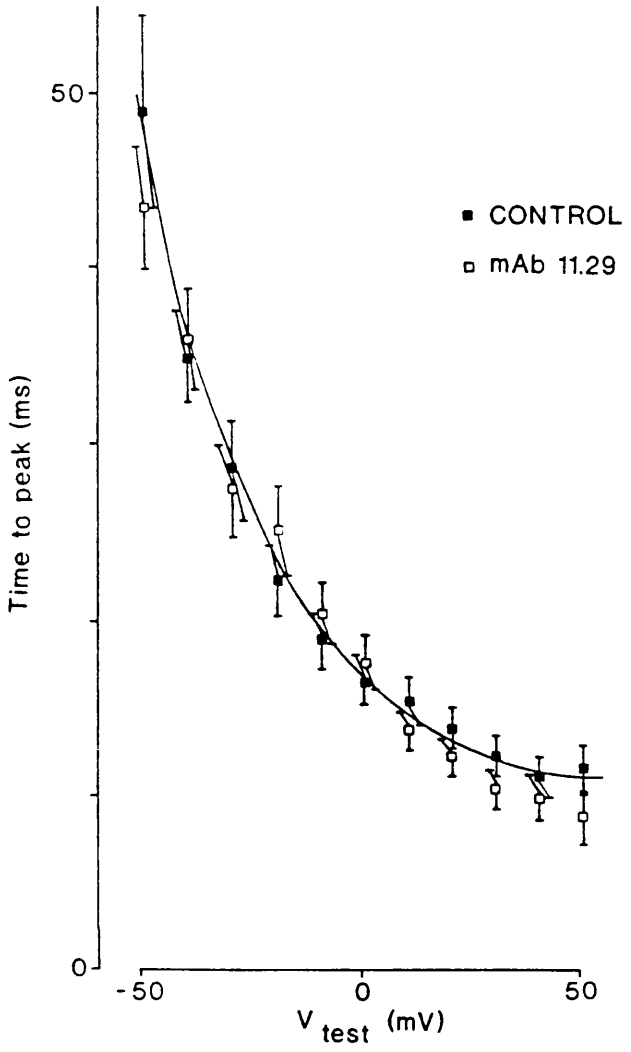

Legend for Figure 3.31 Effect of mAb 11.29 on time to peak current (holding potential -80mV).

This figure shows a plot of the time to peak of inward calcium channel currents versus test membrane potential (V_{test}). Currents were evoked from a holding potential of -80mV. Values plotted are means ± S.E.M from 25 control (■) and 25 monoclonal antibody 11.29 (□) treated differentiated NG 108 15 cells. Monoclonal antibody 11.29 had no significant effect on times to peak at any test potential studied, therefore one curve has been fitted by eye through all data points.

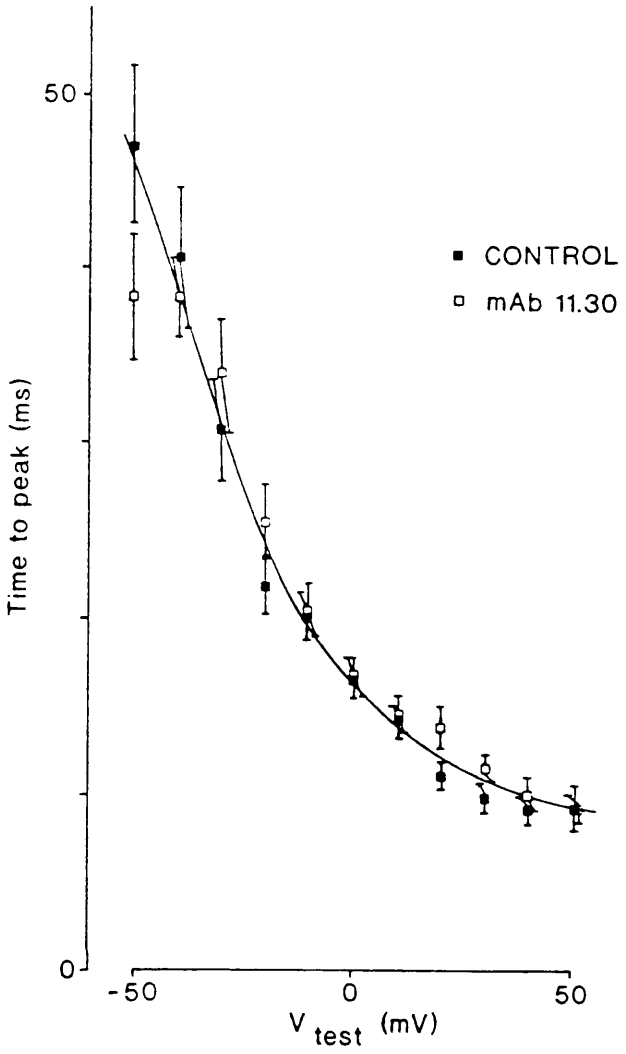

Legend for Figure 3.32 Effect of mAb 11.30 on time to peak current (holding potential -80mV).

This figure shows a plot of time to peak of inward calcium channel currents versus test membrane potential (V_{test}). Currents were evoked from a holding potential of -80mV. Values plotted are means ± S.E.M from 25 control (■) and 26 monoclonal antibody 11.30 (□) treated differentiated NG 108 15 cells. Monoclonal antibody 11.30 had no significant effect on times to peak at any test potential studied, therefore one curve has been fitted by eye through all data points.

a holding potential of -80mV in the same cells as above, again in the presence of either the control or one of the test mAbs. The time to peak inward current was voltage dependent for control and test mAb treated cells. Monoclonal antibodies 11.15, 11.29 and 11.30 had no effects at any test potential on the time to peak as compared with controls. A similar effect was seen for mAb 11.23 except at one test potential at which a significant decrease in time to peak current was seen. This was not a consistent effect over a range of potentials and so probably does not signal a clear effect of this mAb on the channels. On the other hand mAb 11.14 (figure 3.28) caused significant decreases in time to peak inward current at several test potentials. Thus there was a significant increase in the rate of activation of channels by this monoclonal antibody. The decrease in time to peak inward current at a test potential of -40mV by mAb 11.14 in figure 3.28 might be due to an increase in the activation rate of T-type channels. However the decrease is only at one test potential and so it is rather unclear whether this is in fact the case. However the increases in the activation rate at the larger test potentials by mAb 11.14 are more consistent and indicate an increase in the rate of activation of the total inward current. This could be due to an increase in the activation rate of any of the channel types, since at the more depolarised test potentials T-type channels could still be activated to some extent as well as the more likely L-type channels (and any other channel types present).

In summary, none of the monoclonal antibodies affected the amplitude of T-type currents, and four out of the five mAbs tested had no effect on any component of the inward calcium channel currents seen in these differentiated NG 108 15 cells. However mAb 11.14 reduced a sustained component of current which was activated at the more depolarised test potentials and was not inactivated at a relatively depolarised holding

potential (i.e. possibly L-type). This mAb also increased the activation rate of the inward calcium channel currents. It therefore appears that the binding of this mAb can affect the functioning of a high threshold component of current. The nature of this component was investigated further in the following section.

V. Effect of control/11.14 monoclonal antibody on whole cell calcium channel currents in the presence of nitrendipine

The effects of monoclonal antibody 11.14 were studied after currents flowing through dihydropyridine-sensitive L-type channels were blocked with nitrendipine. This was done so that any effect of the antibody on non-dihydropyridine sensitive channels would be studied in isolation. Whole cell currents were recorded from 25 control and 24 mAb 11.14 treated cells (24 hour incubation) in the presence of 5μM nitrendipine throughout.

Figure 3.33 shows a plot of sustained current versus test potential at a holding potential of -40mV in the presence of 5μM nitrendipine. Surprisingly, since a large proportion of the channels activated from this holding potential are expected to be L-type and these should be blocked by the nitrendipine, currents were still evoked under these conditions indicating the presence of a dihydropyridine-insensitive high threshold component. There were no significant effects of mAb 11.14 on the sustained inward current as compared with controls (figure 3.33). Furthermore, the test potential at which the control inward current was maximal (8.0 ± 1.2mV, n=21) was not significantly different from that for mAb 11.14 treated cells (5.4 ± 2.5mV, n=18). This indicates that mAb 11.14 probably inhibits the same component of current as nitrendipine (i.e. "dihydropyridine-sensitive L-type").

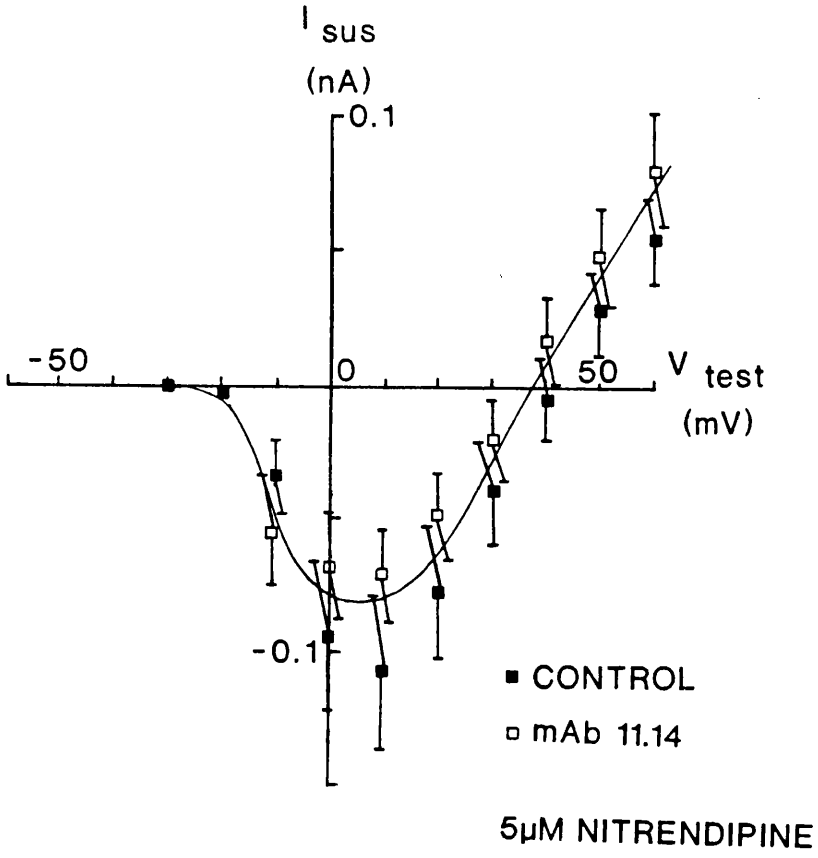

Legend for Figure 3.33 Effect of mAb 11.14 on sustained current in the presence of nitrendipine (holding potential -40mV).

This figure shows the sustained current amplitude (I_{sus}) plotted versus test membrane potential (V_{test}), measured in 25 control (■) and 24 monoclonal antibody 11.14 (□) treated differentiated NG 108 15 cells. All currents were evoked in the presence of 5μM nitrendipine. The values plotted are means ± S.E.M.. In the presence of nitrendipine, monoclonal antibody 11.14 had no significant effect on current amplitude as compared with controls, and so only one curve has been fitted (by eye) through all the data points.

At this holding potential (-40mV) the currents evoked from the control Ab treated cells in the presence of nitrendipine were reduced (approximately 35%) compared to those shown previously recorded in the absence of nitrendipine (figures 3.13). This however may not be a reliable comparison since the currents were not recorded in the same set of experiments and variations do occur in the amplitudes of whole cell currents recorded between experiments.

A similar result was found for the sustained currents evoked from a holding potential of -80mV (see Figure 3.34). There was incomplete block of currents by nitrendipine and there were no significant differences between currents in control and mAb 11.14 treated cells in presence of nitrendipine. Similarly the test potential at which the control inward current was maximal (11.2 ± 1.9mV, n=24) was not significantly different from that for mAb 11.14 treated cells (6.5 ± 2.8mV, n=23). This indicates an action of the antibody on dihydropyridine-sensitive L-type channels.

Figure 3.35 shows the I-V curve for the peak inward currents measured from the same cells as in Figure 3.34, evoked from a holding potential of -80mV. The peak currents were not significantly affected by mAb 11.14 at any test potential. In addition, the test potential at which the control inward current was maximal (4.6 ± 1.6mV, n=25) was not significantly different from that for mAb 11.14 treated cells (0.6 ± 2.3mV, n=24). These results again show that mAb 11.14 had no effect on dihydropyridine-insensitive channels (presumably T-type channels and dihydropyridine-insensitive calcium channels with a voltage dependence like L-type channels).

Figure 3.36 shows the time to peak of the inward currents measured in the same cells from a holding potential of -80mV in the presence of nitrendipine. The

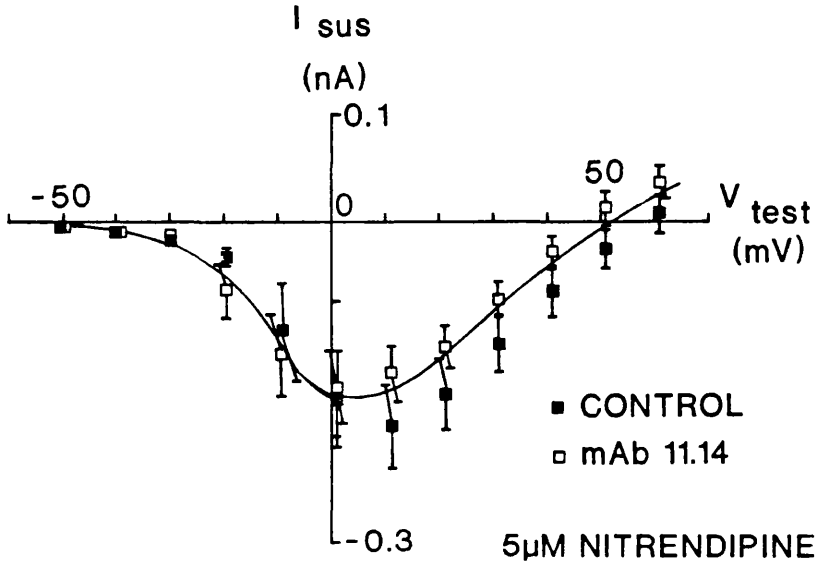

Legend for Figure 3.34 Effect of mAb 11.14 on sustained current in the presence of nitrendipine (holding potential -80mV).

This figure shows the sustained current amplitude (I_{sus}) plotted versus test membrane potential (V_{test}), measured in 25 control (■) and 24 monoclonal antibody 11.14 (□) treated differentiated NG 108 15 cells. All currents were evoked in the presence of 5μM nitrendipine. Values plotted are means ± S.E.M.. Monoclonal antibody 11.14 had no significant effect on the sustained current amplitude at any test potential studied, therefore one curve has been fitted by eye through all data points.

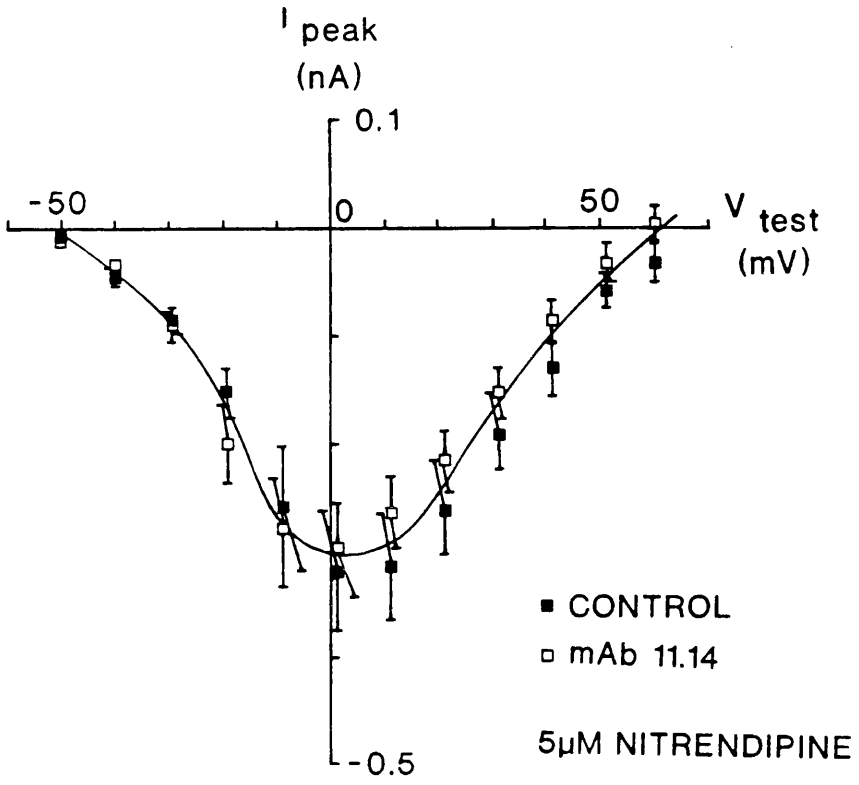

Legend for Figure 3.35 Effect of mAb 11.14 on peak current in the presence of nitrendipine (holding potential -80mV).

This figure shows a plot of peak inward calcium channel current amplitude (I_{peak}) versus test membrane potential (V_{test}), measured in 25 control (■) and 24 monoclonal antibody 11.14 (□) treated differentiated NG 108 15 cells. All currents were evoked in the presence of 5μM nitrendipine. Points plotted are means ± S.E.M.. Since monoclonal antibody 11.14 had no significant effect on peak current amplitude as compared with controls at any test potential, a single curve was fitted through the data points by eye. Data were obtained from the same recordings as in Figures 3.33 and 3.34.

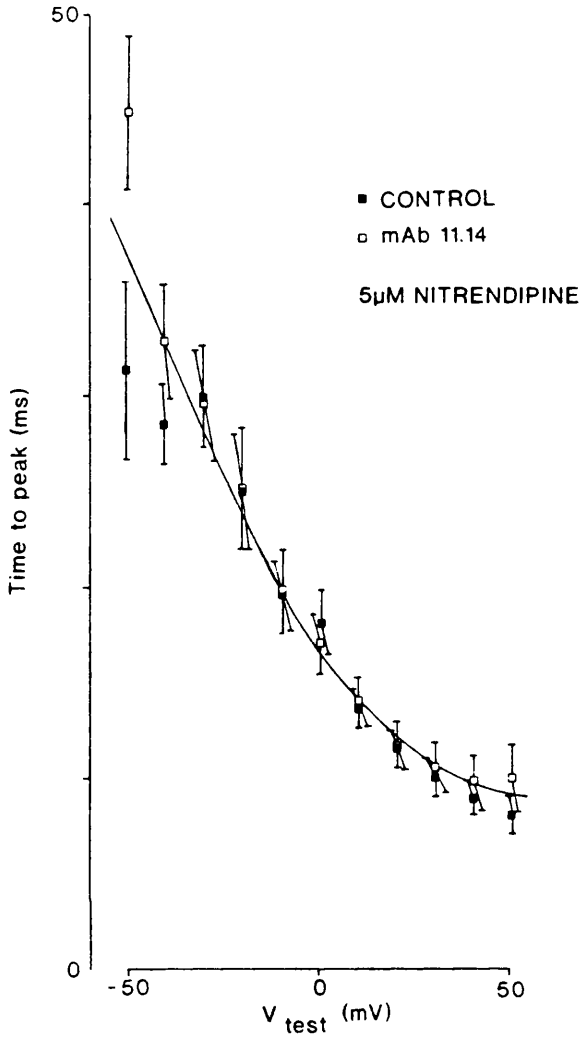

Legend for Figure 3.36 Effect of mAb 11.14 on time to peak current in the presence of nitrendipine (holding potential -80mV).

This figure shows a plot of time to peak inward calcium channel current versus test membrane potential (V_{test}), measured in 25 control (■) and 24 monoclonal antibody 11.14 (□) treated differentiated NG 108 15 cells. All currents were evoked in the presence of 5μM nitrendipine. Points plotted are means ± S.E.M.. Monoclonal antibody 11.14 had no significant effect on time to peak current as compared with controls at any test potential, therefore a single curve was fitted through the data points by eye.

times to peak inward current in cells treated with either control or mAb 11.14 in the presence of nitrendipine were strongly voltage dependent, and were not significantly different between the control and mAb 11.14 treated groups. It therefore appears that mAb 11.14 had no effect on the rate of activation of dihydropyridine-insensitive channels.

In the presence of nitrendipine, capacitance adjusted data also showed no significant differences in I_{sus} (holding potential -40 or -80mV) and I_{peak} between control or mAb 11.14 treated cells.

In summary, combining the results of this set of experiments with the previous ones, mAb 11.14 appears to act only on dihydropyridine-sensitive L-type channels to cause their loss of function.

VI. Effects of acute application of monoclonal antibody 11.14 on whole cell calcium channel currents in NG 108 15 cells

The effect of mAb 11.14 on calcium channel function seen after 24 hours incubation of the cells with the antibody could be due to down regulation of the channels or to direct block of channel function. To decide between these two, in this section, monoclonal antibody 11.14 was applied acutely to the cells. For this, control or monoclonal antibody 11.14 was applied to the bath during whole cell recording (see Methods). Cells were voltage clamped at -80mV and currents evoked in response to repetitive 70mV depolarizing voltage steps (200ms duration, 0.1Hz frequency). Inward calcium channel currents were recorded from 5 cells in which control antibody was applied and 5 in which monoclonal antibody 11.14 was applied.

Figure 3.37 shows a graph of the sustained inward current plotted versus time.

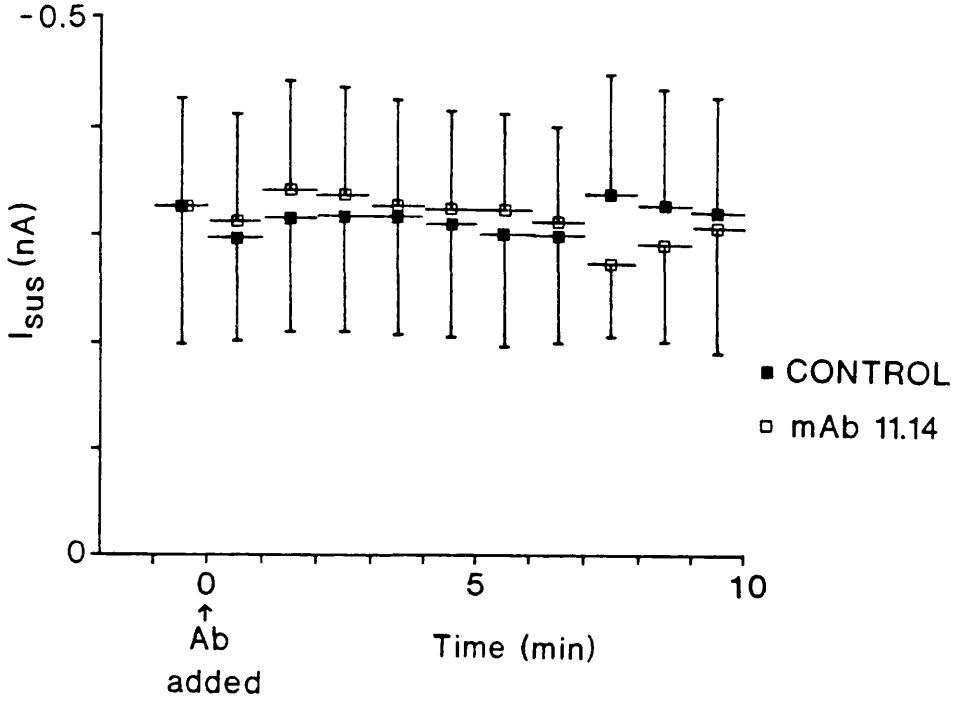

Legend for Figure 3.37 Effect of acute application of mAb 11.14 on sustained current. This figure shows the sustained current amplitude (I_{sus}) plotted versus time measured in differentiated NG 108 15 cells in which the control or mAb 11.14 was added to the bath at time zero. Currents were evoked in response to repetitive 70mV depolarising steps from a membrane holding potential of -80mV. The values plotted are means ± S.E.M. (n=5) of currents averaged over 1 minute intervals.

There were no significant differences in the sustained current recorded in the presence of the control or monoclonal antibody 11.14 over this 10 minute time period.

Figure 3.38 shows a graph of the effect of monoclonal antibody 11.14 (and control) on the peak inward current plotted versus time. As in the case of the sustained current there was no significant effect of the antibody on the peak inward current compared with controls over this 10 minute time period.

In the same experiments, the effect of the acute application of the monoclonal antibody on the time to peak was investigated, see Figure 3.39. There was no significant effect on time to peak by mAb 11.14 as compared with controls.

In summary, for the 24 hour incubation experiments reported in earlier sections we observed effects of mAb 11.14 (figures 3.13, 3.18, 3.23 & 3.28), whereas acute application of the same mAb showed no effects. This indicates that monoclonal antibody 11.14 either has no ~~direct~~ immediate effect on the calcium channels in these cells or, alternatively may have slow access to a possibly partially occluded binding site.

VII. Effects of monoclonal antibodies on ^{45}calcium flux

Potassium-stimulated calcium fluxes were measured with either control antibody or one of the test monoclonal antibodies present. The cells were incubated with the antibody for 24 hours prior to recording. Two separate experiments each with their own control were carried out: firstly mAb 11.14 was tested to try to confirm the result observed above in the whole cell recordings and secondly any effects of the other mAbs were investigated.

The stimulated calcium flux was measured in response to depolarization caused by 144mM potassium and resting flux was measured at a potassium concentration

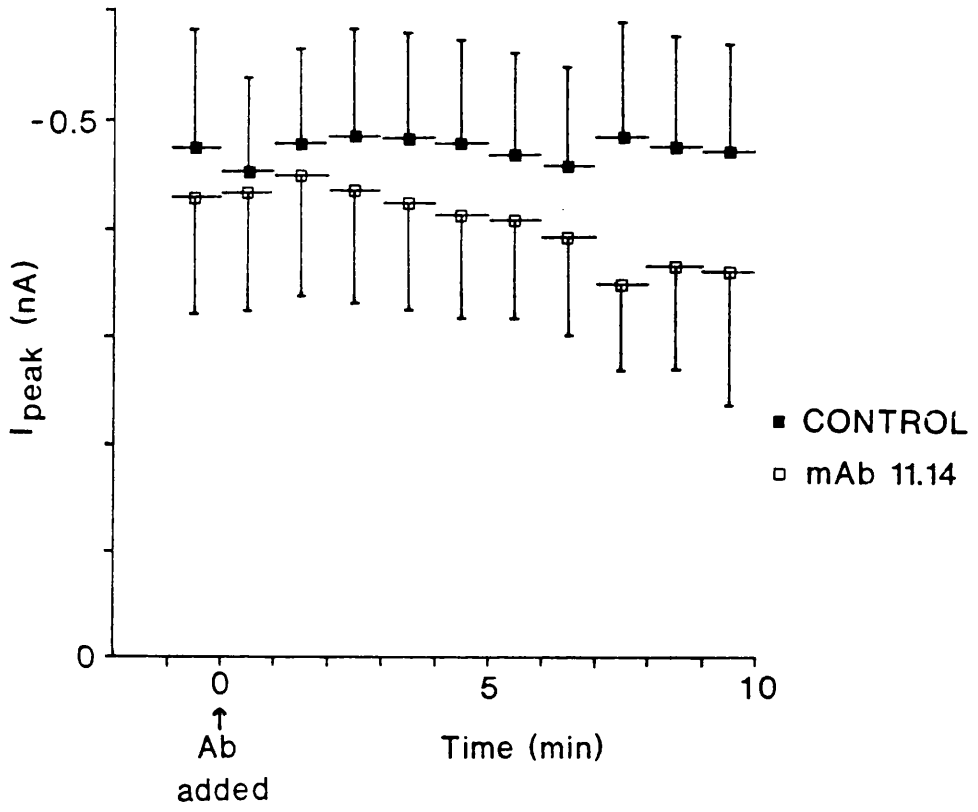

Legend for Figure 3.38 Effect of acute application of mAb 11.14 on peak current. This figure shows the peak current amplitude (I_{peak}) plotted versus time measured in differentiated NG 108 15 cells in which the control or mAb 11.14 was added to the bath at time zero. Currents were evoked in response to repetitive 70mV depolarising steps from a membrane holding potential of -80mV. The values plotted are means ± S.E.M. (n=5) of currents averaged over 1 minute intervals.

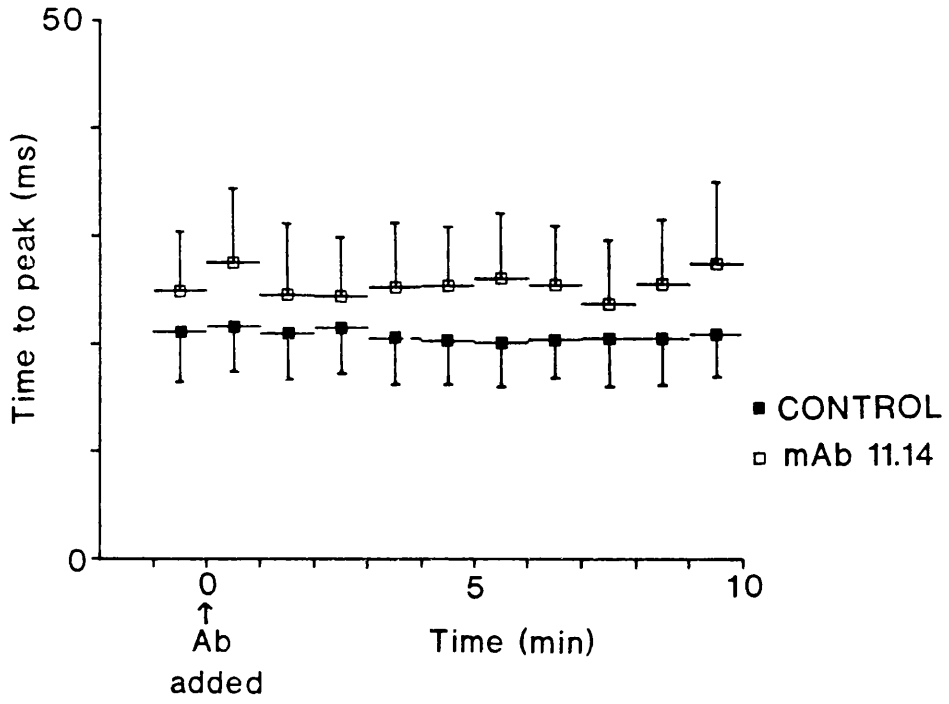

Legend for Figure 3.39 Effect of acute application of mAb 11.14 on time to peak current.

This figure shows the time to peak current plotted versus time measured in differentiated NG 108 15 cells in which the control or mAb 11.14 was added to the bath at time zero. Currents were evoked in response to repetitive 70mV depolarising steps from a membrane holding potential of -80mV. The values plotted are means ± S.E.M. (n=5) of currents averaged over 1 minute intervals.

2.7mM. The K^+-stimulated flux was calculated as the difference between stimulated and resting flux.

Figure 3.40 shows a bar graph for the K^+-stimulated flux in cells incubated for 24 hours with either the control mAb or 11.14 test mAb. In each case the flux plotted is the mean from 8 experiments. There was a significant reduction ($p < 0.05$) in the K^+-stimulated calcium flux by mAb 11.14 as compared with controls, consistent with the effect seen in the electrophysiological recordings.

In the second batch of experiments further monoclonal antibody preparations were tested for their effect on the K^+-stimulated calcium flux in these cells. All had previously been tested for their effect on the whole cell currents in these cells. Figure 3.41 shows a bar graph of the K^+-stimulated calcium flux measured in control mAb treated and test mAb treated cells (11.3, 11.15, 11.23, 11.29). None of these mAbs showed a significant effect on the K^+-stimulated calcium flux in these experiments, consistent with their lack of effect in the electrophysiology experiments above. However standard errors are quite large due to lack of antibodies for large scale repetitive testing.

Also shown (Figure 3.41) are results for the cells treated with verapamil (10μM) in the presence of control mAb. These cells show a significant decrease in the K^+-stimulated calcium flux as compared with controls ($p < 0.005$). This indicates that verapamil can inhibit the voltage-dependent calcium current measured in these experiments. It therefore appears that the currents in these experiments are probably carried predominantly by L-type channels which are blocked by verapamil. However the stimulated flux measured in the presence of verapamil was in fact negative indicating that verapamil is also partially blocking the resting flux. Finally mAb 11.14

Table 3.8 Effect of mAb 11.14 on unstimulated ^{45}calcium flux.

Treatment	Unstimulated flux (nmoles Ca^{2+}/plate)
Control	0.504 ± 0.047
mAb 11.14	0.587 ± 0.054

Values represent unstimulated flux (mean ± S.E.M. of 8 experiments) in control or mAb 11.14 treated differentiated NG 108 15 cells. Monoclonal antibody 11.14 had no significant effect on the unstimulated ^{45}calcium flux as compared with control treated cells.

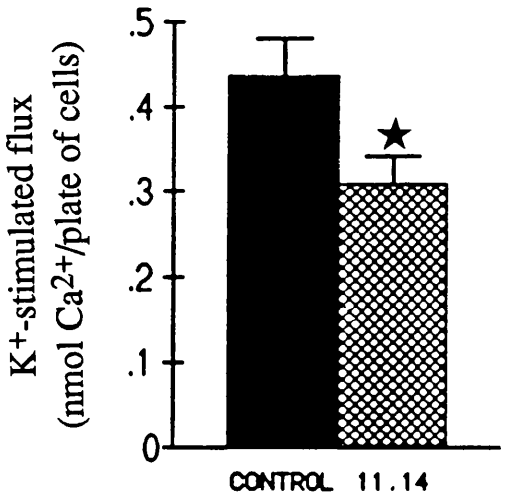

Legend for Figure 3.40 Effect of mAb 11.14 on potassium-stimulated ^{45}calcium flux. This figure shows a plot of potassium-stimulated ^{45}calcium flux measured in 8 control (filled bar) and 8 monoclonal antibody 11.14 (criss-cross bar) treated experiments with differentiated NG 108 15 cells. Values plotted are means ± S.E.M.. Significant reduction by mAb 11.14 as compared with controls: ★ $p < 0.05$.

Table 3.9 Effect of mAbs and verapamil on unstimulated ^{45}calcium flux.

Treatment	Unstimulated flux (nmoles Ca^{2+}/plate)
Control	1.20 ± 0.35
mAb 11.3	0.867 ± 0.062
mAb 11.15	0.849 ± 0.063
mAb 11.23	0.76 ± 0.13
mAb 11.29	1.039 ± 0.073
Control + verapamil (10μM)	1.04 ± 0.10
mAb 11.14 + verapamil (10μM)	0.88 ± 0.12

Values represent unstimulated flux (mean ± S.E.M. of 6 experiments for each treatment, except mAb 11.29 where n=5) in control or test treated differentiated NG 108 15 cells. There were no significant effects on the unstimulated ^{45}calcium flux by any treatment as compared with control treated cells.

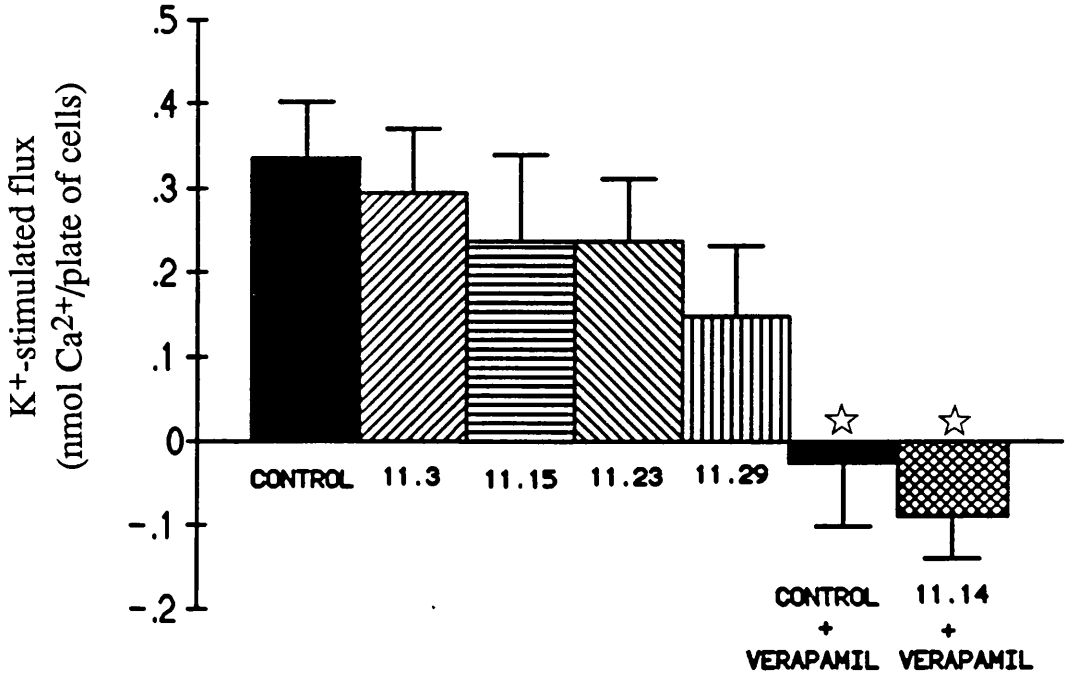

Legend for Figure 3.41 Effect of mAbs and verapamil on potassium-stimulated ^{45}calcium flux.

This figure shows a plot of potassium-stimulated ^{45}calcium flux measured in control (filled bar) and monoclonal antibody treated differentiated NG 108 15 cells. Values plotted are means ± S.E.M. of 6 repeats for each treatment except 11.29 where n=5. Significant reduction by verapamil (10μM + control mAb) treatment as compared with control treated cells (☆ $p < 0.005$).

that reduced the K^+-stimulated flux above was tested in the presence of verapamil. There was no significant difference between the K^+-stimulated calcium flux in verapamil treated cells (plus control mAb) and mAb 11.14 treated cells also in the presence of verapamil. This indicates that the effect of this antibody is on verapamil-sensitive channels i.e. L-type. This result is again consistent with the electrophysiology in which this mAb, capable of reducing currents, had no effect in the presence of a dihydropyridine antagonist, which like verapamil blocks L-type channels.

In summary, these results confirm the earlier findings that the binding of mAb 11.14 can inhibit the functioning of L-type channels whilst none of the other antibodies have any effects.

VIII. Discussion

In this chapter the effect of various monoclonal antibodies raised against the α_2 subunit of the dihydropyridine-sensitive calcium channel from rabbit skeletal muscle were investigated in NG 108 15 cells. In order to do this, the channel types present in differentiated NG 108 15 cells were firstly investigated. The findings show that channels were present with properties resembling a low threshold T-type, a high threshold L-type together with a third high threshold type which was dihydropyridine-insensitive. Secondly, it has been shown that following 24 hour incubation, one of the monoclonal antibodies raised against the α_2 subunit (mAb 11.14) inhibited dihydropyridine-sensitive L-type channels but not the remaining channel types in the cells. This monoclonal antibody also appeared to increase the rate of activation of the total inward current whilst the voltage sensitivity of the channels was unaffected. Other mAbs against the α_2 subunit had no effect on the channels present in either

undifferentiated or differentiated NG 108 15 cells. Finally mAb 11.14 appeared not to have an affect when applied acutely, suggesting that the effect may be due to a longer term loss of function possibly by down-regulation.

The reduction in calcium channel current by mAb 11.14 applied for 24 hours was confirmed in the potassium-stimulated ^{45}calcium flux studies, as was the lack of effect of the antibodies in the presence of a calcium channel antagonist. This is in agreement with an effect (Kowalski *et al.*, 1990) found for the same mAb on aortic smooth muscle cells, in which it produced an inhibition of calcium flux with no further effect being seen in the presence of 10μM nitrendipine.

As just summarised, three channel types were present in the differentiated NG 108 15 cells. More specifically, there was a low threshold transient component which showed almost complete steady-state inactivation at depolarised holding potentials resembling a T-type channel, a high threshold dihydropyridine-sensitive component resembling L-type, and a high threshold dihydropyridine-insensitive component. This dihydropyridine-insensitive component of current although still activated from a holding potential of -40mV like an L-type current, also clearly showed a high degree of steady-state inactivation more characteristic of an N-type current. A similar high threshold dihydropyridine-insensitive component has been found in other studies on NG 108 15 cells chemically differentiated by the same method as used in these experiments (Docherty, 1988). In the latter studies, evidence for the presence of a third type of current in addition to T- and L-type currents was provided by the selective block of a transient, high threshold component by both gadolinium and noradrenaline (Docherty & McFazdean, 1987; Docherty, 1988). This component has a very slow inactivation rate, is dihydropyridine-insensitive (Docherty & McFazdean, 1989), shows

steady-state inactivation at holding potentials more positive than about -70mV (Docherty & McFazdean, 1987) and has been compared to the slowly inactivating variant of the N-type current reported in sympathetic neurons (Brown, Docherty & McFazdean, 1989). This current may correspond to the slowly inactivating (i.e. sustained), dihydropyridine-insensitive component seen in these experiments. However, N-type currents are usually relatively transient with an inactivation rate in between that of T- and L-type (Tsien *et al.*, 1988) and no such transient component was seen. Indeed, results found for I_{diff} at a holding potential of -80mV gave no indication of a second transient component, while I_{diff} reached a maximum at a test potential of around -15mV which is more characteristic of T-type currents than N-type and there were no other peaks or shoulders in the I-V curve.

In conclusion it appears that the dihydropyridine-insensitive sustained component of current seen in these experiments may be a more sustained variant of the N-type current. Further experiments using the possibly selective N-type channel blocker ω-conotoxin, would be needed to confirm this. However, a recent paper using forskolin-differentiated NG 108 15 cells has shown that ω-conotoxin only blocked a component of the dihydropyridine-sensitive current and when applied in the presence of a dihydropyridine, a small component of current was left unblocked (Werth, Hirning & Thayer, 1991). It is therefore possible that the high threshold dihydropyridine-insensitive component observed in the above experiments in fact corresponds to this ω-conotoxin-insensitive component and is not a variant of the N-type channel.

The lack of complete block of the sustained component even at depolarised potentials (where inhibition should be maximal, Sanguinetti & Kass, 1984), is in

contrast to the situation in undifferentiated NG 108 15 cells where this concentration of nitrendipine caused complete block (Peers *et al.*, 1990). The concentration of nitrendipine used here is indeed sufficient to cause complete block of L-type channels when they are the only type of high threshold component present (as in undifferentiated cells).

Experiments in this chapter have shown that mAb 11.14, after 24 hours incubation, can inhibit dihydropyridine-sensitive L-type channels; however no effect was seen on T-type channels nor on the dihydropyridine-insensitive high threshold component. This might have indeed been expected since the antibodies were raised against the dihydropyridine-sensitive channels from skeletal muscle which are comparable with L-type. However the α_2 subunit has been shown to be present in certain channels other than L-type, for example in the N-type channel from mammalian brain (Ahlijanian, Striessnig & Catterall, 1991). Therefore it does show that there must be antigenic differences between the α_2 subunit from L-type channels and the other channel types (if indeed it is present in other channel types in NG 108 15 cells). Antigenic differences between T- and L-type channels have previously been deduced from the effect of LEMS IgG on the channels present in undifferentiated NG 108 15 cells (Peers *et al.*, 1990). LEMS IgG caused an effect comparable with that seen for mAb 11.14; a decrease in the L-type current with no effect on T-type. However in contrast to this, an antibody raised against the α_1 subunit of the L-type channel has revealed an effect on T- type channels (Wilson *et al.*, 1991), suggesting that regions of antigenic similarity must also exist between the channel types. Indeed the α_1 subunit has been shown from cloning studies to be very similar in the dihydropyridine-sensitive L-type channels (skeletal, cardiac and smooth muscle) and

the dihydropyridine-insensitive ω-conotoxin-insensitive channel from brain (Mori *et al.*, 1991).

Monoclonal antibody 11.14 (termed α-DHP-R 14) has also been shown to reduce dihydropyridine-sensitive ^{45}calcium flux in cultured rat aortic smooth muscle cells (Kowalski *et al.*, 1990). This effect on dihydropyridine-sensitive calcium channels in both neuroblastoma and smooth muscle cells along with the cross-reactivity of this antibody between tissues seen in immunoblots (Norman *et al.*, 1987), suggests that mAb 11.14 may bind to a region common to many L-type channels. In addition this antibody still recognizes the SDS-denatured α_2 subunit in immunoblots, which shows that its binding is not dependent on conformation, indicating that it probably recognizes a discrete binding site in the primary sequence (Norman *et al.*, 1987).

From both the recordings of whole cell calcium channel currents and the potassium-stimulated calcium flux studies it appears that the effect of monoclonal antibody 11.14 on the L-type channel is irreversible, since in both cases complete exchange of the culture media containing the antibody was made before recording and so any unbound antibody would have been washed off.

As already mentioned, in contrast to the long-term (24 hour) incubation, acute application of monoclonal antibody 11.14 to the differentiated NG 108 15 cells produced no significant effects. This apparently suggests that the effect of the binding of this monoclonal antibody to the α_2 subunit is not due to a direct pharmacological block of channel function. The long term effect may be due to a mechanism such as cross-linking of the channels leading to their down-regulation; such a mechanism has previously been proposed for the effect of myasthenic syndrome antibodies on L-type

channels (Peers *et al.*, 1990). The α_1 subunit may be down-regulated with the α_2 subunit due to the two being closely associated to cause the loss of channel function. Alternatively, the antibody may cause the loss of only the α_2 subunit leaving the α_1 subunit intact but conducting less current. Co-expression studies (see Introduction) have shown that calcium channel activity is greater when the skeletal muscle α_2 subunit is co-expressed in combination with the α_1 subunit (from brain, cardiac muscle or smooth muscle) than when the α_1 subunit is expressed alone (Mori *et al.*, 1991; Mikami *et al.*, 1989; Biel *et al.*, 1990). Although this could be due to increased expression of the α_1 subunit when co-expressed with the α_2 subunit, these studies have not ruled out the possibility that this is a consequence of the α_2 subunit modulating single channel properties (Mori *et al.*, 1991).

Alternatively the lack of effect of the antibody in the acute studies may be caused by the antibody having limited access to its binding site which may be partially occluded in these neuroblastoma cells and so a longer time period than 10 minutes may have been needed for sufficient antibody binding to occur. Indeed it is clear that different isoforms of the dihydropyridine-sensitive calcium channel occur in neuroblastoma cells and in skeletal muscle cells (against which the antibodies were raised) from the differences in rate of activation of the two channel types (Beam, Tanabe & Numa, 1989).

Antibodies raised against the skeletal muscle α_1 subunit have been found to inhibit the slow dihydropyridine-sensitive current seen in BC_3H1 cells (Morton *et al.*, 1988), an effect which is similar to that seen with mAb 11.14 on the dihydropyridine-sensitive (L-type) current in differentiated NG 108 15 cells. However, unlike mAb 11.14, the maximum effect of the anti-α_1 antibodies was reached within 10 minutes

of application and so appeared to be a direct consequence of binding to a functionally important component of the channel.

Monoclonal antibody 11.14 caused a significant decrease in the time to peak at some test potentials. This effect was observed over a range of potentials at which all three channel types could be contributing partially to the peak current. However there was no effect in the presence of nitrendipine indicating that the effect was probably due to an action on L-type channels. An effect such as this on the activation rate of the channels would be a direct effect (as opposed to down-regulation) and therefore would have been expected to occur with acute application of the antibody. The lack of observation of such an acute effect could possibly again be due to a slow reaction time of the antibody in these cells. However the effect seen after 24 hour incubation on time to peak could also be an indirect effect due to the block of the L-type channels. The time to peak of the current will generally be determined by the slowest activating current so long as its amplitude is not small. Therefore if the L-type current has a slower activation rate than the other components present, this effect may simply be due to block of this component. In contrast to this though, LEMS IgG, which produces a similar reduction in L-type current, has no effect on the time to peak current (Peers *et al.*, 1990).

Apart from monoclonal antibody 11.14, six other antibodies which had been raised against the purified α_2 subunit were tested for their effects on the calcium channel currents in NG 108 15 cells. None of these produced any significant effects on inward calcium channel currents after 24 hours incubation. This could be due to the regions to which these antibodies bind not being important functionally or to the antibodies being unable to bind to the channels. Data establishing the region of antibody binding on the

subunit is not available, therefore it is also quite possible that the antibodies may bind to sites on the α_2 subunit not exposed when the channel is in place in the membrane, since the antibodies were raised against purified α_2 subunit. Another possible reason for the lack of effect of these antibodies on the calcium channels in the NG 108 15 cells is that there may be antigenic differences (probed by the antibodies) between channels in these neuroblastoma cells and the channels in the transverse tubular membranes of skeletal muscle against which they were raised.

As stated above, the mAbs were raised against purified α_2 subunit. In immunoblots of SDS gels using denatured t-tubule membranes, only mAbs 11.14 and 11.15 specifically stained a polypeptide of 140kDa molecular weight under reducing conditions (i.e. α_2) and 165-170kDa under non-reducing conditions (i.e. $\alpha_2\delta$). The other five antibodies have only been shown to definitely bind to the purified dihydropyridine receptor by ELISA (Norman *et al.*, 1987). This lack of binding on immunoblots could possibly be due to SDS gels being denaturing (unlike ELISA) and may indicate that binding of these mAbs requires the α_2 subunit to be conformationally undisturbed. It is therefore possible that these five mAbs are much more dependent on structure for their binding, and so small differences across species and tissue may be more important, leading to weak cross-reactivity.

Although the dihydropyridine-sensitive calcium channel complex from the transverse tubules of skeletal muscle has been proposed to be composed of five subunits (α_1, α_2, ß, γ and δ) there has been some suggestion that the α_2 subunit may not have a role in the complex due to its apparent weak association with the α_1 subunit (Froehner, 1988). In summary, the studies in this chapter, suggest that the α_2 subunit exists in the L-type channel seen in the NG 108 15 cells and is in close

association with the α_1 subunit in which the channel pore is proposed to be located (Tanabe *et al.*, 1987). The effects seen with mAb 11.14 could be interpreted in terms of down-regulation of L-type channels, although a direct modulation of the channel by the α_2 subunit may also have been present.

CHAPTER 4

THE EFFECTS OF MONOCLONAL ANTIBODIES ON CALCIUM CHANNELS IN MOUSE MUSCLE (BC_3H1) CELLS

I. Introduction

In the last chapter the investigations showed a possible functional role for the α_2 subunit within the calcium channel complex in neuroblastoma cells. Further investigations on the effect of the same anti-α_2 monoclonal antibody 11.14 on calcium channel currents are reported in this chapter using a different cell line, BC_3H1. This was chosen because it is a muscle cell line in which the calcium channel currents hopefully more closely resemble those seen in skeletal muscle (see Introduction) against which the antibodies were raised. In the following experiments whole cell patch clamp recordings were made from these cells. After determining the types of calcium channel present (by experiments using different holding potentials and a dihydropyridine antagonist), experiments were carried out to study the effects of mAb 11.14 on channel function. The antibody was applied either for 24 hours or acutely in the bath. Results were compared with effects of mAb 11.6 which had no effect on the neuroblastoma cells.

II. Effect of holding potential on whole cell calcium channel currents in BC_3H1 cells

Experiments were firstly carried out in order to find the most appropriate holding potential for the investigations with the antibody on the BC_3H1 cells and also to give an indication of the channel types present in these cells. For this, inward

calcium channel currents were recorded in these cells at a number of different membrane holding potentials. Currents were recorded in response to depolarizing steps of duration 300 ms, at a frequency of 0.1Hz.

Examples of the calcium channel currents evoked from untreated BC_3H1 cells are shown in figure 4.1. In these cells, when the membrane potential was held at -80mV, with fairly small depolarizing steps, for example to -30mV, only a very small current was present. This current was sustained, inactivating very little during the 300ms pulse. With larger depolarising steps, for example to +10mV, a much larger component of current was observed. This current was slowly inactivating rather like the small component, but in addition had a slower activation rate. At a holding potential of -40mV only the small faster activating component was present.

Figure 4.2 shows I-V curves of the sustained current measured near the end of the pulse (see Methods) at various holding potentials. Steady-state inactivation can clearly be seen at holding potentials which are more positive than -90mV, with almost complete inactivation at -40mV (Figure 4.3A). Therefore it appears that in these cells the major component of current is inactivated at a membrane holding potential of -40mV. At a holding potential of -100mV, there appeared to be a decrease in the amplitudes of the sustained currents compared with those evoked from a holding potential of -90mV but there were large standard errors and the differences were not significant.

If only one calcium channel component were elicited in the experiments, the position of the test potential for maximal inward current should not change. However, there was a progressive shift towards more positive values for this test potential with more depolarised holding potentials (Figure 4.2, Table 4.1). The potential at which the

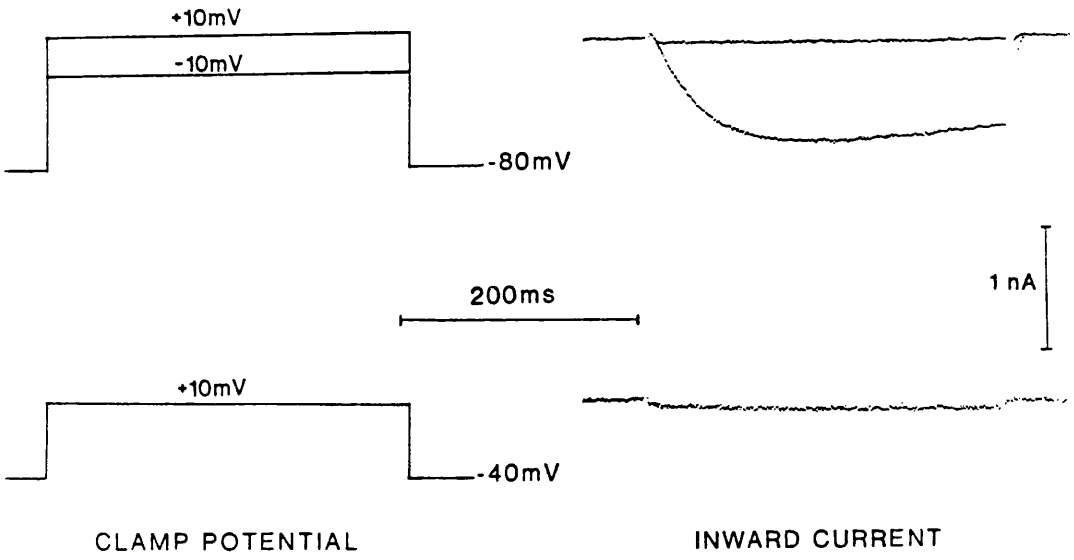

Legend for Figure 4.1 Examples of whole cell calcium channel currents in a differentiated BC_3H1 cells.

Calcium channel currents were evoked in an untreated, differentiated BC_3H1 cell in response to 300ms test depolarisations. Current traces (right) were evoked at different clamp potentials (left). Leakage and capacitance currents have been subtracted.

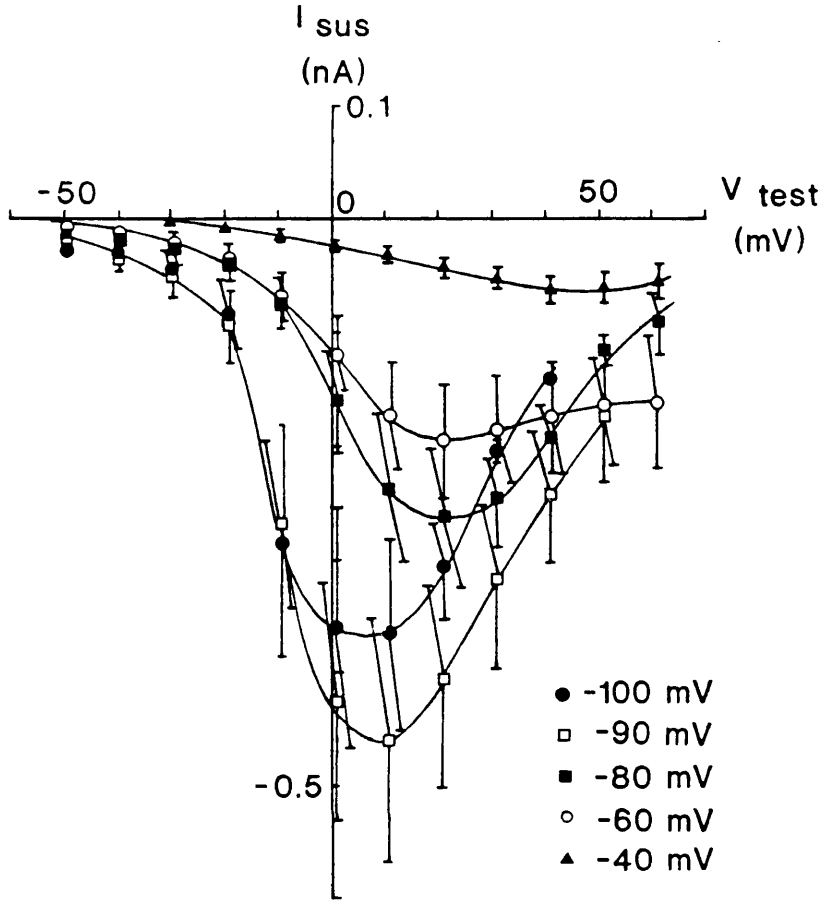

Legend for Figure 4.2 Effect of holding potential on sustained current amplitude.

This figure shows the sustained current amplitude (I_{sus}) plotted versus test membrane potential (V_{test}), measured in untreated BC_3H1 cells held at various membrane holding potentials. Currents were evoked from membrane holding potentials of: ●-100mV, □-90mV, ■-80mV, ○-60mV and ▲-40mV. The values plotted are means ± S.E.M. for 3-7 cells. Curves were fitted by eye to each set of data.

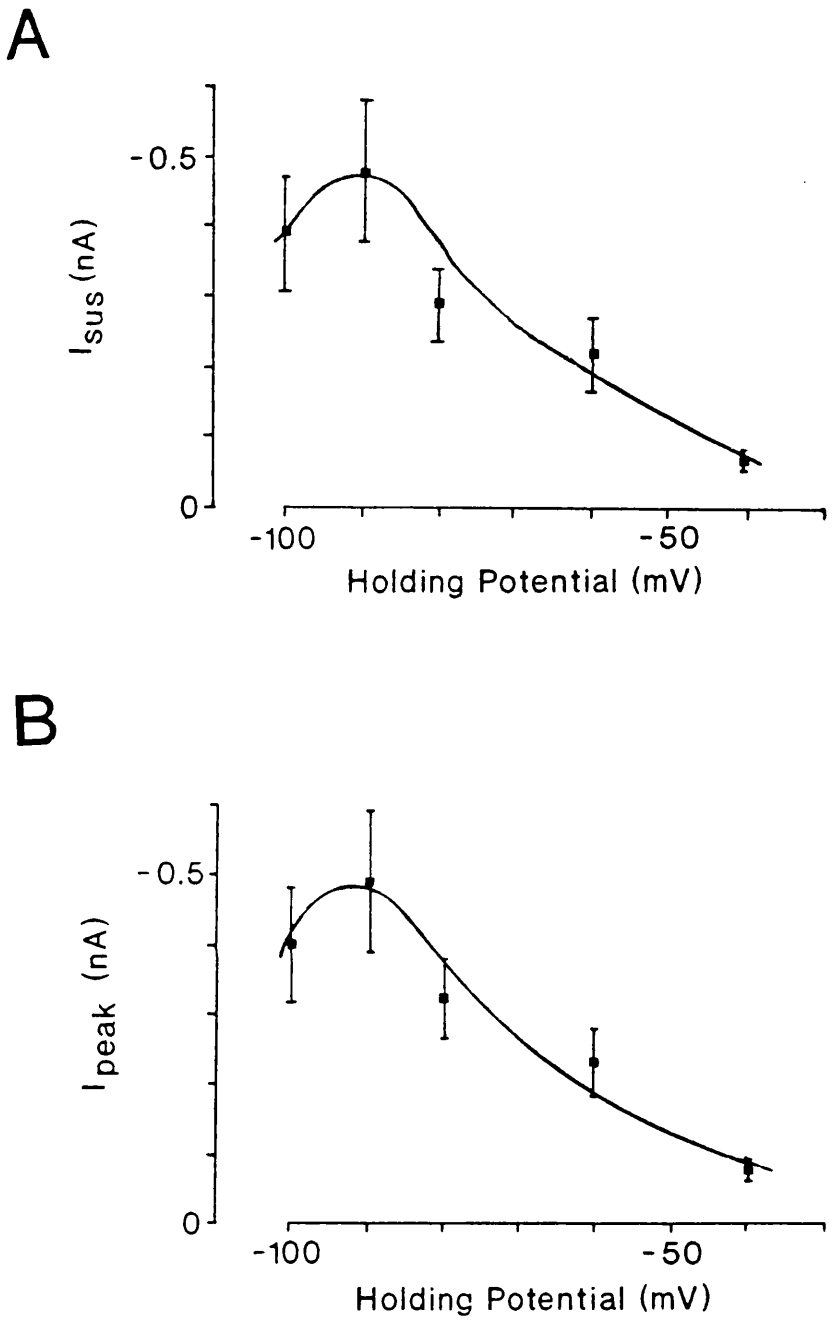

Legend for Figure 4.3 Steady state inactivation of: A. Sustained current, B. Peak current.

The mean ± S.E.M. for 3-7 cells of the maximum sustained current (A) and peak current (B) obtained from original I-V curves plotted against the holding potential from which they were measured. Lines were fitted by eye.

Table 4.1

Effect of holding potential on the test membrane potential at which mean inward calcium channel currents were maximal in BC_3H1 cells.

Holding Potential (mV)	Test potential at which currents were maximal (mV)	
	I_{sus}	I_{peak}
-100	7.7 ± 6.6 (3)	7.7 ± 6.7 (3)
-90	9.0 ± 3.8 (3)	9.0 ± 3.8 (3)
-80	22.7 ± 4.0 (7)	23.6 ± 4.3 (7)
-60	29.8 ± 10.3 (4)	30.0 ± 10.2 (4)
-40	40.4 ± 4.2 (7)	41.4 ± 4.2 (7)

Legend for Table 4.1 Effect of holding potential on the test membrane potential at which mean inward calcium channel currents were maximal in BC_3H1 cells.

This table shows the test potentials at which the mean inward calcium channel currents were maximal for untreated BC_3H1 cells held at various membrane holding potentials. Values given are means S.E.M., averaged in each case from the number of individual current-voltage plots shown in brackets. Significant differences in test potential at which both I_{sus} and I_{peak} were maximal occurred from a holding potential of -40mV as compared with -100mV, -90mV or -80mV ($p < 0.05$).

maximal sustained inward current occurred at a holding potential of -40mV was significantly different from at -100, -90 or -80mV, indicating the presence of more than one component of current.

The I-V curves for the peak current amplitude are shown in figure 4.4. Again steady-state inactivation can clearly be seen at holding potentials more positive than -90mV and the steady-state inactivation curve (figure 4.3B) is similar for both peak and sustained currents. This is different from the situation seen in NG 108 15 cells and suggests that both the peak and sustained currents are composed of the same type(s) of channel. Again there was a decrease in the amplitude of the peak current from a holding potential of -100mV, but standard errors are large.

The similar values for I_{peak} and I_{sus} indicate that no transient component of current is present. Therefore the current seen with small depolarising steps does not appear to be a transient T-type current. With larger depolarising steps a sustained current was seen with a maximal activation at around +10mV which would suggest an identification as an L-type current. However this current was almost totally inactivated at a holding potential of -40mV unlike L-type currents. The channel is slowly activating and is similar to the "slow" channel previously described by Caffrey *et al.*, 1987.

As for the measurements of I_{sus}, there was a shift to more positive potentials for maximal activation of I_{peak} as holding potential was more depolarised (Table 4.1), again indicating the presence of more than one component. Also it is clear from Table 4.1 that sustained and peak currents are maximal at approximately the same test potentials (i.e. the differences are non-significant) again indicating that the channels contributing to the peak current have the same voltage dependence as those which

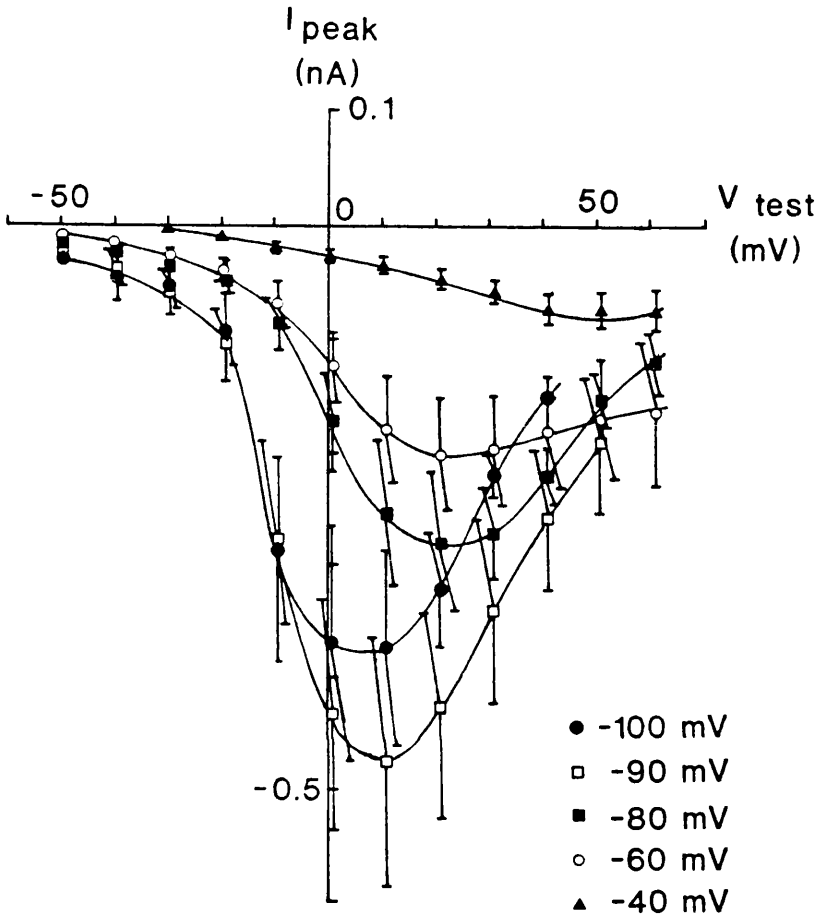

Legend for Figure 4.4 Effect of holding potential on peak current amplitude.

Plot of peak current amplitude (I_{peak}) versus test membrane potential (V_{test}), measured in untreated BC_3H1 cells held at various membrane holding potentials. Currents were evoked from membrane holding potentials of: ●-100mV, □-90mV, ■-80mV, ○-60mV and ▲-40mV. The values plotted are means ± S.E.M. for 3-7 cells. Curves were fitted by eye to each set of data.

produce the sustained current suggesting that both are composed of the same components of current.

For the rest of the experiments a holding potential of -80mV was chosen, since at this holding potential the slowly activating current was still appreciably activated without having to use a very negative holding potential which made recordings unstable.

In summary two sustained components of current appear to be present in these BC_3H1 cells. A small fast activating low threshold component and a much larger slowly activating high threshold component.

III. Effect of nitrendipine on whole cell calcium channel currents in BC_3H1 cells

The channel types present in the cells were studied further by investigating the effect of a dihydropyridine on the currents. Whole cell calcium channel currents were recorded from 26 untreated BC_3H1 cells and 25 cells in the presence of 5μM nitrendipine in the extracellular recording solution. The cells were voltage clamped at a membrane holding potential of -80mV and currents were recorded in response to depolarizing steps at a frequency of 0.1Hz as above.

Figure 4.5 shows I-V curves for the sustained current (I_{sus}) measured at a holding potential of -80mV. There were significant reductions in the sustained current by 5μM nitrendipine as compared with controls, between test potentials of -10 and +50mV i.e over the range for which the major slowly activating calcium channel current type (described above) was clearly activated. The cells recorded in the presence of nitrendipine showed a small fast activating inward current. This small dihydropyridine-resistant current was of a similar magnitude and voltage-dependence to that observed

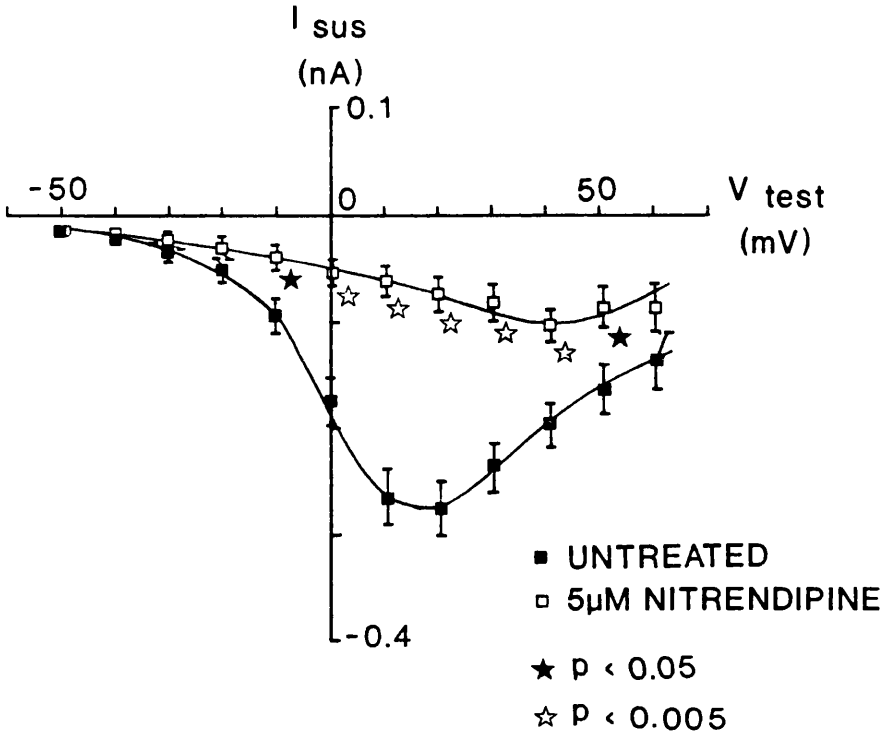

Legend for Figure 4.5 Effect of nitrendipine on sustained current.

This figure shows the sustained current amplitude (I_{sus}) plotted versus test membrane potential (V_{test}), measured in 26 untreated (■) BC_3H1 cells and 25 BC_3H1 cells in the presence of 5μM nitrendipine (□). All currents were evoked from a membrane holding potential of -80mV and values plotted are means ± S.E.M.. Curves were fitted by eye. Significant reductions in sustained current amplitude in cells treated with nitrendipine as compared with untreated cells: ★ $p < 0.05$, ☆ $p < 0.005$.

at a holding potential of -40mV in untreated cells. Therefore this provides further evidence that there are two components of sustained current in these cells.

Figure 4.6 shows the I-V curve for the peak current amplitude measured from the same cells as the sustained currents plotted in figure 4.5. There were again significant decreases in peak inward current in cells in the presence of 5μM nitrendipine compared with the untreated cells. This is expected since the cells do not have a transient component of current. The dihydropyridine-insensitive component was again similar to that in untreated cells at -40mV. Therefore it again appears that there are two components of current present in these cells: a dihydropyridine-insensitive current which is not inactivated at steady-state by depolarised holding potentials and a dihydropyridine-sensitive current (i.e. like L-type) which is inactivated at steady-state by depolarised holding potentials (unlike L-type).

The time to peak of the inward current is shown in figure 4.7. The times to peak show a bell-shaped curve when plotted versus test potential. This indicates that with small depolarising steps the activation rate is fast and slows as the test potential becomes more depolarised which would be consistent with the presence of a low threshold rapidly activating component and a high threshold slowly activating component. There were significant reductions in the time to peak current in the presence of nitrendipine as compared with the untreated cells at the more depolarised test potentials. This suggests that the component of current blocked by nitrendipine is more slowly activating than the dihydropyridine-insensitive component.

In summary these results show that nitrendipine blocks the major component of current in these cells. This high threshold component is both slowly activating and inactivating, and shows steady-state inactivation by depolarised holding potentials. The

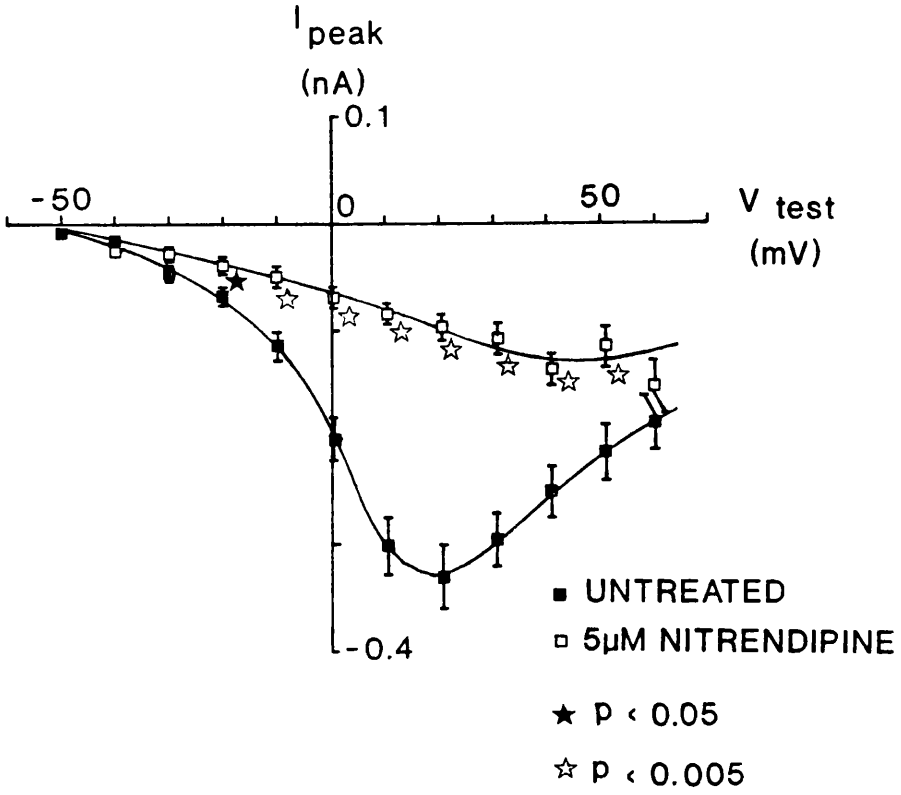

Legend for Figure 4.6 Effect of nitrendipine on peak current.

This figure shows a plot of peak current amplitude (I_{peak}) plotted versus test membrane potential (V_{test}), measured in 26 untreated (■) BC_3H1 cells and 25 BC_3H1 cells in the presence of 5μM nitrendipine (□). All currents were evoked from a membrane holding potential of -80mV and values plotted are means ± S.E.M.. Curves were fitted by eye. Significant reductions in peak current amplitude by nitrendipine as compared with untreated cells: ★ $p < 0.05$, ☆ $p < 0.005$. Data were obtained from the same cells as in figure 4.5.

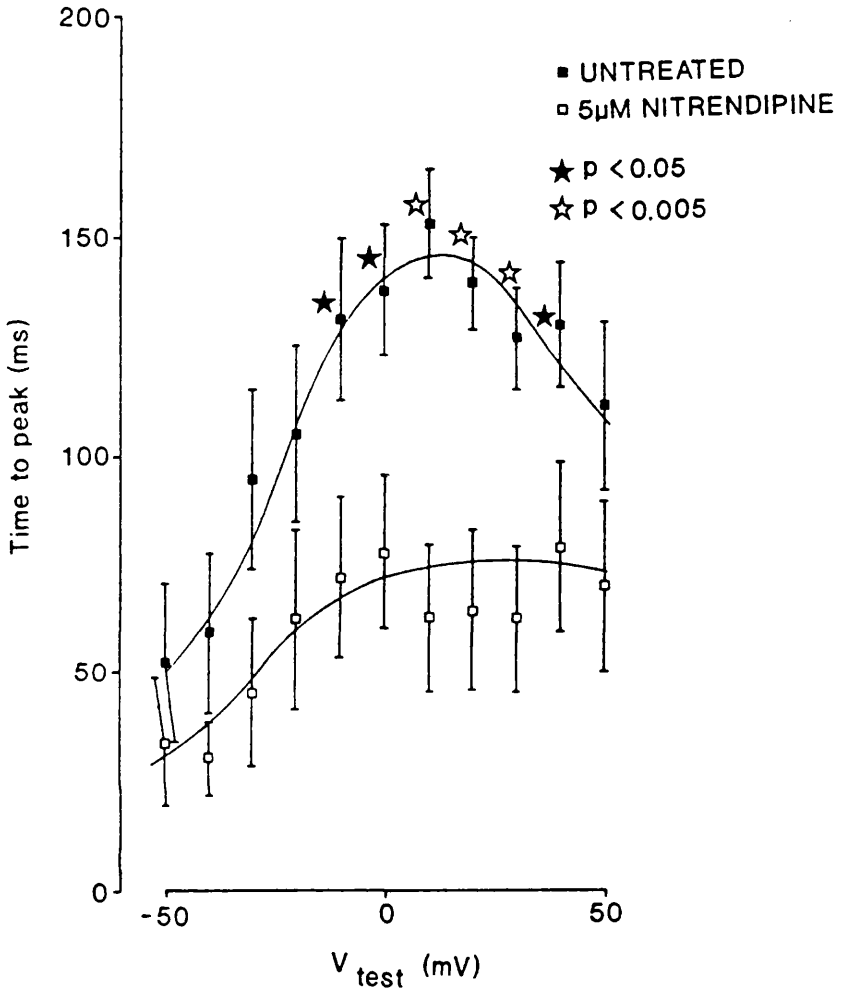

Legend for Figure 4.7 Effect of nitrendipine on time to peak current.

This figure shows a plot of time to peak current plotted versus test membrane potential (V_{test}), measured in 26 untreated (■) BC_3H1 cells and 25 BC_3H1 cells in the presence of 5μM nitrendipine (□). All currents were evoked from a membrane holding potential of -80mV and values plotted are means ± S.E.M.. Curves were fitted by eye. Significant reductions in time to peak current by nitrendipine as compared with untreated cells: ★ $p < 0.05$, ☆ $p < 0.005$.

smaller low threshold dihydropyridine-insensitive current is also slowly inactivating, but has a faster activation rate and does not show steady-state inactivation by depolarised holding potentials. The high threshold current is similar to an L-type current except in respect to steady-state inactivation. Therefore since neither current fits precisely into the T-, N-, and L-type classification they will be distinguished by their activation rates, with the dihydropyridine-insensitive current being referred to as the fast activating current and the dihydropyridine-sensitive component as the slowly activating calcium channel current.

IV. Effects of monoclonal antibodies on whole cell calcium channel currents in BC_3H1 cells

The effects of monoclonal antibody preparations mAb 11.14 (which gave an effect on NG 108 15 cells) and mAb 11.6 (which had no effect on NG 108 15 cells) were tested on BC_3H1 cells. Whole cell calcium channel currents were recorded in response to depolarizing steps of 300 ms duration from cells incubated in the presence of either the control or test monoclonal antibody for 24 hours prior to recording.

Figure 4.8 shows I-V curves for the sustained component of current measured from 25 control and 25 mAb 11.6 treated cells. The currents were evoked from a holding potential of -80mV. There were no significant differences in the sustained inward current by mAb 11.6 as compared with controls over the range of potentials tested. The test potentials at which the maximum sustained inward currents occurred were also not significantly different between control and mAb 11.6 treated cells. For controls, sustained inward currents were maximal at a test potential of $+15.6 \pm 2.0$mV (n=18) and for mAb 11.6 treated cells at a test potential of $+13.1 \pm 1.9$mV (n=22). It

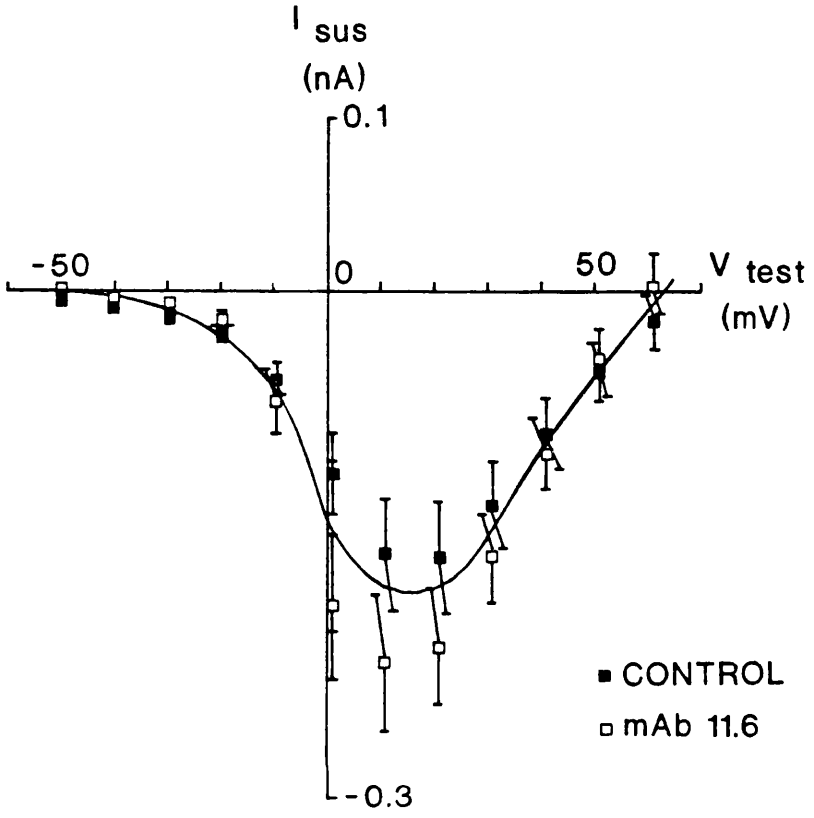

Legend for Figure 4.8 Effect of mAb 11.6 on sustained current.

Plot of sustained current amplitude (I_{sus}) versus test membrane potential (V_{test}), measured in 25 control (■) and 25 monoclonal antibody 11.6 (□) treated BC_3H1 cells. All currents were evoked from a membrane holding potential of -80mV and the values plotted are means ± S.E.M.. The monoclonal antibody 11.6 had no significant effects on the sustained current amplitude in these cells as compared with controls, so only one curve was fitted by eye through both sets of data points.

therefore appears that the mAb 11.6 has no effect on the sustained currents seen in these cells.

Although there was no transient component of current in these cells a possible change in the peak current amplitude was still investigated. Figure 4.9 shows I-V curves for the peak current amplitude measured from the same recordings as the sustained currents (Figure 4.8). There was no significant difference in the peak current amplitude in the test cells as compared with controls. The potential at which the maximum peak inward current occurred was similar to that found for the sustained currents. This again shows that both peak and sustained currents are probably composed of the same components of current. There was also no significant difference between this potential in the control cells (16.6 ± 2.0mV, n=18) and mAb 11.6 treated cells (14.5 ± 1.9mV, n=22).

The difference between the peak and sustained currents (I_{diff}) was calculated (see Methods) and a graph of this plotted against test potential, figure 4.10. There were significant increases in I_{diff} by mAb 11.6 as compared with controls at several test potentials. The capacitance adjusted currents (see Methods) showed a corresponding set of significant increases. Although there were no significant changes in the peak or sustained currents, a change in I_{diff} can occur due to this difference being very small compared with the actual current amplitudes. The increases in I_{diff} indicate very small changes in the current amplitudes either by partial block or possibly by a change in the kinetics of the channel.

Figure 4.11 shows the time to peak amplitude plotted versus test potential. There were no significant differences between the time to peak amplitude in the control antibody treated cells as compared with those treated with the test mAb 11.6.

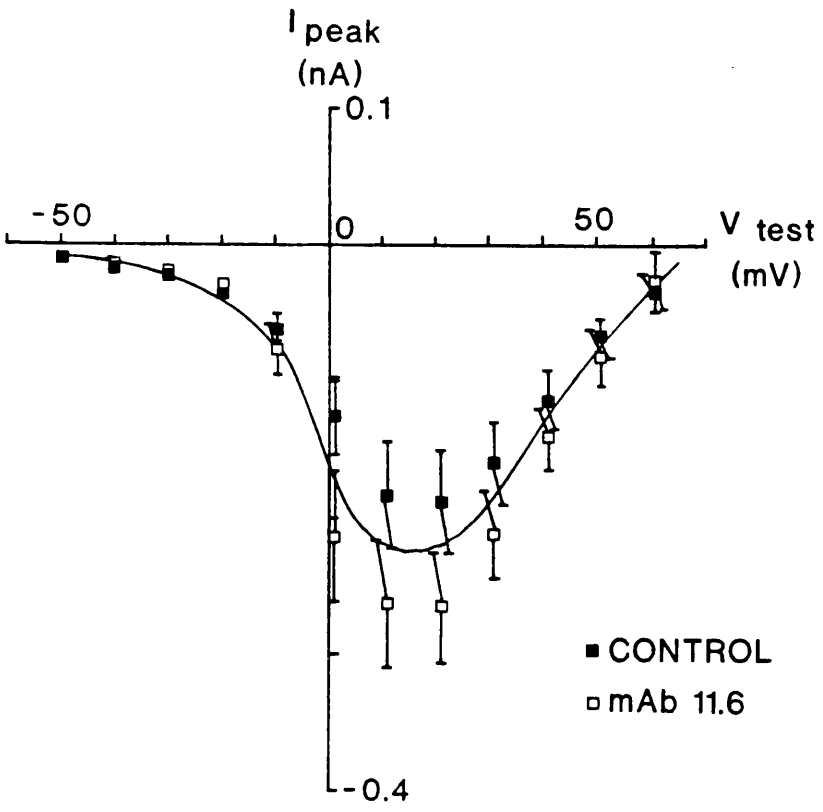

Legend for Figure 4.9 Effect of mAb 11.6 on peak current.

This figure shows the peak inward current amplitude (I_{peak}) plotted versus test membrane potential (V_{test}), measured in control (■) and monoclonal antibody 11.6 (□) treated BC_3H1 cells. All currents were evoked from a membrane holding potential of -80mV. The values plotted are means ± S.E.M from 25 control and 25 monoclonal antibody 11.6 treated cells. Monoclonal antibody 11.6 had no significant effect on peak current amplitude at any test potential studied, therefore one curve has been fitted by eye through all data points. Data were obtained from the same recordings as in Figure 4.8.

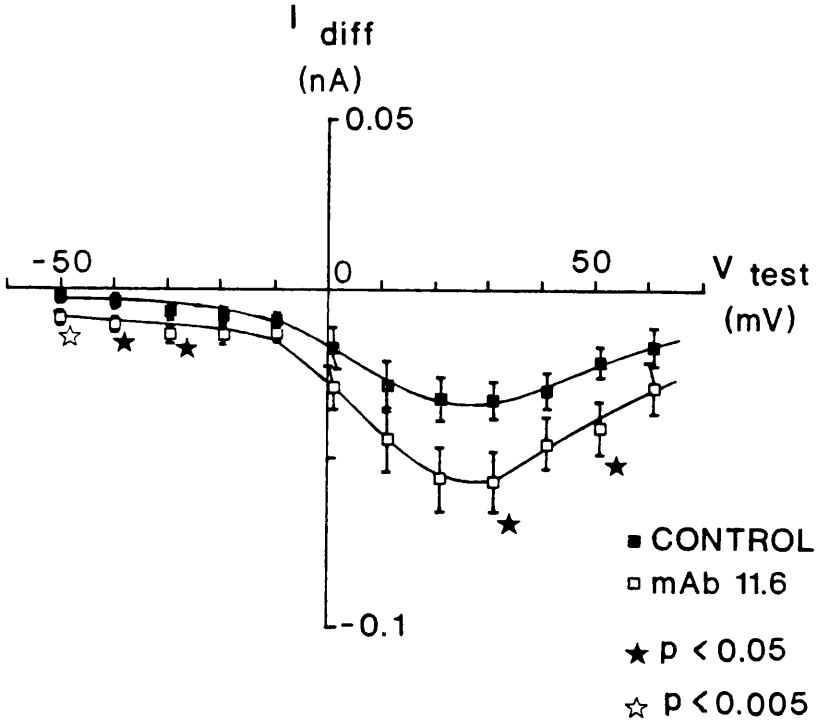

Legend for Figure 4.10 Effect of mAb 11.6 on I_{diff}.

This figure shows the difference between peak and sustained inward calcium channel current amplitudes (I_{diff}) plotted versus test membrane potential (V_{test}), measured in 25 control (■) and 25 monoclonal antibody 11.6 (□) treated BC_3H1 cells. All currents were evoked from a membrane holding potential of -80mV and the values plotted are means ± S.E.M.. Curves were fitted by eye. Values were obtained from the same cells as in figures 4.8 and 4.9. Significant increases in current amplitude by monoclonal antibody 11.6 as compared with controls: ★ $p < 0.05$, ☆ $p < 0.005$.

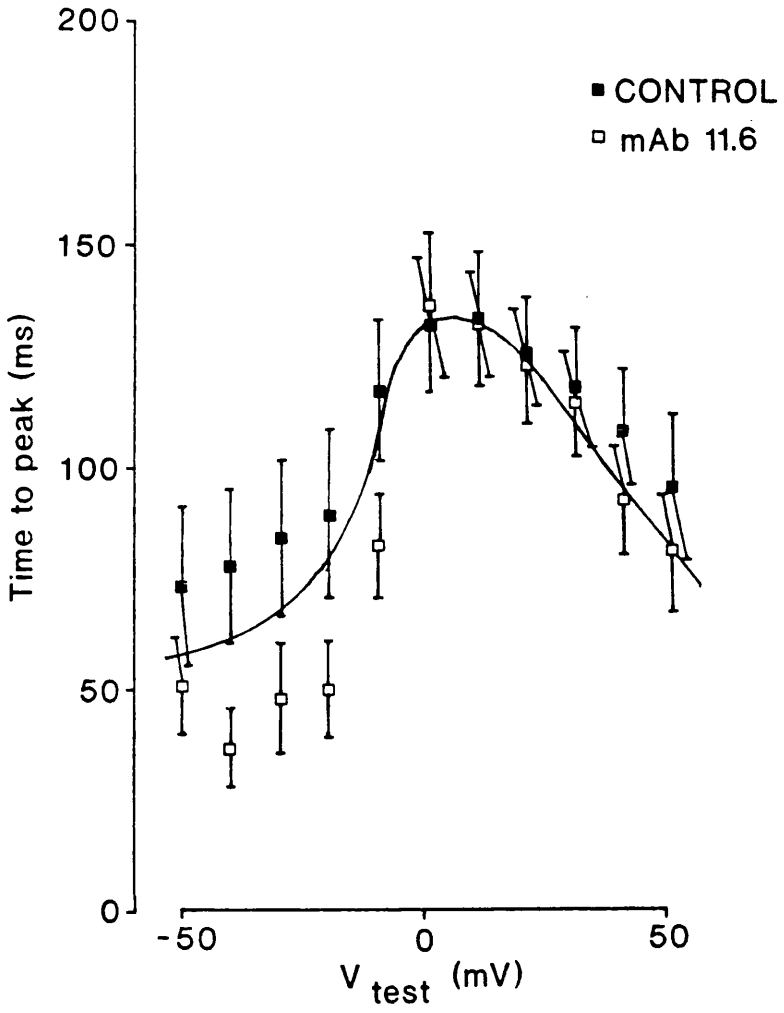

Legend for Figure 4.11 Effect of mAb 11.6 on time to peak current.

Plot of time to peak of inward calcium channel currents versus test membrane potential (V_{test}). Currents were evoked from a holding potential of -80mV. Values plotted are means ± S.E.M from 25 control (■) and 25 monoclonal antibody 11.6 (□) treated BC_3H1 cells. Monoclonal antibody 11.6 had no significant effect on times to peak at any test potential studied, therefore one curve has been fitted by eye through all data points. Data were obtained from the same recordings as in figures 4.8 and 4.9.

This indicates that mAb 11.6 had no effects on the activation rate of the inward calcium channel currents seen in these cells.

In summary the results shown in figures 4.8-4.11 show that mAb 11.6 had very little effect on the calcium channels seen in BC_3H1 cells.

I-V curves for the sustained component of current measured in control and mAb 11.14 treated cells at a holding potential of -80mV are shown in figure 4.12. The results are the means of those from 25 control cells and 26 test mAb 11.14 treated cells. The test mAb 11.14 caused decreases in the sustained inward current at the more positive test potentials, statistically significant at potentials of +40 and +50mV, indicating an effect on the high threshold slowly activating current but not the low threshold fast activating component. When the data was corrected for variations in cell size by taking into account cell capacitance a similar pattern of reductions of current by mAb 11.14 were seen (although at none of the potentials were the reductions statistically significant). The test potentials at which the maximum sustained inward currents occurred were not significantly different between the control mAb treated cells (+14.6 ± 2.0mV, n=24) and the 11.14 test mAb treated cells (+14.3 ± 2.1mV, n=24).

Figure 4.13 shows the I-V curve for the peak current amplitude measured in the same cells as the sustained currents (figure 4.12). In this case there was no significant change in the peak current amplitude in the test mAb 11.14 treated cells as compared with controls at any test potential. Nor was there a significant difference between the potential at which the maximum peak inward currents occurred between the control cells (+14.7 ± 1.9mV, n=24) and mAb 11.14 treated cells (+14.9 ± 1.9mV, n=24). This result shows that mAb 11.14 had no effect on either the fast or slowly

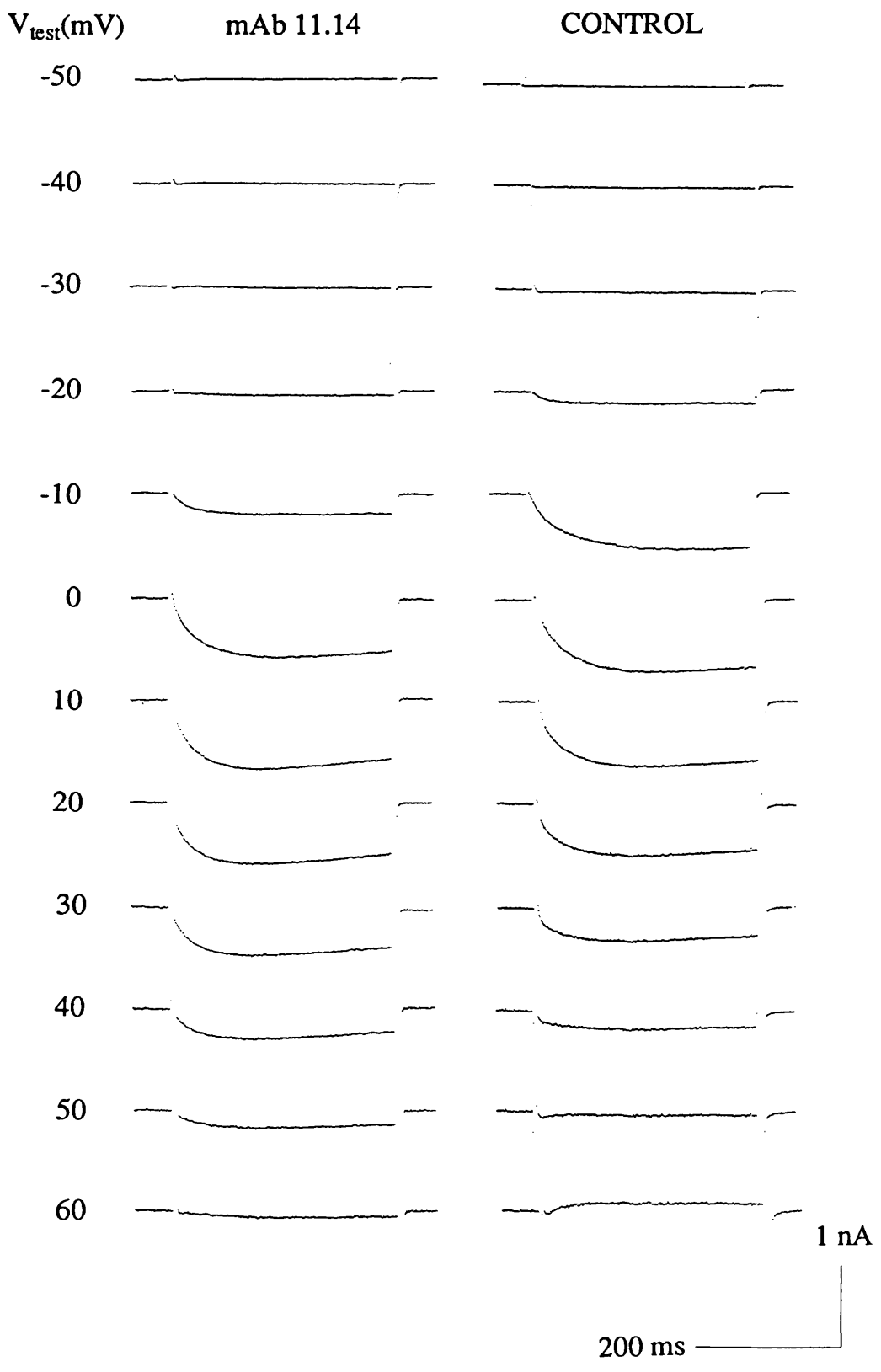

Examples of typical whole cell calcium channel currents in BC_3H1 cells treated with either control or mAb 11.14. The cells were held at a potential of -80mV. All records are leak and capacitance subtracted.

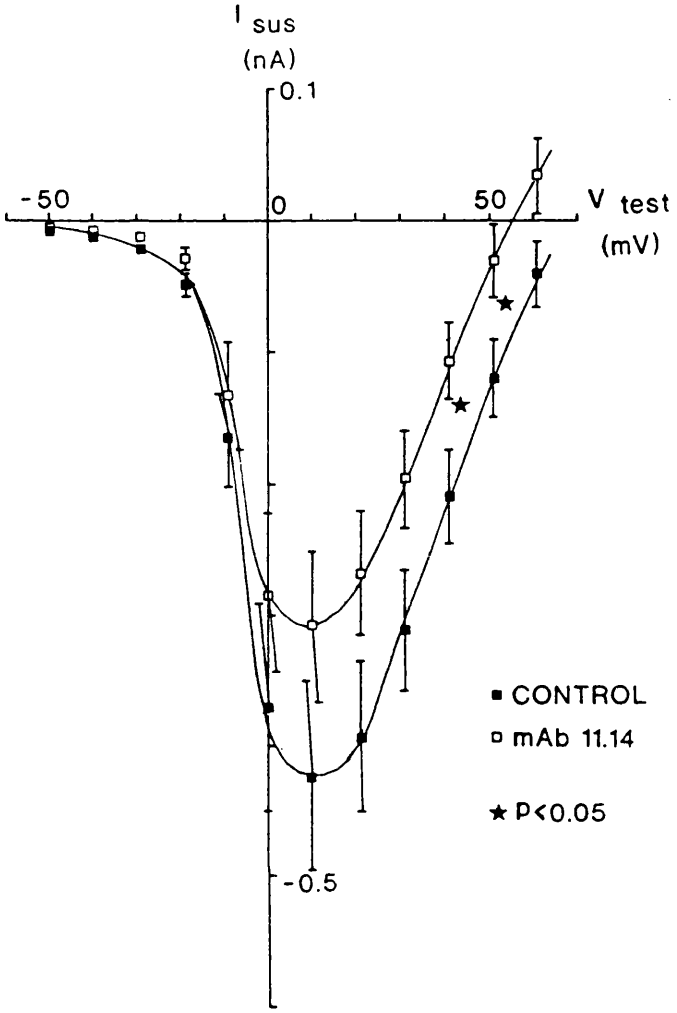

Legend for Figure 4.12 Effect of mAb 11.14 on sustained current.

This figure shows the sustained inward calcium channel current amplitude (I_{sus}) plotted versus test membrane potential (V_{test}), measured in 25 control (■) and 26 monoclonal antibody 11.14 (□) treated BC_3H1 cells. All currents were evoked from a membrane holding potential of -80mV and the values plotted are means ± S.E.M.. Curves were fitted by eye. Significant reductions in current amplitude by monoclonal antibody 11.14 as compared with controls: ★ $p < 0.05$.

Table 4.2 Effect of mAb 11.14 on capacitance adjusted sustained current (holding potential -80mV).

mAb 11.14		Control	
V_{test}±S.E.M.(mV)	I_{sus}±S.E.M.(AF^{-1})	V_{test}±S.E.M.(mV)	I_{sus}±S.E.M.(AF^{-1})
-49.55 ± 0.04	-0.05 ± 0.03	-49.59 ± 0.04	-0.05 ± 0.02
-39.40 ± 0.05	-0.07 ± 0.04	-39.51 ± 0.04	-0.10 ± 0.02
-29.26 ± 0.06	-0.11 ± 0.05	-29.34 ± 0.06	-0.17 ± 0.03
-19.15 ± 0.07	-0.26 ± 0.08	-19.27 ± 0.06	-0.36 ± 0.07
-9.02 ± 0.08	-1.04 ± 0.26	-9.17 ± 0.07	-1.20 ± 0.27
+1.10 ± 0.09	-2.16 ± 0.37	+0.95 ± 0.08	-2.43 ± 0.41
+11.18 ± 0.10	-2.40 ± 0.33	+10.99 ± 0.09	-2.88 ± 0.35
+21.26 ± 0.11	-2.13 ± 0.29	+21.08 ± 0.09	-2.72 ± 0.29
+31.38 ± 0.12	-1.56 ± 0.26	+31.16 ± 0.11	-2.16 ± 0.23
+41.43 ± 0.14	-0.83 ± 0.26	+41.17 ± 0.11	-1.44 ± 0.18
+51.53 ± 0.15	-0.18 ± 0.28	+51.20 ± 0.13	-0.81 ± 0.16
+61.51 ± 0.15	+0.35 ± 0.31	+61.26 ± 0.14	-0.26 ± 0.18

This table shows the capacitance adjusted sustained calcium channel current amplitudes (I_{sus}) evoked from the given test potentials (V_{test}) with a membrane holding potential of -80mV. Values shown are means ± S.E.M from 25 control and 26 mAb 11.14 treated BC_3H1 cells. Monoclonal antibody 11.14 had no significant effect on capacitance adjusted sustained current amplitude at any test potential studied.

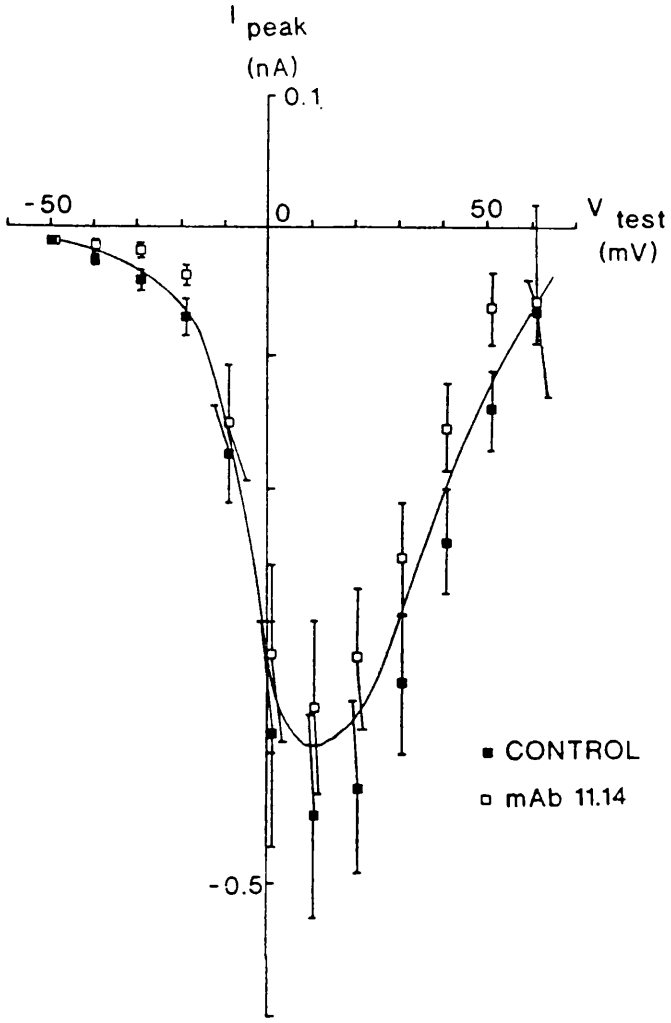

Legend for Figure 4.13 Effect of mAb 11.14 on peak current.

This figure shows the peak inward calcium channel current amplitude (I_{peak}) plotted versus test membrane potential (V_{test}), measured in control (■) and monoclonal antibody 11.14 (□) treated BC_3H1 cells. All currents were evoked from a membrane holding potential of -80mV. The values plotted are means ± S.E.M from 25 control and 26 monoclonal antibody 11.14 treated cells. Monoclonal antibody 11.14 had no significant effect on peak current amplitude at any test potential studied, therefore one curve has been fitted by eye through all data points. Data were obtained from the same recordings as in Figure 4.12.

Table 4.3 Effect of mAb 11.14 on capacitance adjusted peak current (holding potential -80mV).

mAb 11.14		Control	
V_{test}±S.E.M.(mV)	I_{peak}±S.E.M.(AF^{-1})	V_{test}±S.E.M.(mV)	I_{peak}±S.E.M.(AF^{-1})
-49.55 ± 0.04	-0.10 ± 0.03	-49.59 ± 0.04	-0.09 ± 0.02
-39.40 ± 0.05	-0.14 ± 0.04	-39.51 ± 0.04	-0.19 ± 0.03
-29.26 ± 0.06	-0.18 ± 0.05	-29.34 ± 0.06	-0.28 ± 0.05
-19.15 ± 0.07	-0.34 ± 0.08	-19.27 ± 0.06	-0.48 ± 0.09
-9.02 ± 0.08	-1.19 ± 0.27	-9.17 ± 0.07	-1.26 ± 0.27
+1.10 ± 0.09	-2.50 ± 0.42	+0.95 ± 0.08	-2.53 ± 0.43
+11.18 ± 0.10	-2.86 ± 0.39	+10.99 ± 0.09	-3.04 ± 0.37
+21.26 ± 0.11	-2.64 ± 0.33	+21.08 ± 0.09	-2.94 ± 0.31
+31.38 ± 0.12	-2.04 ± 0.29	+31.16 ± 0.11	-2.39 ± 0.25
+41.43 ± 0.14	-1.25 ± 0.26	+41.17 ± 0.11	-1.63 ± 0.19
+51.53 ± 0.15	-0.94 ± 0.17	+51.20 ± 0.13	-0.94 ± 0.17
+61.51 ± 0.15	-0.11 ± 0.37	+61.26 ± 0.14	-0.43 ± 0.17

This table shows the capacitance adjusted peak calcium channel current amplitudes (I_{peak}) evoked from the given test potentials (V_{test}) with a membrane holding potential of -80mV. Values shown are means ± S.E.M from 25 control and 26 mAb 11.14 treated BC_3H1 cells. Monoclonal antibody 11.14 had no significant effect on capacitance adjusted peak current amplitude at any test potential studied.

activating components of peak current.

Figure 4.14 shows I-V curves for I_{diff} which has been calculated at each of the test potentials from the same cells as for the previous two figures (4.12 & 4.13). Interestingly there was an increase in I_{diff} by mAb 11.14 which was statistically significant at several test potentials as compared with controls. When the results had been capacitance adjusted, there were still significant differences between I_{diff} measured in the control and mAb 11.14 treated cells over a large range of test potentials from -10mV - +50mV. Therefore mAb 11.14 caused a significant increase in the difference between peak and sustained current amplitudes as compared with controls indicating a possible change in the kinetics of the high threshold slowly activating channel.

Figure 4.15 shows the time to peak amplitude plotted versus test potential. There were significant decreases in the time to peak amplitude in the mAb 11.14 treated cells compared with those treated with the control antibody over a range of test potentials from 0 - +40mV. The time to peak current would be expected to be determined by the most slowly activating component of current. Over a range of test potentials from 0 - +40mV, the major component of current present is the slowly activating current and the effect observed is most likely to be due to an increase in the activation rate of these channels by mAb 11.14. No effect was seen at test potentials more negative than 0mV indicating no effect on the low threshold fast activating component.

In summary the results indicate possible effects of mAb 11.14 on the activation kinetics of the slowly activating dihydropyridine-sensitive calcium channel seen in BC_3H1 cells whilst no effects were observed on the fast activating calcium channel.

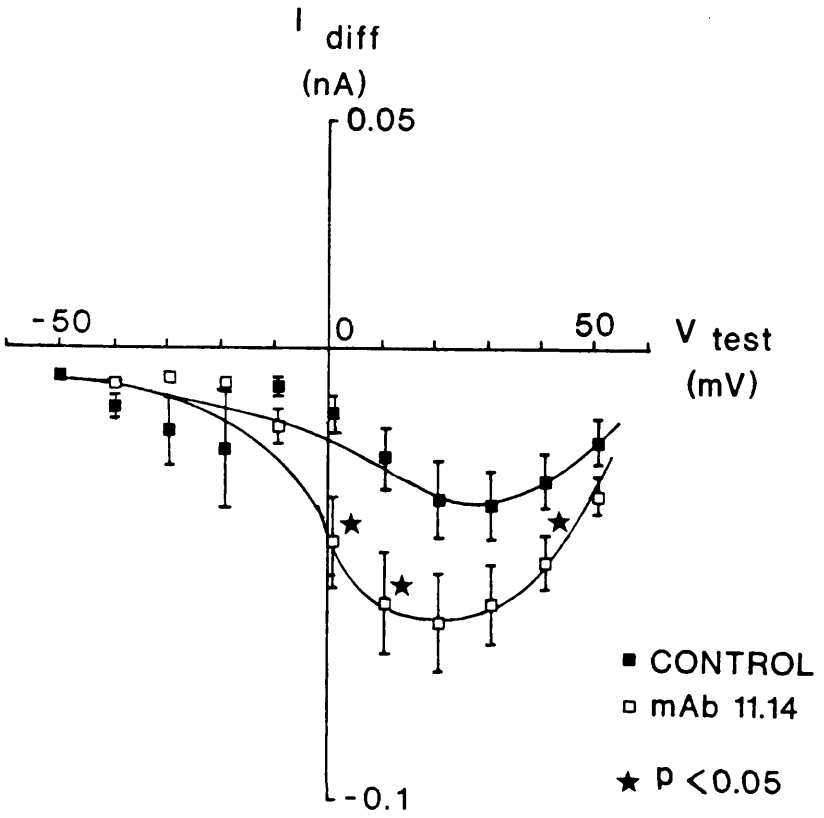

Legend for Figure 4.14 Effect of mAb 11.14 on I_{diff}.

This figure shows the difference between peak and sustained inward calcium channel current amplitudes (I_{diff}) plotted versus test membrane potential (V_{test}), measured in 25 control (■) and 26 monoclonal antibody 11.14 (□) treated BC_3H1 cells. All currents were evoked from a membrane holding potential of -80mV and the values plotted are means ± S.E.M.. Curves were fitted by eye. Significant increases in current amplitude by monoclonal antibody 11.14 as compared with controls: ★ $p < 0.05$.

Table 4.4 Effect of mAb 11.14 on capacitance adjusted I_{diff} (holding potential -80mV).

mAb 11.14		Control	
V_{test}±S.E.M.(mV)	I_{diff}±S.E.M.(AF^{-1})	V_{test}±S.E.M.(mV)	I_{diff}±S.E.M.(AF^{-1})
-49.55 ± 0.04	-0.05 ± 0.01	-49.59 ± 0.04	-0.04 ± 0.01
-39.40 ± 0.05	-0.07 ± 0.01	-39.51 ± 0.04	-0.10 ± 0.02
-29.26 ± 0.06	-0.06 ± 0.01	-29.34 ± 0.06	-0.11 ± 0.04
-19.15 ± 0.07	-0.08 ± 0.02	-19.27 ± 0.06	-0.12 ± 0.07
-9.02 ± 0.08	-0.15 ± 0.03 ☆	-9.17 ± 0.07	-0.06 ± 0.01
+1.10 ± 0.09	-0.35 ± 0.07 ☆	+0.95 ± 0.08	-0.10 ± 0.02
+11.18 ± 0.10	-0.46 ± 0.08 ☆	+10.99 ± 0.09	-0.16 ± 0.04
+21.26 ± 0.11	-0.51 ± 0.09 ★	+21.08 ± 0.09	-0.22 ± 0.04
+31.38 ± 0.12	-0.48 ± 0.07 ☆	+31.16 ± 0.11	-0.23 ± 0.04
+41.43 ± 0.14	-0.42 ± 0.05 ☆	+41.17 ± 0.11	-0.19 ± 0.03
+51.53 ± 0.15	-0.29 ± 0.04 ☆	+51.20 ± 0.13	-0.13 ± 0.02

This table shows the capacitance adjusted difference between peak and sustained inward calcium channel current amplitudes (I_{diff}) evoked from the given test potentials (V_{test}) with a membrane holding potential of -80mV. Values shown are means ± S.E.M from 25 control and 26 mAb 11.14 treated BC_3H1 cells. Significant reductions by monoclonal antibody 11.14 as compared with controls: ★ $p < 0.05$, ☆ $p < 0.005$.

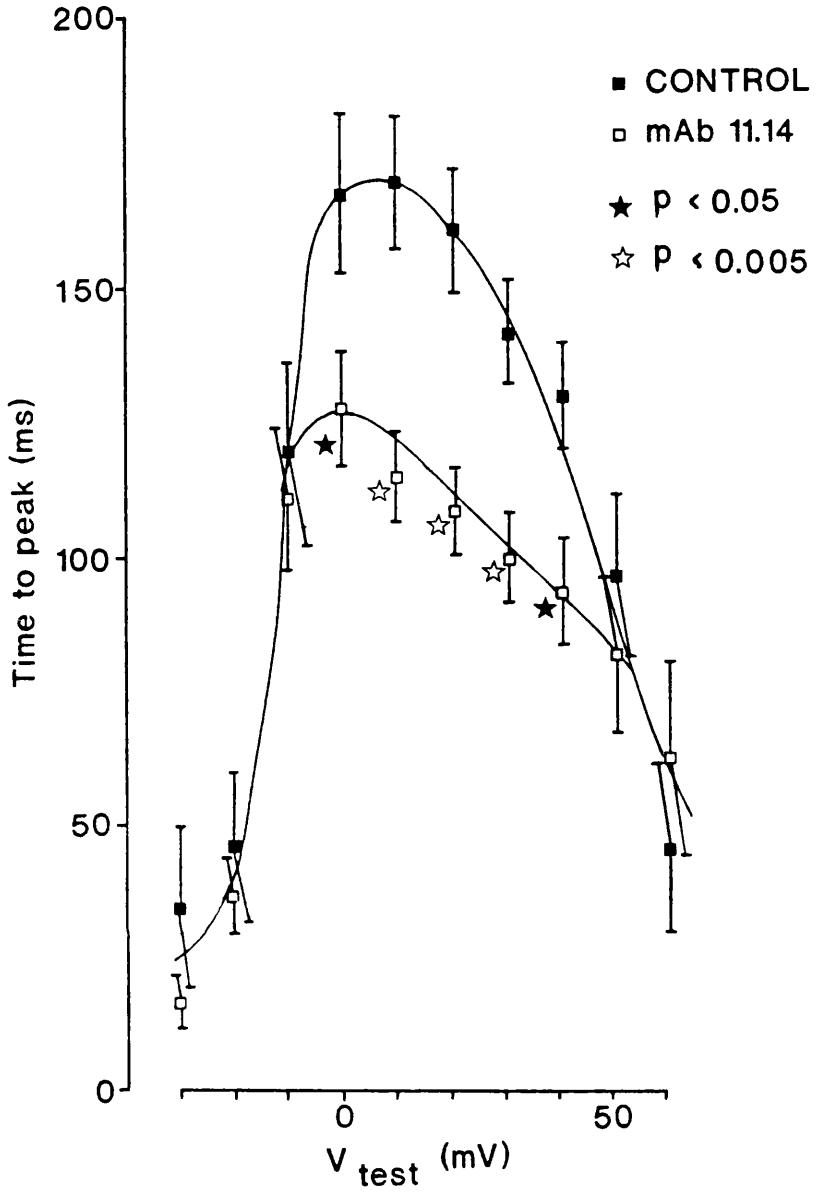

Legend for Figure 4.15 Effect of mAb 11.14 on time to peak current.

Plot of time to peak of inward calcium channel current versus test membrane potential (V_{test}). Currents were evoked from a holding potential of -80mV. Values plotted are means ± S.E.M from 25 control (■) and 26 monoclonal antibody 11.14 (□) treated BC_3H1 cells. Curves were fitted by eye. Significant reductions by monoclonal antibody 11.14 as compared with controls: ★ $p < 0.05$, ☆ $p < 0.005$.

V. Effects of acute application of monoclonal antibody 11.14 on whole cell calcium channel currents in BC_3H1 cells

In this section the monoclonal antibody was applied to the cells during whole cell recording, in order to investigate if the antibody had a direct effect on the inward calcium channel currents. Control antibody was applied to 6 cells and monoclonal antibody 11.14 to 6 cells. Cells were voltage clamped at -80mV and currents evoked in response to 90mV depolarizing voltage steps (300ms duration, 0.1Hz frequency). At this test potential, the major component of current that will be activated is the slowly activating dihydropyridine-sensitive channel.

Before application of test or control antibody, I-V curves obtained for the two groups of cells showed no significant differences in sustained, peak, difference between peak and sustained current amplitudes or time to peak current (figures 4.16-4.19 respectively). This indicates that the currents in the two groups of cells were similar before application of the antibody and so comparisons between groups after application would be expected to be justified.

The effect of acute application of control and monoclonal antibody 11.14 on the sustained inward currents over a 10 minute time period is shown in figure 4.20. In agreement with the experiments involving 24 hour incubation with the antibodies, the sustained inward currents were smaller in the presence of mAb 11.14 as compared with controls, but this reduction was not statistically significant over the time period tested.

Figure 4.21 shows a graph of the effect of control and monoclonal antibody 11.14 on the peak inward current plotted versus time. As in the experiments involving 24 hour incubation with the antibodies there was again no significant effect of

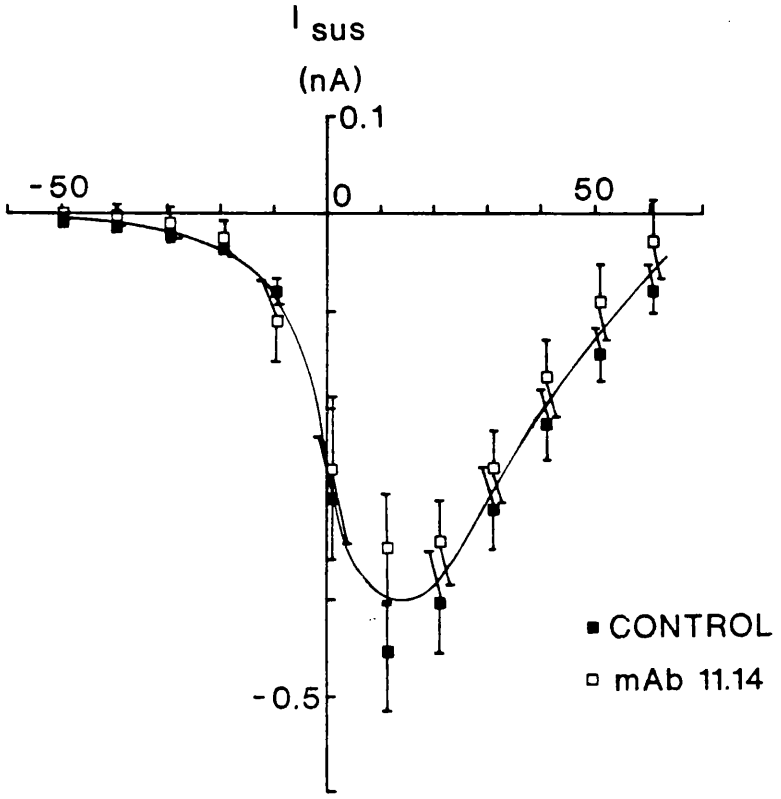

Legend for Figure 4.16 Sustained currents before acute application of control or mAb 11.14.

This figure shows the sustained calcium channel current amplitude (I_{sus}) plotted versus test membrane potential (V_{test}), from 6 cells subsequently treated with control antibody (■) and 6 cells subsequently treated with mAb 11.14 (□). All currents were evoked from a membrane holding potential of -80mV and the values plotted are means ± S.E.M.. There were no significant differences between the two groups at any test potential studied, therefore one curve has been fitted by eye through all data points.

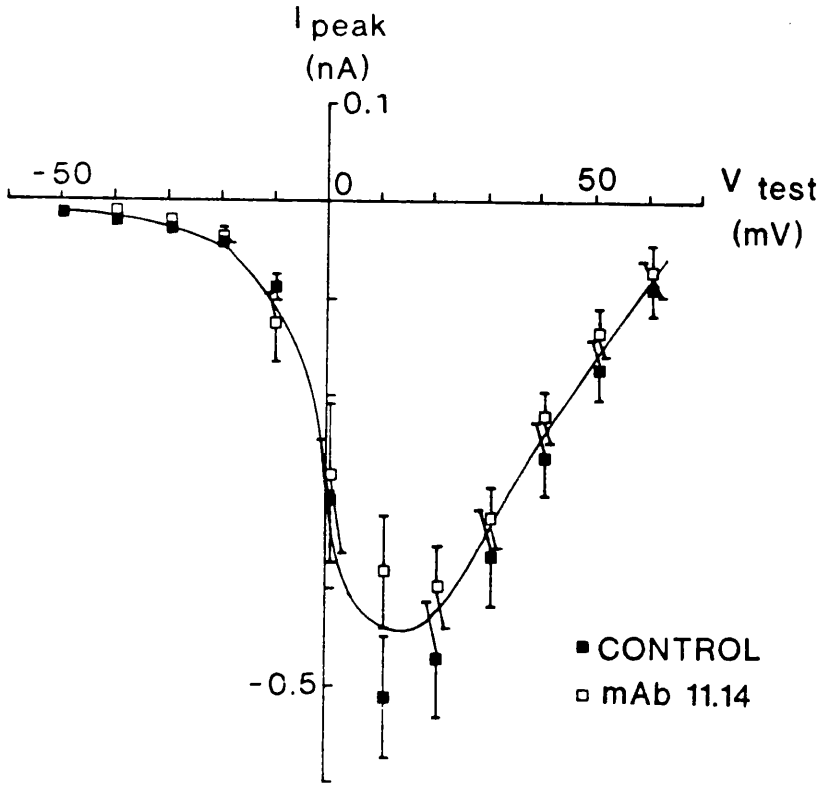

Legend for Figure 4.17 Peak currents before acute application of control or mAb 11.14.

This figure shows the peak calcium channel current amplitude (I_{peak}) plotted versus test membrane potential (V_{test}), from 6 cells subsequently treated with control antibody (■) and 6 cells subsequently treated with mAb 11.14 (□). All currents were evoked from a membrane holding potential of -80mV and the values plotted are means ± S.E.M.. There were no significant differences between the two groups at any test potential studied, therefore one curve has been fitted by eye through all data points.

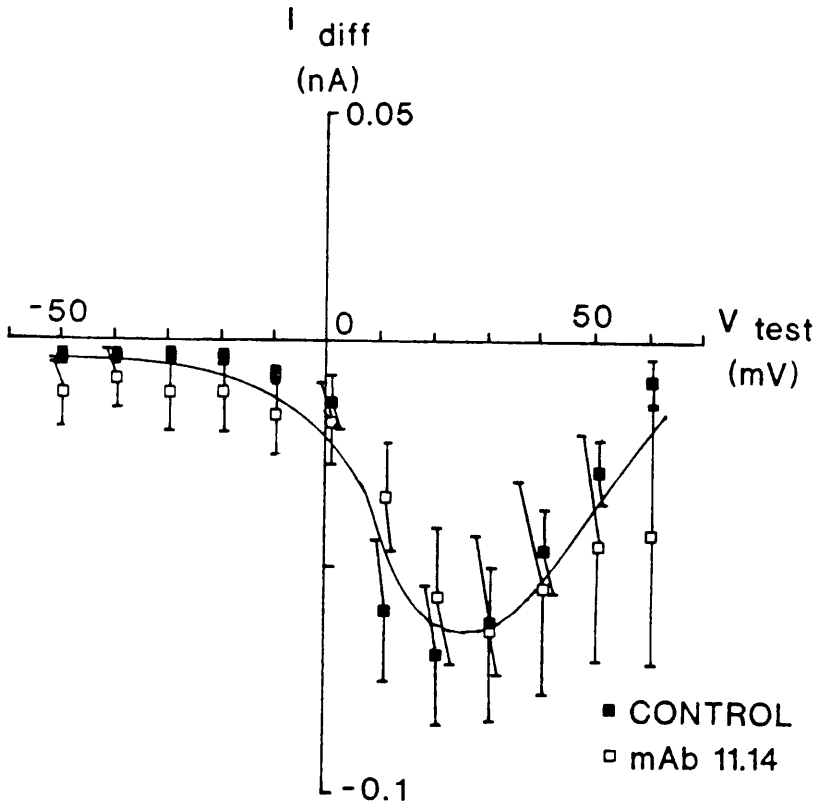

Legend for Figure 4.18 I_{diff} before acute application of control or mAb 11.14.

This figure shows the difference between peak and sustained inward calcium channel current amplitudes (I_{diff}) plotted versus test membrane potential (V_{test}), from 6 cells subsequently treated with control antibody (■) and 6 cells subsequently treated with mAb 11.14 (□). All currents were evoked from a membrane holding potential of -80mV and the values plotted are means ± S.E.M.. There were no significant differences between the two groups at any test potential studied, therefore one curve has been fitted by eye through all data points. Data were obtained from the same cells as figures 4.16 and 4.17.

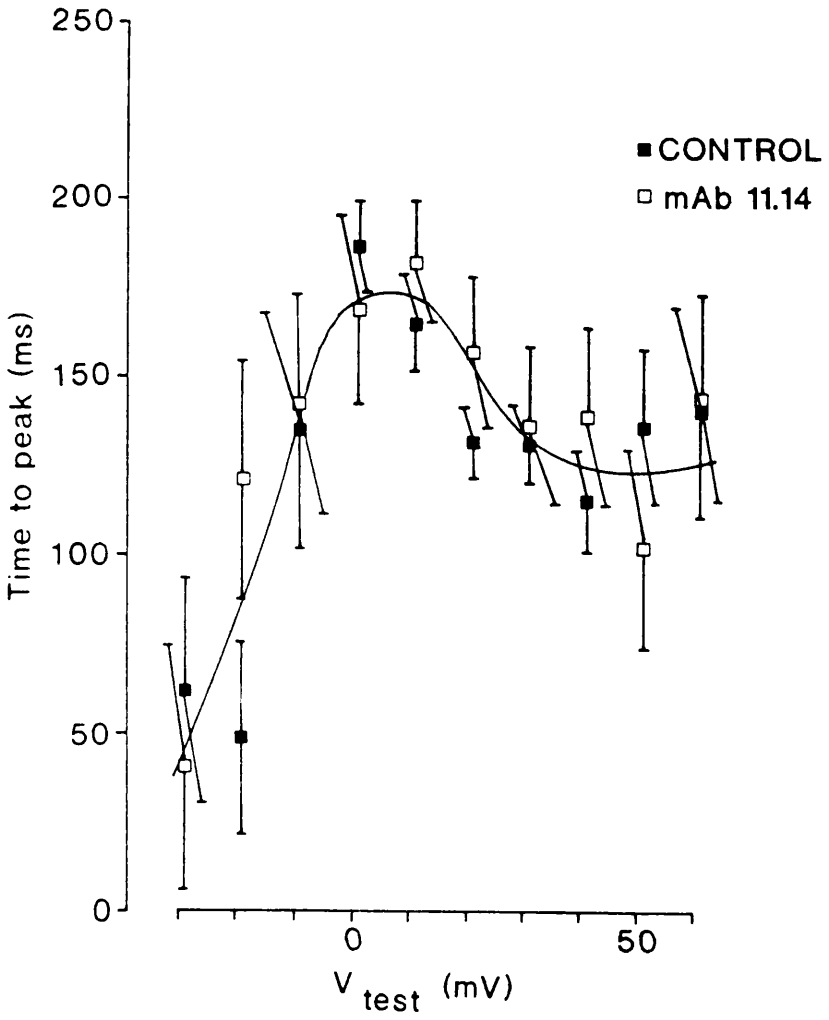

Legend for Figure 4.19 Time to peak currents before acute application of control or mAb 11.14.

Plot of time to peak of inward calcium channel current versus test membrane potential (V_{test}), from 6 cells subsequently treated with control antibody (■) and 6 cells subsequently treated with mAb 11.14 (□). All currents were evoked from a membrane holding potential of -80mV and the values plotted are means ± S.E.M.. There were no significant differences between the two groups at any test potential studied, therefore one curve has been fitted by eye through all data points. Data were obtained from the same cells as figures 4.16-4.18.

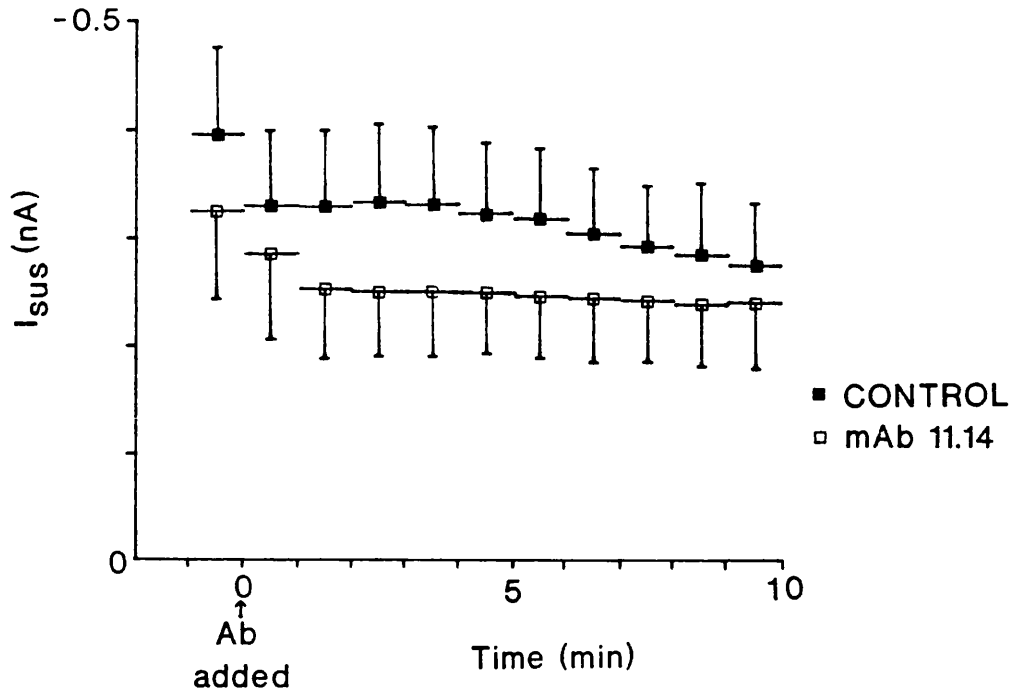

Legend for Figure 4.20 Effect of acute application of mAb 11.14 on sustained current. This figure shows the sustained current amplitude (I_{sus}) plotted versus time measured in BC_3H1 cells in which the control/11.14 mAb was added at time 0. Currents were evoked in response to 90mV depolarising steps from a membrane holding potential of -80mV. Six cells were treated with the control antibody (■) and six with mAb 11.14 (□). The values plotted are means ± S.E.M. of currents averaged over 1 minute intervals from 1 minute before the antibody was added until 10 minutes after adding the antibody.

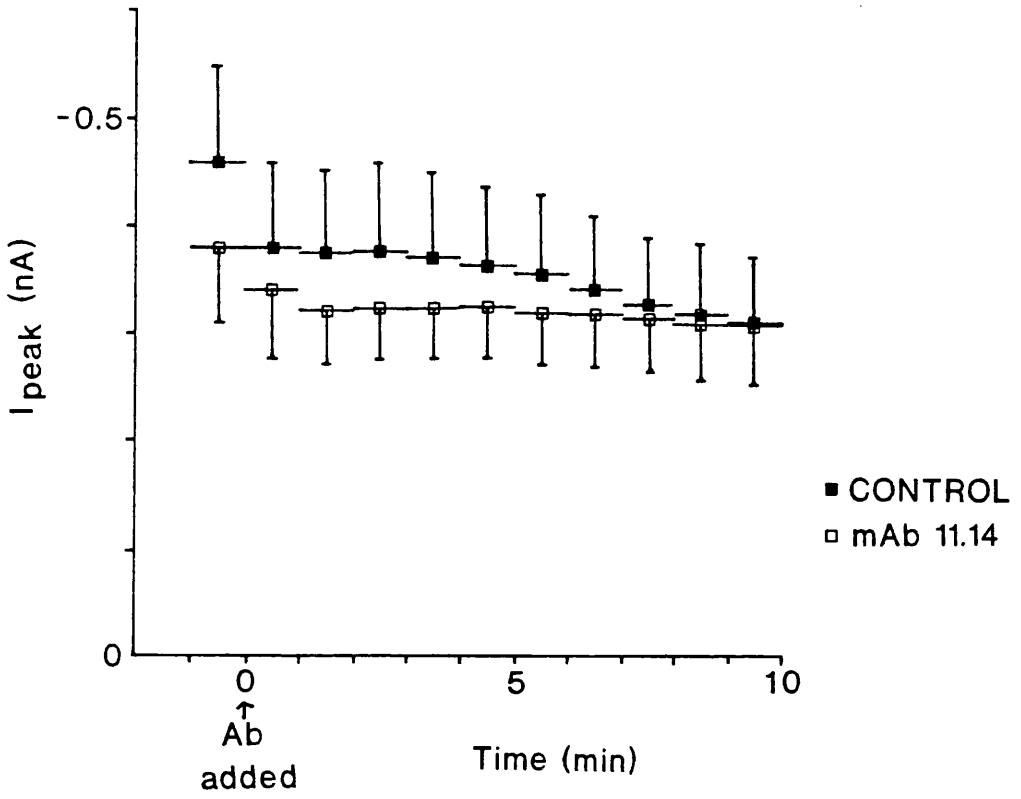

Legend for Figure 4.21 Effect of acute application of mAb 11.14 on peak current. This figure shows the peak current amplitude (I_{peak}) plotted versus time measured in BC_3H1 cells in which the control/11.14 mAb was added at time 0. Currents were evoked in response to 90mV depolarising steps from a membrane holding potential of -80mV. Six cells were treated with the control antibody (■) and six with mAb 11.14 (□). The values plotted are means ± S.E.M. of currents averaged over 1 minute intervals from 1 minute before the antibody was added until 10 minutes after adding the antibody.

monoclonal antibody 11.14 on the peak inward current compared with controls over the 10 minute time period.

In contrast to the effect on I_{diff} of monoclonal antibody 11.14 on the cells after 24 hour incubation (Figure 4.14), there was no effect when the antibody was applied acutely (Figure 4.22). Although I_{diff} in the presence of monoclonal antibody 11.14 was always greater than the comparable control value the increase was never significant.

Figure 4.23 shows the time to peak inward current plotted versus time. From this, it can be seen that the time to peak current was significantly decreased by monoclonal antibody 11.14 as compared with controls from 1 minute after adding the antibody until the end of these recordings 10 minutes after adding the antibody. This decrease in the time to peak current was similarly seen after 24 hour incubation with the antibody (see above).

Current-voltage plots taken after either the control or monoclonal antibody 11.14 had been present in the bath for 10 minutes showed no significant differences in the sustained, peak or I_{diff} currents between control and test treated cells (figures 4.24-4.26 respectively). However there were again significant decreases in the time to peak currents at test potentials around where the maximum activation of the currents occurred (figure 4.27).

In summary the results from these experiments show that monoclonal antibody 11.14 while not having clear effects on the amplitude of the current appeared to have a direct, acute effect on the activation rate of the inward calcium channel currents seen in these BC_3H1 cells. At the test potential used for these acute application experiments, the major component activated is the slowly activating channel. Therefore the binding of this antibody to the α_2 subunit possibly affects the kinetics of the slowly activating

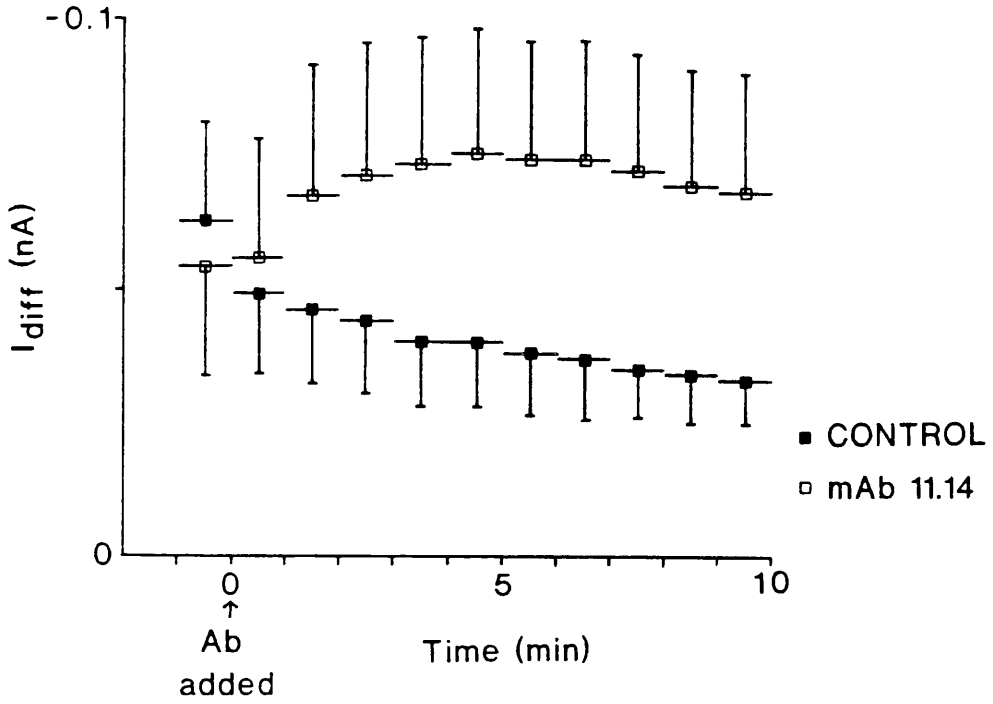

Legend for Figure 4.22 Effect of acute application of mAb 11.14 on I_{diff}.

This figure shows I_{diff} plotted versus time measured in BC_3H1 cells in which the control/11.14 mAb was added at time 0. Currents were evoked in response to 90mV depolarising steps from a membrane holding potential of -80mV. Six cells were treated with the control antibody (■) and six with mAb 11.14 (□). The values plotted are means ± S.E.M. of currents averaged over 1 minute intervals from 1 minute before the antibody was added until 10 minutes after adding the antibody.

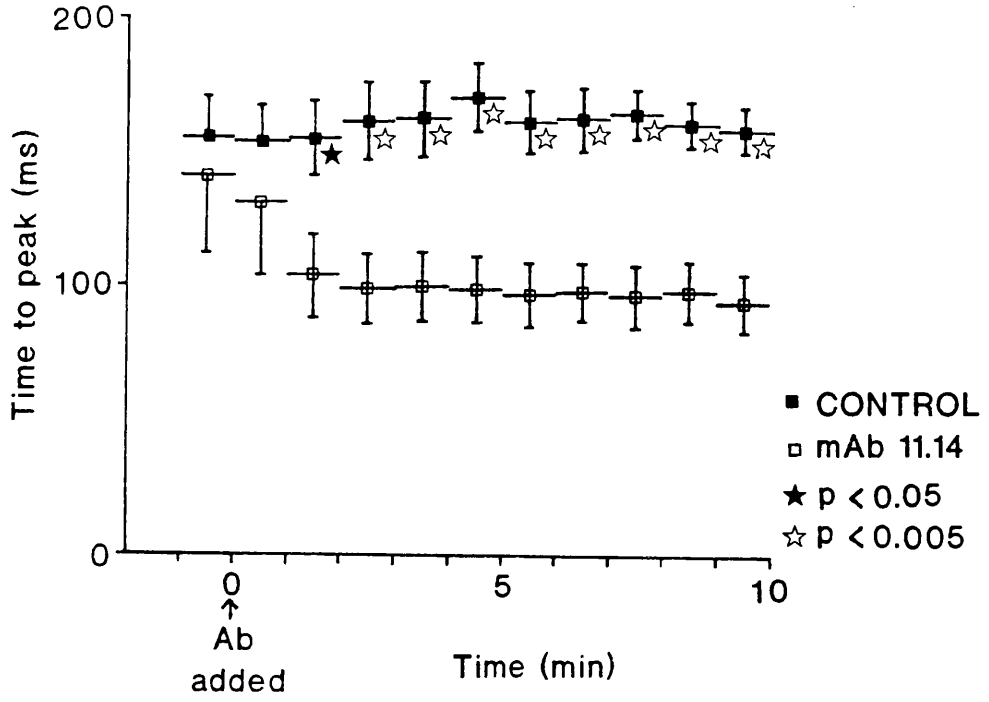

Legend for Figure 4.23 Effect of acute application of mAb 11.14 on time to peak current.

This figure shows the time to peak current plotted versus time measured in BC_3H1 cells in which the control/11.14 mAb was added at time 0. Currents were evoked in response to 90mV depolarising steps from a membrane holding potential of -80mV. Six cells were treated with the control antibody (■) and six with mAb 11.14 (□). The values plotted are means ± S.E.M. of currents averaged over 1 minute intervals from 1 minute before the antibody was added until 10 minutes after adding the antibody. Significant decreases in time to peak current by monoclonal antibody 11.14 as compared with controls: ★ $p < 0.05$, ☆ $p < 0.005$.

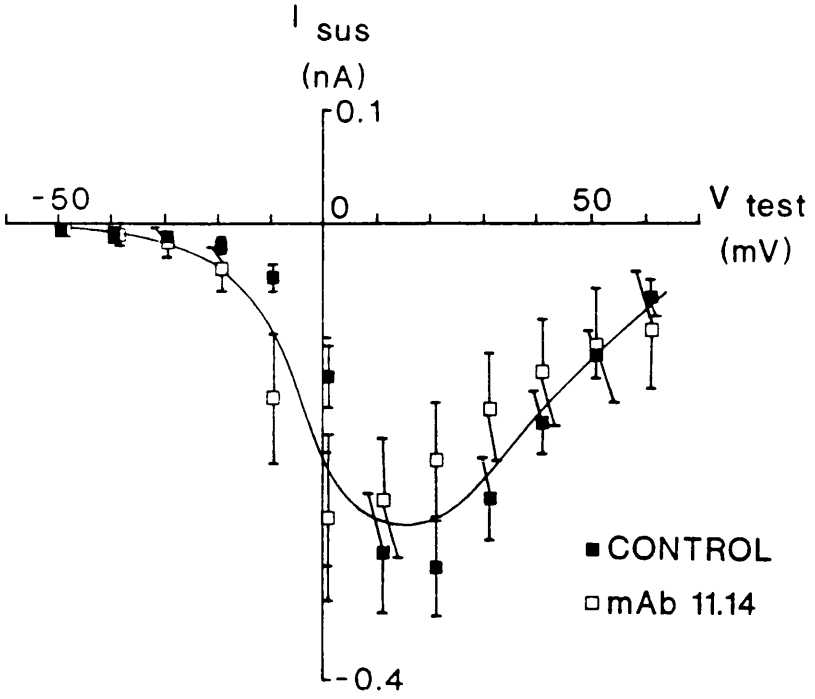

Legend for Figure 4.24 Effect of mAb 11.14 on the I-V relationship of the sustained currents 10 minutes after antibody application.

This figure shows the sustained calcium channel current amplitude (I_{sus}) plotted versus test membrane potential (V_{test}) taken after either control antibody (■) or mAb 11.14 (□) had been present in the bath for 10 minutes. All currents were evoked from a membrane holding potential of -80mV and the values plotted are means ± S.E.M. of 6 cells from each group. There were no significant differences between the two groups at any test potential studied, therefore one curve has been fitted by eye through all data points.

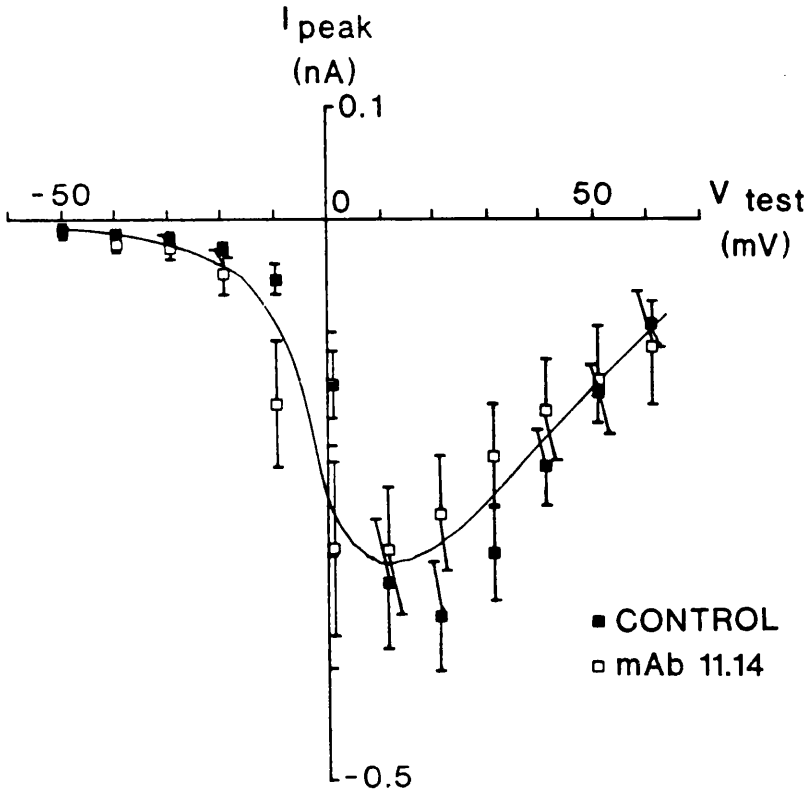

Legend for Figure 4.25 Effect of mAb 11.14 on the I-V relationship for the peak current 10 minutes after antibody application.

This figure shows the peak calcium channel current amplitude (I_{peak}) plotted versus test membrane potential (V_{test}) taken after either control antibody (■) or mAb 11.14 (□) had been present in the bath for 10 minutes. All currents were evoked from a membrane holding potential of -80mV and the values plotted are means ± S.E.M. of 6 cells from each group. There were no significant differences between the two groups at any test potential studied, therefore one curve has been fitted by eye through all data points.

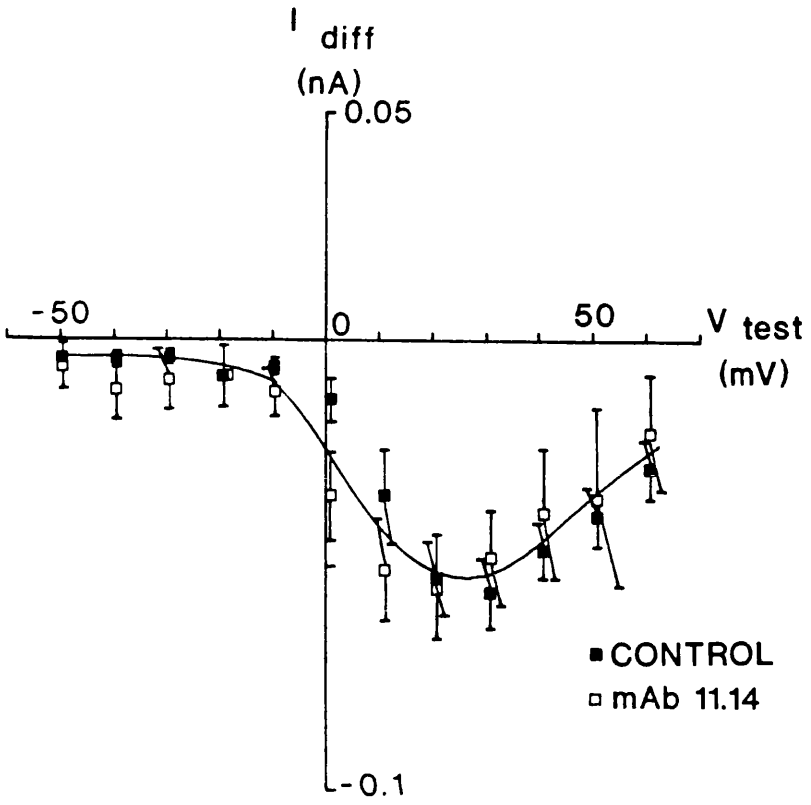

Legend for Figure 4.26 Effect of mAb 11.14 on the I-V relationship for I_{diff} 10 minutes after antibody application.

This figure shows I_{diff} plotted versus test membrane potential (V_{test}) taken after either control antibody (■) or mAb 11.14 (□) had been present in the bath for 10 minutes. All currents were evoked from a membrane holding potential of -80mV and the values plotted are means ± S.E.M. of 6 cells from each group. There were no significant differences between the two groups at any test potential studied, therefore one curve has been fitted by eye through all data points.

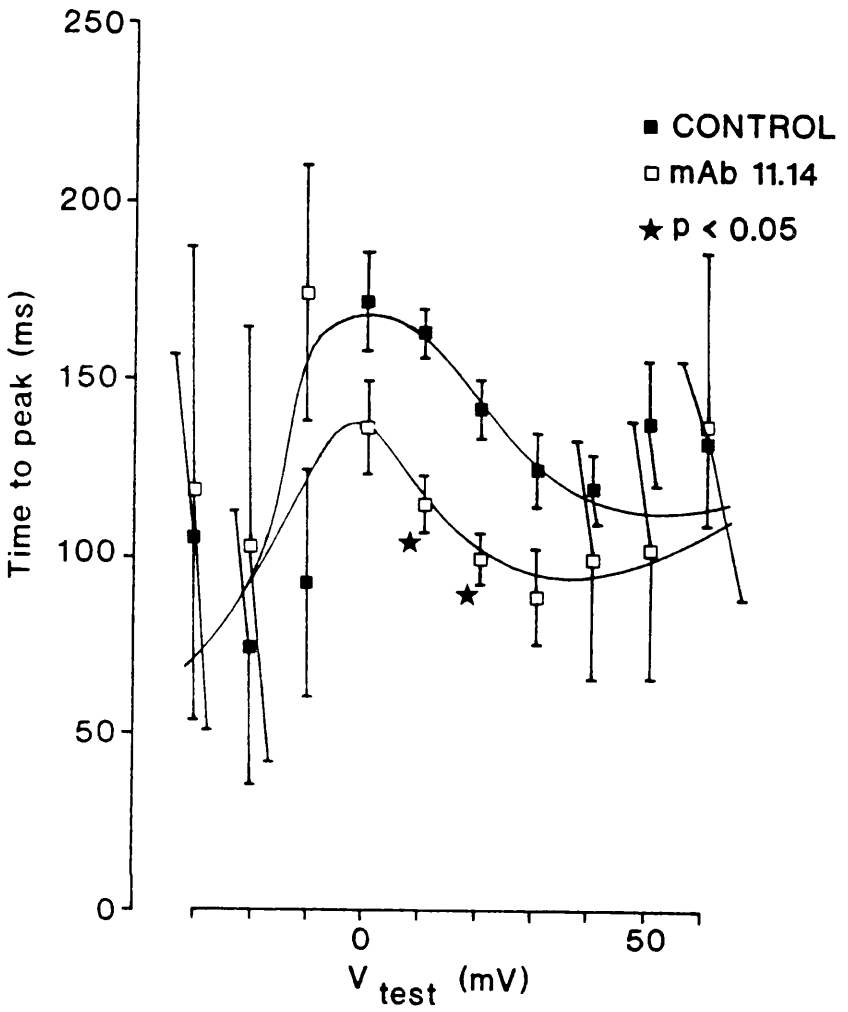

Legend for Figure 4.27 Effect of mAb 11.14 on time to peak current 10 minutes after antibody application.

Plot of time to peak current versus test membrane potential (V_{test}) taken after either control antibody (■) or mAb 11.14 (□) had been present in the bath for 10 minutes. All currents were evoked from a membrane holding potential of -80mV and the values plotted are means ± S.E.M. of 6 cells from each group. Curves were fitted by eye. Significant decreases in time to peak current by monoclonal antibody 11.14 as compared with controls: ★ $p < 0.05$.

dihydropyridine-sensitive channels whilst not causing a direct block of function.

VI. Discussion

In this chapter the effect of the monoclonal antibodies against the α_2 subunit have been investigated on the calcium channel current seen in cultured muscle cells (BC_3H1). The results presented indicate that there are two components of calcium channel current present in these cells. The dominant component was activated by large depolarising steps (i.e. high threshold) but only from a strongly negative holding potential. This current was both slowly inactivating and slowly activating, with a time to peak current in the region of 170 ms at a potential where the channels were maximally activated. In addition, this major component was sensitive to dihydropyridines; nitrendipine was able to block the inward current leaving only a small, fast component remaining. Thus the high threshold component of current appears to be similar to the "slow" calcium channel type described by others in this cell line (Caffrey, Brown & Schneider, 1987). They also found a slowly activating and inactivating, high threshold calcium current which was inactivated at steady-state by a depolarised holding potential (-50mV) and was dihydropyridine-sensitive (Morton *et al.*, 1988). The slowly activating current in the BC_3H1 cells is also similar to the predominant type of current in skeletal muscle which again is a high threshold current that both activates and inactivates slowly (Sanchez & Stefani, 1978). These "slow" channels of skeletal muscle have also been shown to be dihydropyridine-sensitive (Cognard, Lazdunski & Romey, 1986). It therefore appears that the major current seen in the BC_3H1 cells is very similar to dihydropyridine-sensitive current of skeletal muscle and it is against these latter channels that the antibodies were raised.

The second (small) component present in these cells was activated with small depolarising steps (i.e. low threshold) but appeared to be activated over a large range of potentials. It was observed to be a fast activating current but slowly inactivating and could be isolated by using a relatively depolarised holding potential or by evoking the currents in the presence of nitrendipine. It does not fit into the T-, N- or L-type channel classification. This type of calcium channel current has also been observed in these cells by others (Caffrey, Brown & Schneider, 1987), who found a low threshold component of current that could similarly be isolated by using a more depolarised holding potential and was dihydropyridine-insensitive. Again, a current similar to this fast activating current in BC_3H1 cells has been found in skeletal muscle, where in addition to the "slow" calcium current, a low threshold, fast activated current is present (Avila-Sakar *et al.*, 1986). This current only has a small amplitude, is not sensitive to diltiazem and is very slowly inactivating (Cota and Stefani, 1986). Thus it appears that the currents observed in these studies in the BC_3H1 cells are similar to those found by others in these cells and are comparable with those present in skeletal muscle. Thus it is reasonable to regard the channels in BC_3H1 cells as a good model for skeletal muscle channels.

Experiments in this chapter investigated the effects of two monoclonal antibodies on the two components of calcium channel current present in these cells. One antibody (mAb 11.6) had no effect whilst the other (mAb 11.14) showed both long term and acute effects on the slowly activating current. After long term incubation with mAb 11.14 there was a small decrease in the sustained current amplitude and increases in I_{diff} and the activation rate (i.e. a decrease in time to peak). However with the acute application of the antibody only the increase in activation rate was still significant. An

increase in the activation rate could cause the apparent changes in the current amplitudes to occur since if the activation rate was faster, assuming that there is no change in the inactivation rate, the current will have decayed more within the duration of the test pulse.

The clear effect of monoclonal antibody 11.14 on the time to peak suggests that this monoclonal antibody can increase the activation rate of the slowly activating dihydropyridine-sensitive calcium channel present in these cells. Furthermore this must be a direct, acute effect on the functioning of the calcium channels and could therefore possibly be due to the antibody binding to a functionally significant site. Since the binding of this antibody to the α_2 subunit appears to affect the activation kinetics of the channel it could be postulated that the α_2 subunit is functionally significant, possibly modulating calcium channel function. However another possibility is that the binding of this antibody to the α_2 subunit alters the conformation of the channel within the membrane so having an effect on the channel properties rather than directly affecting a functionally significant site.

Although no effects by antibodies have previously been observed on calcium channel kinetics, antibodies against the sodium channel α subunit have been shown to be capable of altering the inactivation rate (Meiri *et al.*, 1987; Vassilev, Scheuer & Catterall, 1988; Vassilev, Scheuer & Catterall, 1989). These effects are comparable with that of mAb 11.14 on the activation rate in that both occur acutely and in the case of Meiri *et al.* the antibody was also able to produce the action when applied externally.

Differences in the activation kinetics of the calcium channel, which depend on which subunits are present, have however been observed recently in co-expression

studies (Varadi *et al.*, 1991; Singer *et al.*, 1991). When skeletal muscle α_1 subunit was co-expressed with the ß subunit the activation rate of the currents was faster than that seen for the α_1 subunit alone (Varadi *et al.*, 1991). Another similar study, co-expressing the α_2/δ, ß, and/or γ subunits with cardiac α_1 subunit, showed that the activation rate of the currents was slower in groups not containing the $\alpha_2\delta$ subunit (Singer *et al.*, 1991). These effects indicate that the $\alpha_2\delta$ and ß subunits may modulate the activation kinetics of the channels. This is a similar finding to that reported in this chapter produced by the anti-α_2 antibody (mAb 11.14) on the calcium channel currents in BC_3H1 cells. In contrast however, co-expression of mRNA specific for the α_2 subunit from skeletal muscle with mRNA for the α_1 subunit from skeletal muscle (Varadi *et al.*, 1991), cardiac muscle (Mikami *et al.*, 1989), smooth muscle (Biel *et al.*, 1990) or for a brain calcium channel (Mori *et al.*, 1991), resulted in larger calcium channel currents with no effect on the channel kinetics (Biel *et al.*, 1990).

From studies expressing cloned subunits, the α_1 subunit alone is thought to be sufficient to form a functional calcium channel in the brain as well as skeletal, cardiac and smooth muscle (Mori *et al.*, 1991, Perez-Reyes *et al.*, 1989, Kim *et al.*, 1990; Mikami *et al.*, 1989, Biel *et al.*, 1990). However these studies have also provided evidence for a possible role of the α_2 subunit within the complex since the calcium channel currents observed are larger when the α_2 subunit is co-expressed with the α_1 calcium channel containing subunit. Another indication that the α_1 subunit, although able to form channels alone, may require other subunits for normal functioning, has come from investigations which involve reconstitution of the α_1 subunit into planar lipid bilayers (Pelzer, D. *et al.*, 1989). In these studies, in only 3% of experiments did the reconstitution of the α_1 subunit alone result in single-channel currents which were

sensitive to D600, BayK 8644 and cAMP-dependent phosphorylation. However this low success rate could also possibly be due to the finding that not all of the dihydropyridine receptors in skeletal muscle act as voltage-sensitive calcium channels (Schwartz, McCleskey & Almers, 1985).

With acute application of the antibody, the currents were recorded over a longer time period than for the 24 hour incubations. For both the test and controls there was a slow decrease in current with time (approximately 15-20% in 10 minutes). This rate of decrease was not fast enough to cause any problems in interpreting the results, so long as the control values were compared with test values at corresponding times following application. However it does show that these channels possibly also require phosphorylation like L-type channels for normal functioning.

It is clear from the results presented in this and the previous chapter that the effect of mAb 11.14 on the dihydropyridine-sensitive calcium channel in neuroblastoma cells is different from that observed on the slowly activating dihydropyridine-sensitive channel expressed in the muscle cell line. The predominant effect on NG 108 15 cells is simply a reduction in the current amplitude which is only produced after long term incubation. This could be caused by the antibody cross-linking the channels resulting in their down-regulation (i.e. a reduction in number), since there was no acute effect. However in both cell types there were significant increases in the activation rates. The effect on the activation rate of the slowly activating calcium channel in the muscle cells is direct and could not simply be due to a decrease in number of channels and therefore does not appear to be due to cross-linking and down-regulation of the channels. However this same effect on the NG 108 15 cells does not occur with acute application and therefore may simply be due to the

channels lost by down-regulation being the most slowly activating. This variation in the effects of the antibody does however show that there must be differences in the channel types between NG 108 15 and BC_3H1 cells. One possibility is that small variations in the sequences of the subunits may affect the orientation of the subunits within the membrane, so the binding of the antibody, particularly if it is simply acting by distorting the channel, may affect the channel pore in different ways. However the α_2 subunits of the two channels must share an antigenically similar region since the antibody appears to bind to both. Slight differences in the orientation of the channel in the membrane could also possibly account for the apparent lack of an acute action of the antibody on the neuroblastoma cells since changes in orientation may affect the access of the antibody to the subunit.

Monoclonal antibody 11.6 raised against the α_2 subunit had no effects on the calcium channels in the BC_3H1 and neuroblastoma cells. Although it appears that the calcium channels seen in the BC_3H1 cells are more closely related to the channels found in skeletal muscle (see above), against which the antibodies were raised, it is still possible that there may be antigenic differences between the channel types in BC_3H1 and skeletal muscle cells. It is also possible that they were raised against a region that is not important for the channel functioning or an intracellular or transmembrane site which could have been exposed on the purified protein but not in the intact cell.

No other studies have been done by other workers for antibodies raised against the α_2 subunit although similar investigations for the other subunits of the calcium channel have revealed effects on function. Antibodies raised against the α_1 subunit were found to inhibit the slow activating dihydropyridine-sensitive current without

having any effect on the fast activating dihydropyridine-insensitive current seen in BC_3H1 cells (Morton *et al.*, 1988). This effect was maximal within 10 minutes of applying the antibody and so like the effect seen with the anti-α_2 antibody on the same cell line, appears to be a direct consequence of binding to a functionally important component of the channel. Another antibody that binds to a smaller subunit of the calcium channel (45-50kDa, comparable with the ß subunit), in BC_3H1 cells (Caffrey & Farach, 1988) also altered the amplitude of the calcium currents. The effect of this antibody was again both acute and specific for the slowly activating channel like the effect reported above for the anti-α_2 monoclonal antibody (mAb 11.14). This again provides evidence that the non-channel forming subunits of the dihydropyridine-sensitive calcium channel may have modulatory roles within the complex.

In conclusion, the results presented in this thesis show that the α_2 subunit must be part of the dihydropyridine receptor complex in both the neuronal-type and the skeletal muscle-type cells studied. The α_2 subunit is probably closely associated with the α_1 subunit. In addition, it appears that the α_2 subunit may have a modulatory role within the dihydropyridine receptor complex. The α_2 subunit if present in other channel types seems to be antigenically different from that found in dihydropyridine-sensitive channels. Monoclonal antibody 11.14 may be a useful probe in further studies on the role of the α_2 subunit in calcium channels.

Additional useful experiments which could be carried out with these mAbs would be: Firstly, to confirm that they bind to both cell lines by immunocytochemistry. Secondly, to use Fab fragments of mAb 11.14 to determine whether its effect on the differentiated NG 108 15 cells is due to cross-linking and down-regulation of the channels. Finally, to determine the site of binding of mAb

11.14 to the α_2 subunit by synthesising small peptides (possibly 6 amino acids each) which correspond to the sequence of the α_2 subunit. Binding by the mAbs to these peptide sequences could then be tested by ELISA.

In addition to these experiments with the existing mAbs, polyclonal Abs could be raised against small sequences of peptides specific for the α_2 subunit of the dihydropyridine-sensitive calcium channel. This approach could also be extended to the other subunits. Finally, it would also be interesting to further investigate the current types present in the NG 108 15 cells using in particular, ω-conotoxin.

REFERENCES

AHLIJANIAN, M.K., STRIESSNIG, J. & CATTERALL, W.A. (1991) Phosphorylation of an α_1-like subunit of an ω-conotoxin-sensitive brain calcium channel by cAMP-dependent protein kinase and protein kinase C. J.Biol.Chem. **266**, 20192-20197.

AKASU, T., TSURUSAKI, M. & TOKIMASA, T. (1990) Reduction of the N-type calcium current by noradrenaline in neurones of rabbit vesical parasympathetic ganglia. J.Physiol. **426**, 439-452.

ALMERS, W. & McCLESKEY, E.W. (1984) Non-selective conductance in calcium channels of frog muscle: calcium selectivity in a single-file pore. J.Physiol. **353**, 585-608.

ALMERS, W., McCLESKEY, E.W. & PALADE, P.T. (1985) Calcium channels in vertebrate skeletal muscle. In: Calcium in biological systems 321-330. Ed. Rubin, R.P., Weiss, G.B. & Putney, J.W. Plenum Publishing Corp.

ARMSTRONG, D. & ECKERT, R. (1987) Voltage-activated calcium channels that must be phosphorylated to respond to membrane depolarization. Proc.Natl.Acad.Sci. **84**, 2518-2522.

ARREOLA, J., CALVO, J., GARCIA, M.C. & SANCHEZ, J.A. (1987) Modulation of calcium channels of twitch skeletal muscle fibres of the frog by adrenaline and cyclic adenosine monophosphate. J.Physiol. **393**, 307-330.

ASHCROFT, F.M., RORSMAN, P. & TRUBE, G. (1989) Single calcium channel activity in mouse pancreatic beta-cells. Ann.N.Y.Acad.Sci. **560**, 410-412.

AVILA-SAKAR, A.J., COTA, G., GAMBOA-ALDECO, R., GARCIA, J., HUERTA, M., MUNIZ, J. & STEFANI, E. (1986) Skeletal muscle calcium channels. J. Musc. Res. Cell Motility **7**, 291-298.

BEAM, K.G., TANABE, T. & NUMA, S. (1989) Structure, function and regulation of the skeletal muscle dihydropyridine receptor. Ann.N.Y.Acad.Sci. **560**, 127-137.

BEAN, B.P. (1989) Multiple types of calcium channels in heart muscle and neurons. Ann.N.Y.Acad.Sci. **560**, 334-345.

BEAN, B.P., STUREK, M., PUGA, A. & HERMSMEYER, K. (1986) Calcium channels in muscle cells isolated from rat mesenteric arteries: modulation by dihydropyridine drugs. Circ. Res. **59**, 229-235.

BENHAM, C.D., HESS, P. & TSIEN, R.W. (1987) Two types of calcium channels in single smooth muscle cells from rabbit ear artery studied with whole-cell and single-channel recordings. Circ. Res. **61**, 10-16.

BIEL, M., RUTH, P., BOSSE, E., HULLIN, R., STUHMER, W., FLOCKERZI, V. & HOFMANN, F. (1990) Primary structure and functional expression of a high voltage activated calcium channel from rabbit lung. Febs Lett. **269**, 409-412.

BORSOTTO, M., BARHANIN, J., NORMAN, R.I. & LAZDUNSKI, M. (1984) Purification of the dihydropyridine receptor of the voltage-dependent Ca^{2+} channel from skeletal muscle transverse tubules using (+) [^{3}H]PN 200-110. Biochem. Biophys. Res. Comm. **122**, 1357-1366.

BOSSE, E., REGULLA, S., BIEL, M., RUTH, P., MEYER, H.E., FLOCKERZI, V. & HOFMANN, F. (1990) The cDNA and deduced amino acid sequence of the γ subunit of the L-type calcium channel from rabbit skeletal muscle. Febs Lett. **267**, 153-156.

BROWN, D.A., DOCHERTY, R.J. & McFADZEAN, I. (1989) Calcium channels in vertebrate neurons. Experiments on a neuroblastoma hybrid model. Ann.N.Y.Acad.Sci. **560**, 358-372.

BRUM, G., OSTERRIEDER, V.W. & TRAUTWEIN, W. (1984) ß-Adrenergic increase in the calcium conductance of cardiac myocytes studied with the patch clamp. Pflugers Arch. **401**, 111-118.

BURGESS, A.J. & NORMAN, R.I. (1988) The large glycoprotein subunit of the skeletal muscle voltage-sensitive calcium channel. Deglycosylation and development. Eur. J. Biochem. **178**, 527-533.

CAFFREY, J.M., BROWN, A.M. & SCHNEIDER, M.D. (1987) Mitogens and oncogenes can block the induction of specific voltage-gated ion channels. Science **236**, 570-573.

CAFFREY, J.M. & FARACH, M.C. (1988) A monoclonal antibody specifically modulates dihydropyridine-sensitive calcium current in BC_3H1 myocytes. Molecular Pharmacology **34**, 518-526.

CATTERALL, W.A. (1988) Structure and function of voltage-sensitive ion channels. Science **242**, 50-61.

CATTERALL, W.A., SEAGAR, M.J., TAKAHASHI, M. & NUNOKI, K. (1989) Molecular properties of dihydropyridine-sensitive calcium channels. Ann.N.Y.Acad.Sci. **560**, 1-14.

CAVALIE, A., OCHI, R., PELZER, D. & TRAUTWEIN, W. (1983) Elementary currents through Ca^{2+} channels in guinea pig myocytes. Pflugers Arch. **398**, 284-297.

CHAD, J.E. & ECKERT, R. (1986) An enzymatic mechanism for calcium current inactivation in dialysed Helix neurones. J. Physiol. **378**, 31-51.

CHAPLIN, E.R., NELL, G.W. & WALKER, S.M. (1970) Excitation-contraction latencies in postnatal skeletal muscle fibers. Exp. Neurol. **29**, 142-151.

CHEN, C., CORBLEY, M.J., ROBERTS, T.M. & HESS, P. (1988) Dihydropyridine-sensitive and -insensitive Ca^{2+} channels in normal and transformed fibroblasts. In: The Calcium Channel: Structure, Function and Implications 92-102. Ed. Morad, M., Nayler, W., Kazda, S. & Schramm, M. Springer-Verlag.

COGNARD, C., LAZDUNSKI, M. & ROMEY, G. (1986) Different types of calcium channels in mammalian skeletal muscle cells in culture. Proc. Natl. Acac. Sci. **83**, 517-521.

COOPER, C.L., VANDAELE, S., BARHANIN, J., FOSSET, M., LAZDUNSKI, M. & HOSEY, M.M. (1987) Purification and characterization of the dihydropyridine-sensitive voltage-dependent calcium channel from cardiac tissue. J.Biol.Chem. **262**, 509-512.

COTA, G., NICOLA SIRA, L. & STEFANI, E. (1984) Calcium channel inactivation in frog (Rana pipiens and Rana moctezuma) skeletal muscle fibres. J.Physiol. **354**, 99-108.

COTA, G. & STEFANI, E. (1986) A fast-activated inward calcium current in twitch muscle fibres of the frog (rana montezume). J.Physiol. **370**, 151-163.

CURTIS, B.M. & CATTERALL, W.A. (1984) Purification of the calcium antagonist receptor of the voltage-sensitive calcium channel from skeletal muscle transverse tubules. Biochemistry **23**, 2113-2118.

CURTIS, B.M. & CATTERALL, W.A. (1985) Phosphorylation of the calcium antagonist receptor of the voltage-sensitive calcium channel by cAMP-dependent protein kinase. Proc. Natl. Acad. Sci. USA **82**, 2528-2532.

DE JONGH, K.S., MERRICK, D.K. & CATTERALL W.A. (1989) Subunits of purified calcium channels: A 212-kDa form of the α_1 and partial amino acid sequence of a phosphorylation site of an independent ß subunit. Proc.Natl.Acad.Sci. **86**, 8585-8589.

DE JONGH, K.S., WARNER, C. & CATTERALL, W.A. (1990) Subunits of purified calcium channels. J.Biol.Chem. **265**, 14738-14741.

DOCHERTY, R.J. (1988) Gadolinium selectively blocks a component of calcium current in rodent neuroblastoma x glioma hybrid (NG 108-15) cells. J.Physiol. **398**, 33-47.

DOCHERTY, R.J. & McFAZDEAN, I. (1987) Noradrenaline decreases voltage-dependent calcium current in neuroblastoma x glioma hybrid (NG 108 15) cells. J. Physiol. **390**, 79P.

DOCHERTY, R.J. & McFAZDEAN, I. (1989) Noradrenaline-induced inhibition of voltage-sensitive calcium currents in NG 108 15 hybrid cells. European Journal of Neurosciences 132-140.

DOLPHIN, A.C. & SCOTT, R.H. (1986) Inhibition of calcium currents in cultured rat dorsal root ganglion neurones by (-)-baclofen. Br. J. Pharmac. **88**, 213-220.

DOLPHIN, A.C. & SCOTT, R.H. (1987) Calcium channel currents and their inhibition by (-)-baclofen in rat sensory neurones: modulation by guanine nucleotides. J. Physiol. **386**, 1-17.

DONALDSON, P.L. & BEAM, K.G. (1983) Calcium currents in a fast-twitch skeletal muscle of the rat. J. Gen. Physiol. **82**, 449-468.

DUNLAP, K. & FISCHBACH, G.D. (1981) Neurotransmitters decrease the calcium conductance activated by depolarization of embryonic chick sensory neurones. J. Physiol. **317**, 519-535.

ECKERT, R. & TILLOTSON, D.L. (1981) Calcium-mediated inactivation of the calcium conductance in caesium-loaded giant neurones of Aplysia californica. J. Physiol. **314**, 265-280.

EDGE, M.B. (1970) Development of apposed sarcoplasmic reticulum at the T system and sarcolemma and the change in orientation of triads in rat skeletal muscle. Dev. Biol. **23**, 634-650.

ELLIS, S.B., WILLIAMS, M.E., WAYS, N.R., BRENNER, R., SHARP, A.H., LEUNG, A.T., CAMPBELL, K.P., McKENNA, E., KOCH, W.J., HUI, A., SCHWARTZ, A. & HARPOLD, M.M. (1988) Sequence and expression of mRNAs encoding the α_1 and α_2 subunits of a DHP-sensitive calcium channel. Science **241**, 1661-1664.

FEDULOVA, S.A., KOSTYUK, P.G. & VESELOVSKY, N.S. (1985) Two types of calcium channels in the somatic membrane of new-born rat dorsal root ganglion neurones. J. Physiol. **359**, 431-446.

FLOCKERZI, V., OEKEN, H-J & HOFMANN, F. (1986) Purification of a functional receptor for calcium-channel blockers from rabbit skeletal-muscle microsomes. Eur.J.Biochem. **161**, 217-224.

FLOCKERZI, V., OEKEN, H-J, HOFMANN, F.,PELZER, D., CAVALIE, A. & TRAUTWEIN, W. (1986) Purified dihydropyridine-binding site from skeletal muscle t-tubules is a functional calcium channel. Nature **323**, 66-68.

FORSCHER, P. & OXFORD, G.S. (1985) Modulation of calcium channels by norepinephrine in internally dialysed avian sensory neurons. J. Gen. Physiol. **85**, 743-763.

FOSSET, M., JAIMOVICH, E., DELPONT, E. & LAZDUNSKI, M. (1983) [^{3}H]Nitrendipine receptors in skeletal muscle. J.Biol.Chem. **258**, 6086-6092.

FOX, A.P., NOWYCKY, M.C. & TSIEN, R.W. (1987) Kinetic and pharmacological properties distinguishing three types of calcium currents in chick sensory neurones. J. Physiol. **394**, 149-172.

FOX, A.P., NOWYCKY, M.C. & TSIEN, R.W. (1987a) Single-channel recordings of three types of calcium channels in chick sensory neurones. J. Physiol. **394**, 173-200.

FROEHNER, S.C. (1988) New insights into the molecular structure of the dihydropyridine-sensitive calcium channel. TINS **11**, 90-92.

GARCIA, J. & STEFANI, E. (1987) Appropriate conditions to record activation of fast Ca^{2+} channels in frog skeletal muscle (Rana pipiens). Pflugers Arch. **408**, 646-648.

GLOSSMANN, H., FERRY, D.R., GOLL, A. & ROMBUSCH, M. (1984) Molecular pharmacology of the calcium channel: Evidence for subtypes, multiple drug-receptor sites, channel subunits, and the development of a radioiodinated 1,4-dihydropyridine calcium channel label, [^{125}I]iodipine. J.Cardiovascular Pharmacol. **6**, S608-S621.

GRAY, R. & JOHNSTON, D. (1987) Noradrenaline and ß-adrenoceptor agonists increase activity of voltage-dependent calcium channels in hippocampal neurons. Nature **327**, 620-622.

HAGIWARA, S. & BYERLY, L. (1981) Calcium channel. Ann. Rev. Neurosci. **4**, 69-125.

HAMILL, O.P., MARTY, A., NEHER, E., SAKMANN, B. & SIGWORTH, F.J. (1981) Improved patch-clamp techniques for high-resolution current recording from cells and cell-free membrane patches. Pflugers Arch. **391**, 85-100.

HAMPRECHT, B. (1977) Structural, electrophysiological and pharmacological properties of neuroblastoma-glioma cell hybrids in cell culture. Int. Rev. Cytol. **49**, 99-170.

HARRISON, T.M., NORMAN, R.I., PHILLIPS, H.J. & WRAY, D.W.- (1990) Effect of monoclonal antibody on calcium channel function in neuroblastoma cells. J. Physiol. **422**, 20P.

HESCHELER, J., ROSENTHAL, W., TRAUTWEIN, W. & SCHULTZ, G. (1987) The GTP-binding protein, G_o, regulates neuronal calcium channels. Nature **325**, 445-447.

HESS, P., LANSMAN, J.B. & TSIEN, R.W. (1984) Different modes of Ca channel gating behaviour favoured by dihydropyridine Ca agonists and antagonists. Nature **311**, 538-544.

HILLE, B. (1984) Ionic channels of excitable membranes. Sinauer Associates, Inc., Sunderland, Mass.

HIRNING, L.D., FOX, A.P., McCLESKEY, E.W., OLIVERA, B.M., THAYER, S.A., MILLER, R.J. & TSIEN, R.W. (1988) Dominant role of N type Ca^{2+} channels in evoked release of norepinephrine from sympathetic neurons. Science **239**, 57-61.

HOFMANN, F., NASTAINCZYK, W., ROHRKASTEN, A., SCHNEIDER, T. & SIEBER, M. (1987) Regulation of the L type calcium channel. TIPS **8**, 393-398.

HOLZ IV, G.G., RANE, S.G. & DUNLAP, K. (1986) GTP-binding proteins mediate transmitter inhibition of voltage-dependent calcium channels. Nature **319**, 670-672.

HOSEY, M.M., BORSOTTO, M. & LAZDUNSKI, M. (1986) Phosphorylation and dephosphorylation of dihydropyridine-sensitive voltage-dependent Ca^{2+} channel in skeletal muscle membranes by cAMP- and Ca^{2+}-dependent processes. Proc. Natl. Acad. Sci. USA **83**, 3733-3737.

HOSEY, M.M., CHANG, F.C., O'CALLAHAN, C.M. & PTASIENSKI, J. (1989) L-type calcium channels in cardiac and skeletal muscle. Purification and phosphorylation. Ann.N.Y.Acad.Sci. **560**, 27-38.

HUI, A., ELLINOR, P.T., KRIZANOVA, O., WANG, J-J., DIEBOLD, R.J. & SCHWARTZ, A. (1991) Molecular cloning of multiple subtypes of a novel rat brain isoform of the α_1 subunit of the voltage-dependent calcium channel. Neuron **7**, 35-44.

IMAGAWA, T., LEUNG, A.T. & CAMPBELL, K.P. (1987) Phosphorylation of the 1,4-dihydropyridine receptor of the voltage-dependent Ca^{2+} channel by an intrinsic protein kinase in isolated triads from rabbit skeletal muscle. J.Biol.Chem. **262**, 8333-8339.

JAY, S.D., SHARP, A.H., KAHL, S.D., VEDVICK, T.S.,HARPOLD, M.M. & CAMPBELL, K.P. (1991) Structural characterization of the dihydropyridine-sensitive calcium channel α_2-subunit and the associated δ peptides. J.Biol.Chem. **266**, 3287-3293.

KASAI, H. & AOSAKI, T. (1989) Modulation of Ca-channel current by an adenosine analog mediated by a GTP-binding protein in chick sensory neurons. Pflugers Arch. **414**, 145-149.

KASAI, H., AOSAKI, T. & FUKUDA, J. (1987) Presynaptic Ca-antagonist *w*-conotoxin irreversibly blocks N-type Ca-channels in chick sensory neurons. Neurosci. Res. **4**, 228-235.

KIM, H.S., WEI, X., RUTH, P., PEREZ-REYES, E., FLOCKERZI, V., HOFMANN, F. & BIRMBAUMER, L. (1990) Studies on the structural requirements for the activity of the skeletal muscle dihydropyridine receptor/slow Ca^{2+} channel. J.Biol.Chem. **265**, 11858-11863.

KOCH, W.J., ELLINOR, P.T. & SCHWARTZ, A. (1990) cDNA cloning of a dihydropyridine-sensitive calcium channel from rat aorta. J.Biol.Chem. **265**, 17786-17791.

KOCH, W.J., HUI, A., SHULL, G.E., ELLINOR, P. & SCHWARTZ, A. (1989) Characterization of cDNA clones encoding two putative isoforms of the α_1 subunit of the dihydropyridine-sensitive voltage-dependent calcium channel isolated from rat brain and rat aorta. Febs Lett. **250**, 386-388.

KONGSAMUT, S., LIPSCOMBE, D. & TSIEN, R.W. (1989) The N-type Ca channel in frog sympathetic neurons and its role in α-adrenergic modulation of transmitter release. Ann.N.Y.Acad.Sci. **560**, 312-333.

KOWALSKI, M.T., GEORGE, P.R., HARRISON, T.M., WRAY, D. & NORMAN, R.I. (1990) Effects of anti-calcium channel α_2-subunit antibodies on calcium flux and 1,4-dihydropyridine binding. Biochem. Soc. Transac. **18**, 890.

LEE, K.S. & TSIEN, R.W. (1983) Mechanism of calcium channel blockade by verapamil, D600, diltiazem and nitrendipine in single dialysed heart cells. Nature **302**, 790-794.

LEES, G., PEARSON, H.A. & W.-WRAY, D. (1989) Calcium channels in isolated locust thoracic ganglia. J.Physiol. **410**, 13P.

LEUNG, A.T., IMAGAWA, T. & CAMPBELL, K.P. (1987) Structural characterization of the 1,4-dihydropyridine receptor of the voltage-dependent Ca^{2+} channel from rabbit skeletal muscle. J.Biol.Chem. **262**, 7943-7946.

LIPSCOMBE, D. & TSIEN, R.W. (1987) Noradrenaline inhibits N-type Ca channels in isolated frog sympathetic neurones. J. Physiol. **390**, 84P.

LLINAS, R.R., SUGIMORI, M. & CHERKSEY, B. (1989) Voltage-dependent calcium channels in mammalian neurons. The P channel. Ann.N.Y.Acad.Sci. **560**, 103-111.

LLINAS, R., SUGIMORI, M., LIN, J.-W. & CHERKSEY, B. (1989) Blocking and isolation of a calcium channel from neurons in mammals and cephalopods utilizing a toxin fraction (FTX) from funnel-web spider poison. Proc.Natl.Acad.Sci.USA **86**, 1689-1693.

McCLESKEY, E.W. (1985) Calcium channels and intracellular calcium release are pharmacologically different in frog skeletal muscle. J.Physiol. **361**, 231-249.

McCLESKEY,E.W., FOX, A.P., FELDMAN, D.H., CRUZ, L.J., OLIVERA, B.M., TSIEN, R.W. & YOSHIKAMI, D. (1987) ω-conotoxin: direct and persistent blockade of specific types of calcium channels in neurons but not muscle. Proc. Natl. Acad. Sci. **84**, 4327-4331.

McKENNA, E.J., SMITH, J.S., MA, J., VILVEN, J., VAGHY, P., SCHWARTZ, A. & CORONADO, R. (1987) Reconstitution of a purified voltage-dependent calcium channel (VDCC) into planar lipid bilayers. Biophys. J. **51**, 29a.

MEIRI, H., SPIRA, G., SAMMAR, M., NAMIR, M., SCHWARTZ, A., KOMORIYA, A., KOSOWER, E.M. & PALTI, Y. (1987) Mapping a region associated with Na channel inactivation using antibodies to a synthetic peptide corresponding to a part of the channel. Proc. Natl. Acad. Sci. **84**, 5058-5062.

MIKAMI, A., IMOTO, K., TANABE, T., NIIDOME, T., MORI, Y., TAKESHIMA, H., NARUMIYA, S. & NUMA, S. (1989) Primary structure and functional expression of the cardiac dihydropyridine-sensitive calcium channel. Nature **340**, 230-233.

MORI, Y., FRIEDRICH, T., KIM, M-S., MIKAMI, A., NAKAI, J., RUTH, P., BOSSE, E., HOFMANN, F., FLOCKERZI, V., FURUICHI, T., MIKOSHIBA, K., IMOTO, K., TANABE, T. & NUMA, S. (1991) Primary structure and functional expression from complementary DNA of a brain calcium channel. Nature **350**, 398-402.

MORTON, M.E., CAFFREY, J.M., BROWN, A.M. & FROEHNER, S.C. (1988) Monoclonal antibody to the α_1 subunit of the dihydropyridine complex inhibits calcium currents in BC_3H1 myocytes. J. Biol. Chem. **263**, 613-616.

MORTON, M.E. & FROEHNER, S.C. (1987) Monoclonal antibody identifies a 200kDa subunit of the dihydropyridine-sensitive calcium channel. J.Biol.Chem. **262**, 11904-11907.

MORTON, M.E. & FROEHNER, S.C. (1989) The α_1 and α_2 polypeptides of the dihydropyridine-sensitive calcium channel differ in developmental expression and tissue distribution. Neuron **2**, 1499-1506.

NARAHASHI, T., TSUNOO, A. & YOSHII, M. (1987) Characterization of two types of calcium channels in mouse neuroblastoma cells. J. Physiol. **383**, 231-249.

NASTAINCZYK, W., ROHRKASTEN, A., SIEBER, M., RUDOLPH, C., SCHACHTELE, C. MARNE, D. & HOFMANN, F. (1987) Phosphorylation of the purified receptor for calcium channel blockers by cAMP kinase and protein kinase C. Eur.J.Biochem. **169**, 137-142.

NILIUS, B., HESS, P., LANSMAN, J.B. & TSIEN, R.W. (1985) A novel type of cardiac calcium channel in ventricular cells. Nature **316**, 443-446.

NODA, M., IKEDA, T., KAYANO, T., SUZUKI, H., TAKESHIMA, H., KURASAKI, M., TAKAHASHI, H. & NUMA, S. (1986) Existence of distinct sodium channel messenger RNAs in rat brain. Nature **320**, 188-192.

NODA, M., SHIMIZU, S., TANABE, T., TAKAI, T., KAYANO, T., IKEDA, T., TAKAHASHI, H., NAKAYAMA, H., KANAOKA, Y., MINAMINO, N., KANGAWA, K., MATSUO, H., RAFTERY, M.A., HIROSE, T., INAYAMA, S., HAYASHIDA, H., MIYATA, T. & NUMA, S. (1984) Primary structure of *Electrophorus electricus* sodium channel deduced from cDNA sequence. Nature **312**, 121-127.

NORMAN, R.I., BURGESS, A.J., ALLEN, E. & HARRISON, T.M. (1987) Monoclonal antibodies against the 1,4-dihydropyridine receptor associated with voltage-sensitive Ca^{2+} channels detect similar polypeptides from a variety of tissues and species. Febs Lett. **212**, 127-132.

NORMAN, R.I., BURGESS, A.J., ALLEN, E. & HARRISON, T.M. (1987a) Monoclonal antibodies to Ca^{2+} channel component. Biochem. Soc. Trans. **15**, 895-896.

NORMAN, R.I., BURGESS, A.J. & HARRISON, T.M. (1989) Monoclonal antibodies against calcium channels. Ann.N.Y.Acad.Sci. **560**, 258-268.

NOWYCKY, M.C., FOX, A.P. & TSIEN R.W. (1985) Three types of neuronal calcium channel with different calcium agonist sensitivity. Nature **316**, 440-443.

PEERS, C., LANG, B., NEWSOM-DAVIS, J. & WRAY, D.W.- (1990) Selective action of myasthenic syndrome antibodies on calcium channels in a rodent neuroblastoma x glioma cell line. J. Physiol. **421**, 293-308.

PELZER, D., GRANT, A.O., CAVALIE, A., PELZER, S., SIEBER, M., HOFMANN, F. & TRAUTWEIN, W. (1989) Calcium channels reconstituted from the skeletal muscle dihydropyridine receptor protein complex and its α_1 peptide subunit in lipid bilayers. Ann.N.Y.Acad.Sci. **560**, 138-154.

PELZER, S., BARHANIN, J., PAURON, D., TRAUTWEIN, W., LAZDUNSKI, M. & PELZER, D. (1989) Diversity and novel pharmacological properties of Ca^{2+} channels in *Drosophila* brain membranes. EMBO J. **8**, 2365-2371.

PEREZ-REYES, E., KIM, H.S., LACERDA, A.E., HORNE, W., WEI, X., RAMPE, D., CAMPBELL, K.P., BROWN, A.M. & BIRNBAUMER, L. (1989) Induction of calcium currents by the expression of the α_1-subunit of the dihydropyridine receptor from skeletal muscle. Nature **340**, 233-236.

PEREZ-REYES, E., WEI, X., CASTELLANO, A. & BIRNBAUMER, L. (1990) Molecular diversity of L-type calcium channels. J.Biol.Chem. **265**, 20430-20436.

PHILLIPS, H.J., WILSON, G., BALDWIN, S., NORMAN, R. & WRAY, D. (1991) Effect of antibodies on calcium channels. Ann.N.Y.Acad.Sci. **635**, 489-492.

QUANDT, F.N. & NARAHASHI, T. (1984) Isolation and kinetic analysis of inward currents in neuroblastoma cells. Neuroscience **13**, 249-262.

RANE, S.G., HOLZ IV, G.G. & DUNLAP, K. (1987) Dihydropyridine inhibition of neuronal calcium current and substance P release. Pflugers Arch. **409**, 361-366.

REGAN, L.J., SAH, D.W.Y. & BEAN, B.P. (1991) Calcium channels in rat central and peripheral neurons: High-threshold current resistant to dihydropyridine blockers and ω-conotoxin. Neuron **6**, 269-280.

REUTER, H. (1983) Calcium channel modulation by neurotransmitters, enzymes and drugs. Nature **301**, 569-574.

RIOS, E. & BRUM, G. (1987) Involvement of dihydropyridine receptors in excitation-contraction coupling. Nature **325**, 717-720.

ROBERTSON, B. & TAYLOR, R. (1986) Effects of γ-aminobutyric acid and (-)-baclofen on calcium and potassium currents in cat dorsal root ganglion neurones in vitro. Br.J.Pharmac. **89**, 661-672.

ROSENBERG, R.L., HESS, P., REEVES, J.P., SMILOWITZ, H. & TSIEN, R.W. (1986) Calcium channels in planar lipid bilayers: Insights into mechanisms of ion permeation and gating. Science **231**, 1564-1566.

RUTH, P., ROHRKASTEN, A., BIEL, M., BOSSE, E., REGULLA, S., MEYER, H.E., FLOCKERZI, V. & HOFMANN, F. (1989) Primary structure of the ß subunit of the DHP-sensitive calcium channel from skeletal muscle. Science **245**, 1115-1118.

SANCHEZ, J.A. & STEFANI, E. (1978) Inward calcium current in twitch muscle fibres of the frog. J.Physiol. **283**, 197-209.

SANGUINETTI, M.C. & KASS, R.S. (1984) Voltage-dependent block of calcium channel current in the calf cardiac purkinje fiber by dihydropyridine calcium channel antagonists. Circ. Res. **55**, 336-348.

SCHWARTZ, L.M., McCLESKEY, E.W. & ALMERS, W. (1985) Dihydropyridine in muscle are voltage-dependent but most are not functional calcium channels. Nature **314**, 747-751.

SCROGGS, R.S. & FOX, A.P. (1992) Calcium current variation between acutely isolated adult rat dorsal root ganglion neurons of different size. J.Physiol. **445**, 639-658.

SIEBER, M, NASTAINCZYK, W, ZUBOR, V, WERNET, W. & HOFMANN, F. (1987) The 165-kDa peptide of the purified skeletal muscle dihydropyridine receptor contains the known regulatory sites of the calcium channel. Eur.J.Biochem. **167**, 117-122.

SINGER, D., BIEL, M., LOTAN, I., FLOCKERZI, V., HOFMANN, F. & DASCAL, N. (1991) The roles of the subunits in the function of the calcium channel. Science **253**, 1553-1557.

SNUTCH, T.P., TOMLINSON, W.J., LEONARD, J.P. & GILBERT, M.M. (1991) Distinct calcium channels are generated by alternative splicing and are differentially expressed in the mammalian CNS. Neuron **7**, 45-57.

SPIZZ, G., ROMAN, D., STRAUSS, A. & OLSON, E.N. (1986) Serum and fibroblast growth factor inhibit myogenic differentiation through a mechanism dependent on protein synthesis and independent of cell proliferation. J.Biol.Chem. **261**, 9483-9488.

STRIESSNIG, J., KNAUS, H-G., GRABNER, M., MOOSBURGER, K., SEITZ, W., LIETZ, H. & GLOSSMANN, H. (1987) Photoaffinity labelling of the phenylalkylamine receptor of the skeletal muscle transverse-tubule calcium channel. FEBS Lett. **212**, 247-253.

STUHMER, W., CONTI, F., HARUKAZU, S., WANG, X., NODA, M., YAHAGI, N., KUBO, H. & NUMA, S. (1989) Structural parts involved in activation and inactivation of the sodium channel. Nature **339**, 597-603.

TAKAHASHI, M. & CATTERALL, W.A. (1987) Dihydropyridine-sensitive calcium channels in cardiac and skeletal muscle membranes: studies with antibodies against the α subunits. Biochem. **26**, 5518-5526.

TAKAHASHI, M., SEAGAR, M.J., JONES, J.F., REBER, B.F.X. & CATTERALL, W.A. (1987) Subunit structure of dihydropyridine-sensitive calcium channels from skeletal muscle. Proc.Natl.Acad.Sci.USA **84**, 5478-5482.

TALVENHEIMO, J.A., WORLEY, J.F. & NELSON, M.T. (1987) Heterogeneity of calcium channels from a purified dihydropyridine receptor preparation. Biophys.J. **52**, 891-899.

TANABE, T., BEAM, K.G., POWELL, J.A. & NUMA, S. (1988) Restoration of excitation-contraction coupling and slow calcium current in dysgenic muscle by dihydropyridine receptor complementary DNA. Nature **336**, 134-139.

TANABE, T., MIKAMI, A., NUMA, S. & BEAM, K.G. (1990) Cardiac-type excitation-contraction coupling in dysgenic skeletal muscle injected with cardiac dihydropyridine receptor cDNA. Nature **344**, 451-453.

TANABE, T., TAKESHIMA, H., MIKAMI, A., FLOCKERZI, V., TAKAHASHI, H., KANGAWA, K., KOJIMA, M., MATSUO, H., HIROSE, T. & NUMA, S. (1987) Primary structure of the receptor for calcium channel blockers from skeletal muscle. Nature **328**, 313-318.

TANG, C.M., PRESSER, F. & MORAD, M. (1988) Amiloride selectively blocks the low threshold (T) calcium channel. Science **240**, 213-215.

TRAUTWEIN, T., CAVALIE, A., FLOCKERZI, V., HOFMANN, F. & PELZER, D. (1987) Modulation of calcium channel function by phosphorylation in guinea pig ventricular cells and phospholipid bilayer membranes. Circ. Res. **61**, 17-23.

TSIEN, R.W., ELLINOR, P.T. & HORNE, W.A. (1991) Molecular diversity of voltage-dependent Ca^{2+} channels. TIPS **12**, 349-354.

TSIEN, R.W., LIPSCOMBE, D., MADISON, D.V., BLEY, K.R. & FOX, A.P. (1988) Multiple types of neuronal calcium channels and their selective modulation. TINS **11**, 431-438.

VAGHY, P.L., STRIESSNIG, J., MIWA, K., KNAUS, H-G., ITAGAKI, K., McKENNA, E., GLOSSMANN, H. & SCHWARTZ, A. (1987) Identification of a novel 1,4-dihydropyridine- and phenylalkylamine-binding polypeptide in calcium channel preparations. J.Biol.Chem. **262**, 14337-14342.

VARADI, G., LORY, P., SCHULTZ, D., VARADI, M. & SCHWARTZ, A. (1991) Acceleration of activation and inactivation by the ß subunit of the skeletal muscle calcium channel. Nature **352**, 159-162.

VASSILEV, P., SCHEUER, T. & CATTERALL, W.A. (1988) Identification of an intracellular peptide segment involved in sodium channel inactivation. Science **241**, 1658-1661.

VASSILEV, P., SCHEUER, T. & CATTERALL, W.A. (1989) Inhibition of inactivation of single sodium channels by a site-directed antibody. Proc. Natl. Acad. Sci. **86**, 8147-8151.

VILVEN, J., LEUNG, A.T., IMAGAWA, T., SHARP,A.H., CAMPBELL, K.P. & CORONADO, R. (1988) Interaction co calcium channels of skeletal muscle with monoclonal antibodies specific for its dihydropyridine receptor. Biophys. J. **53**, 556a.

WANG, R., KARPINSKI, E., WU, L. & PANG, P.K.T. (1990) Flunarizine selectively blocks transient calcium channel currents in N1E-115 cells. J.Pharmacol.Exp.Ther. **254**, 1006-1011.

WERTH, J.L., HIRNING, L.D. & THAYER, S.A. (1991) ω-conotoxin exerts functionally distinct low and high affinity effects in the neuronal cell line NG108-15. Mol.Pharmacol. **40**, 742-749.

WILSON, G., BALDWIN, S., NORMAN, R. & WRAY, D. (1991) Effect of peptide-specific antibody on calcium channel function in neuroblastoma cells. J. Physiol. **435**, 48P.

WRAY, D.W.-, NORMAN, R.I. & PHILLIPS, H.J. (1990) Action of monoclonal antibody against calcium channels. Eur.J.Pharmacol. **183**, 248.

WRAY, D.W-., PHILLIPS, H.J., HARRISON, T.M. & NORMAN, R.I. (1989) Monoclonal antibodies as probes of calcium channels. Eur.J.Neurosci., **S2**, 277.

YAARI, Y., HAMON,B. & LUX, H.D. (1987) Development of two types of calcium channels in cultured mammalian hippocampal neurons. Science **235**, 680-682.